The development and optimisation of a Theiler's murine encephalomyelitis virus antiviral assay

A dissertation submitted in partial fulfilment of the requirements for the degree of
MASTER OF SCIENCE IN MICROBIOLOGY

Department of Biochemistry and Microbiology
Rhodes University
Makhanda
South Africa

ORCID ID
https://orcid.org/0000-0002-7684-7457

By:
Urisha Tirah Naidoo
Feb 2023

Supervisor: Professor Caroline Knox

Co-supervisor: Doctor Nicole Upfold

Abstract

Picornaviruses belong to the *Picornaviridae* family which are one of the largest and most diverse family of RNA viruses that cause a broad spectrum of infections in both humans and animals. These diseases range from severe infections such as poliomyelitis, meningitis, myocarditis to mild illnesses such as the common cold. Picornavirus outbreaks are a worldwide threat as they are continuously occurring. A recent outbreak of foot-and-mouth disease caused by a picornavirus occurred in South Africa, resulting in a temporary ban on the movement of cattle. Currently, the FDA has not approved any antiviral drugs against this virus, increasing the urgency for identifying effective antivirals. Picornaviruses have similar genomes and capsid organisation as such, those that are non-hazardous to humans can be used as a model system. A Theiler's murine encephalomyelitis virus (TMEV) strain GDVII and Baby Hamster Kidney fibroblasts (BHK-21 cells) was used as a replication system to develop and optimise a medium-throughput antiviral screening assay.

The TMEV GDVII replication system in BHK-21 cells was validated, and preliminary experiments were performed that were necessary for the development of the TMEV GDVII antiviral assay. This was achieved by conducting a CPE assay to visually monitor the onset and development of CPE induced by TMEV GDVII. Plaque assays accurately quantified the number of infectious virus particles required for calculating the MOI in downstream experiments. Lastly, indirect immunofluorescence and Western blot analysis detected the expression of viral proteins using previously generated antibodies against the TMEV GDVII VP1 capsid and 2C protein, thereby confirming infection in BHK-21 cells.

The development of robust and reproducible assays is an essential component in antiviral drug discovery. Therefore, the confirmed replication system was then used as a foundation to develop a medium-throughput CPE-based TMEV GDVII antiviral assay whereby the parameters were optimised to produce one of high quality. Firstly, the quantitation of viral-induced CPE was examined and confirmed in a 96-well plate using resazurin as a cell viability indicator. Each parameter was tested at varying conditions, and the optimal was concluded as 2 % FBS in the assay media, a 15 000 cells/well seeding density, infecting the cells with TMEV GDVII at an MOI of 0.00625 and measuring resazurin at an endpoint of 72 hpi. Furthermore, the parameters were

validated by calculating the Z'- factor, which consistently produced scores above 0.5, indicative of a reliable, robust, reproducible antiviral assay.

Currently, there are no inhibitors against TMEV GDVII that have been reported or confirmed in cell lines, animal models or clinical trials. Therefore, once the optimal assay parameters were selected, it presented an opportunity to assess whether potential compounds, including itraconazole (ITZ) and dipyridamole (DIP), possessed antiviral activity that could firstly, be utilised as a control inhibitor when screening compounds against TMEV GDVII and secondly, contribute to research on this virus. Additionally, the previously produced anti-TMEV GDVII capsid antibody was shown to neutralise viral infection and was also included as a potential control. The sensitivity of the cells towards DMSO, a solution in which the compounds were solubilised, was first investigated. It was found that concentrations above 1 % are toxic to the cells; as such, the final DMSO concentrations were always kept below 1 % when screening compounds. Lastly, the generation of dose-response curves aided in the conclusion that the antibody was the most suitable control inhibitor as it displayed potent antiviral activity and no cytotoxicity towards the cells. In contrast, ITZ and DIP did not possess effective antiviral action and were toxic to cells at high concentrations.

Finally, after all the components of the medium-throughput TMEV GDVII antiviral assay were identified, it was possible to screen 24 compounds from a coumarin and marine natural product library for cell cytotoxicity and antiviral activity. After generating dose-response curves, it was concluded that no compound effectively inhibited virus-induced CPE, and most were toxic to cells at relatively high concentrations.

In conclusion, this is the first study that describes the development and optimisation of a robust medium-throughput CPE-based antiviral assay that has immense potential to screen other libraries of compounds for antiviral activity against TMEV GDVII.

Acknowledgements

- Firstly, I would like to sincerely thank my primary supervisor, Prof Caroline Knox, for your support, guidance, encouragement and inspiration throughout my time in her lab. Thank you for always helping whenever I encountered a problem in the project. Your willingness to always help will not be forgotten.
- To my co-supervisor Dr Nicole Upfold, even though you have moved to the UK, you have still found time to help me get through this project. Thank you for all your guidance and advice.
- Thank you to Dr Tarryn Swart, for the assistance and tips regarding assay development.
- Thank you to Prof Rosalyn Klein, the Rhodes Department of Chemistry, for supplying the coumarin compounds.
- Thank you to Prof Rosemary Dorrington, the Rhodes Department of Biochemistry and Microbiology, for supplying the MNP library of compounds.
- Thank you to Rhodes University and the National Research Foundation (NRF) for the financial support.
- Thank you to the members of lab 425 for the words of encouragement in the short time spent together.
- Thank you to my closest friends, Nomxolisi Mqwathi and Gabriella Jackson, for your friendship, motivation and presence.
- Finally, thank you to my mum Ashika Naidoo, my late father Sean Naidoo and family, Kamisha Fortuin, Lawrenzo Fortuin, Tyron Joseph and my two beautiful nieces, Azariah Fortuin and Lily Fortuin, for everything!

Table of contents

List of figures

List of tables

List of abbreviations

Abbreviations

μ	Mean
σ	Standard Deviation
%	Percentage
°C	Degrees Celsius
x g	Times Gravitational Force
α	Alpha
β	Beta
µg	Microgram/s
µg/ml	Microgram/s per millilitre
µl	Microlitre/s
µM	Micromolar
2 °	Secondary
BHK-21 cells	Baby Hamster Kidney Cells Clone 21
BSL-2	Biosafety Level 2
cm^2	Square centimetre
CPE	Cytopathic Effect
DAPI	4′,6-diamino-2 phenylindole
ddH_2O	Deionised Water
DIP	Dipyridamole

DMEM	Dulbecco's Modified Eagle Medium
DMSO	Dimethyl Sulfoxide
FBS	Foetal Bovine Serum
g/mol	Gram/s per mole
h	Hour/s
HeLa cells	Henrietta Lacks cells
Hpi	Hours Post-infection
Hsp90	Heat Shock Protein 90
HTS	High-throughput screen
HEp-2	Human Epithelioma cells
ITZ	Itraconazole
kDa	Kilo Daltons
M	Molar
mg	Milligram/s
min	Minute/s
ml	Millilitre/s
mM	Millimolar
mm	Millimetres
MNP	Marine Natural Product
MOI	Multiplicity of Infection
MTS	Medium-throughput screen
nm	Nanometre
PBS	Phosphate Buffered Saline
PFU/ml	Plaque Forming Units per millilitre
PSA	Penicillin Streptomycin Amphotericin
RFU	Relative Fluorescence Units
RT	Room Temperature
SDS	Sodium Dodecyl Sulphate
SDS-PAGE	Sodium Dodecyl Sulphate Polyacrylamide gel electrophoresis
TBS	Tris-buffered saline
TBS-T	Tris-buffered saline with Tween

TEMED	N, N, N', N'-Tetramethyl ethylene diamine Thymidine
Tntc	Too Numerous to Count
U	Units
v/v	Volume over Volume
w/v	Weight over Volume

Viruses

CV	Coxsackievirus
EMCV	Encephalomyocarditis Virus
EV	Enterovirus
FMDV	Foot-and-Mouth Disease Virus
HAV	Hepatitis A Virus
HCV	Hepatitis C Virus
HIV	Human Immunodeficiency Virus
HPeV	Human Parechovirus
PV	Poliovirus
RV	Rhinovirus
SAFV	Saffold Virus
SARS-CoV-2	Severe Acute Respiratory Syndrome Type 2 virus
TMEV	Theiler’s murine encephalomyelitis virus

Chapter 1 Literature review

1.1 Introduction and classification of picornaviruses

Picornaviridae is one of the largest and most diverse families of viruses that have caused a multitude of epidemics globally. Picornaviruses are characterised as small, icosahedral, non-enveloped positive-sense RNA viruses (Zell, 2017; Kuhn et al., 2020). Currently, there are 68 genera that consist of 158 species (International Committee on Taxonomy of Viruses, 2021); however, these figures are constantly changing as many viruses await classification. Genera with pathological importance include *Enterovirus* (EV), *Parechovirus, Aphthovirus*, *Cardiovirus* and *Hepatovirus* (Tuthill et al., 2010; Lemon, 2022; Novikov and Melentev, 2022; Sarry et al., 2022; Zhang et al., 2022; Foglia et al., 2023) (**Table 1.1**).

Picornaviruses cause a broad range of infections in humans and animals. These diseases can range from severe infections such as poliomyelitis, meningitis, and encephalitis to mild illnesses like the common cold (Jiang et al., 2014). The largest genus in this family is EVs which are ubiquitous and responsible for a substantial number of infections annually around the globe (Sinclair and Omar, 2021). EVs consist of 12 species and over 300 types (Palmenberg et al., 2009; Simmonds et al., 2010; McIntyre et al., 2013; Sinclair and Omar, 2021). They are mainly transmitted via the faecal-oral route with the possibility of spreading to other organs via blood circulation. Infections may also occur in the upper and lower respiratory tracts (Rubsamen-Schaeff and Buschmann, 2021). EVs include the species *Enterovirus A-D, Rhinovirus A-C,* which infect humans and *Enterovirus E-J* (**Table 1.1**), which cause animal disease. EV-A consists of numerous coxsackievirus (CV) A serotypes and EV-A71, the foremost causative agent of hand-foot-and-mouth disease (HFMD). The serotype EV-A71 has been accountable for several global outbreaks of HFMD since 1990, where symptoms include skin rashes and mouth sores commonly affecting young children (Wang et al., 2015; Dai et al., 2019, Wang et al., 2022). EV-B is the largest EV species and consists of several CV-B serotypes and echoviruses causing diseases such as meningitis, encephalitis, myocarditis, and pancreatitis (Tapparel et al., 2013; Lugo and Krogstad, 2016; Alhazmi et al., 2022). EV-C includes polioviruses (PV) 1,2,3 and many other serotypes. PV infections are mild; however, some cases can lead to poliomyelitis or non-paralytic meningitis. Poliomyelitis, also

known as polio, is a form of flaccid paralysis and has been the source of a multitude of epidemics with high morbimortality since the 19th century (de Jesus, 2007). In 1988 the Forty-first World Health Assembly launched the Global Polio Eradication Initiative (GPEI). Since the GPEI was introduced, polio cases have decreased by over 99% globally, with 80% of the world's population certified as polio-free (World Health Organization, 2019). However, there have been recent unexpected outbreaks in the UK, the United States and parts of Africa (Sethi et al., 2022). EV-D contains serotypes such as EV-D68, EV-D70 and EV-D94. EV-D68 has recently re-emerged with an increase in epidemics worldwide, causing severe respiratory illness in children (Khetsuriani et al., 2006; Furuse et al., 2015; Messacar et al., 2015). The last human-related EV species are the rhinoviruses (RV). Unlike most EVs, RVs infect the respiratory tract causing the most widespread infectious disease worldwide, the common cold. The common cold has a significant economic impact as it leads to countless losses of working and school days, an increase in medical assistance costs, and an upsurge in prescription medication (Heikkinen and Jarvinen, 2003). In addition, RVs can also infect the lower respiratory tract and are linked to diseases such as pneumonia, bronchiolitis (Papadopoulos et al., 2002; Renwick et al., 2007), asthma (Edwards et al., 2012), and chronic obstructive pulmonary disease (COPD) exacerbations (Mirabelli et al., 2017).

Parechovirus is another genus of pathological importance. The genus is classified into six species: *Parechovirus A-F. Parechovirus A* comprises 19 serotypes, whereas *Parechovirus B* consists of Ljungan virus 1-6 (Chuchaona et al., 2015; Zhao et al., 2017) (International Committee on Taxonomy of Viruses, 2021) (**Table 1.1**). The human parechovirus (HPeV) prevalence is said to be as high as EVs, and due to an upsurge of HPeVs circulating worldwide, this virus has gained more attention and awareness. HPeV-1 induces mild to severe gastrointestinal and respiratory illness, HPeV-3 is the most pathogenic HPeV and is associated with viral sepsis-like illness, meningitis, paralysis and even fatality in infants (Boivin et al., 2005; Harvala et al., 2009; Schuffenecker et al., 2012). Other noteworthy genera in the picornavirus family include *Hepatovirus,* which consists of hepatitis A virus (HAV) known to cause hepatitis, a liver disease (Smith and Simmonds, 2018; Lemon, 2022). The genus *Aphthovirus* includes the species Foot-and-mouth disease virus (FMDV), which threatens livestock, resulting in extreme economic challenges. Foot-and-mouth disease (FMD) is one of the most contagious and devastating animal diseases to occur (Tulloch et al., 2018).

Table 1.1 Classification of picornaviruses that are clinically important to humans/animals.

Genus	Selected species	Serotypes	Clinical infections
Enterovirus	*Enterovirus A*	Coxsackievirus A8, A16 EV-A71	Hand-foot-and-mouth disease, herpangina, encephalitis, paralysis, myelitis, meningitis
	Enterovirus B	Coxsackievirus B1, B3, B4 Echoviruses 3, 30	Neonatal sepsis, insulin-dependent diabetes mellitus, meningitis, encephalitis, myocarditis, pancreatitis
	Enterovirus C	Poliovirus 1,2,3	Poliomyelitis, non-paralytic meningitis
	Enterovirus D	EV-D68, EV-D70, EV-D94	Severe respiratory illness, acute haemorrhagic conjunctivitis, acute flaccid paralysis
	Rhinovirus A, B, C		Common cold, asthma, pneumonia, bronchiolitis, COPD
Parechovirus	*Parechovirus A*	Human parechovirus 1, 2, 3, 4	Gastroenteritis, respiratory illness, viral sepsis-like illness, meningitis, paralysis
	Parechovirus B	Ljungan virus 1-6	Diabetes mellitus, neurological disease, myocarditis (rodents)
Hepatovirus	*Hepatovirus A*	Hepatitis A virus	Hepatitis
Aphthovirus	*Foot-and-mouth disease virus*	Foot-and-mouth disease virus O, A, C, Asia 1	Foot-and-mouth disease, acute fatal myocarditis
	Bovine rhinitis A, B virus	Bovine rhinitis A virus 1,2, Bovine rhinitis B virus 1,2,3,4,5	Respiratory illness
Cardiovirus	*Cardiovirus A*	Encephalomyocarditis 1, 2	Encephalitis, myocarditis
	Cardiovirus B	Theiler's murine encephalomyelitis virus	Polioencephalomyelitis, chronic persistent demyelinating disease
	Cardiovirus D	Saffold virus	Respiratory and gastrointestinal disease

Agricultural production is impeded due to FMDV infecting domestic animals such as cattle, pigs and sheep by causing blistering of limb epithelia, myocarditis in younger animals and after an extended period of infection, milk and meat production can decline (Paton et al., 2021). More relevantly, a recent outbreak of FMD occurred in South Africa, followed by a temporary suspension of the movement of cattle within the entire country, resulting in significant economic losses (Orabi, 2022). Lastly, the *Cardiovirus* genus consists of the six species *Cardiovirus A-F* (**Table 1.1**). It has long been thought that cardioviruses mainly infect rodents. However, in 2007, the first human cardiovirus was discovered and was named the Saffold virus (SAFV), belonging to the species *Cardiovirus D.* SAFV has been isolated from nasal and stool samples predominantly from children, presenting respiratory and gastrointestinal disease (Jones et al., 2007; Abed et al., 2008; Zoll et al., 2009). Encephalomyocarditis virus (EMCV) (*Cardiovirus A*) infections result in encephalitis and myocarditis in rodents, pigs, and many other mammals (Carocci and Bakkali-Kassimi, 2012). Theiler's murine encephalomyelitis virus (TMEV) belonging to the species *Cardiovirus B* infects mice either causing a fatal polio-encephalomyelitis or a chronic persistent demyelinating disease depending on the subgroup (Gerhauser et al., 2019). TMEV consists of two major subgroups. These subgroups are differentiated by their neurovirulence and antigenicity (Oleszak et al., 2004). GDVII and FA strains are part of the first subgroup and are highly neurovirulent, causing fatal acute encephalitis (Theiler and Gard, 1940). Theiler's original (TO) is the second subgroup and consists of the more persistent BeAn and DA strains. These strains result in mild encephalitis and can induce late chronic demyelinating disease. The GDVII, BeAn and DA strains have been sequenced and characterised (Lehrich et al., 1976; Lipton, 1980). TMEV GDVII can infect BHK-21 cells causing CPE in culture, but poses a low risk to human health as TMEV has been shown to only infect mice and not any other species (Omura et al., 2018). It can thus be used as a biosafe replication system to study picornaviruses in conventional BSL 2 tissue culture facilities and was the subject of this study.

1.2 Genome structure and polyprotein processing

Although picornaviruses of different genera infect different hosts and cause diverse diseases, these viruses share a notable similarity in their genome structure and capsid organisation (Francisco-Velilla et al., 2022). Picornavirus genomes consist of single-stranded positive-sense RNA, ranging from 6.7 to 10.1 kb in size (Zell et al., 2017). Generally, the genome comprises a single open

reading frame (ORF) encoding a large polyprotein. The ORF is flanked on the 5' and 3' ends by untranslated regions (UTR) of different lengths (**Figure 1.1**) (Bedard and Semler, 2004; Zell et al., 2021). The 5' UTR consists of a cloverleaf structure that functions in the initiation of replication and the internal ribosome entry site (IRES), which allows translation of RNA in a CAP-independent manner (Mokrejš et al., 2010). The 3' ends of all RNAs in the picornavirus family are polyadenylated like eukaryotic mRNAs. However, the 5' ends do not have the usual triphosphate cap; instead, they have viral-coded, genome-linked proteins (VPg) attached to the RNA via a tyrosine phosphodiester bond. The exact function of VPg is unclear, but it is believed to be involved in the initiation of RNA synthesis (Palmenberg, 1990; Francisco-Velilla et al., 2022).

The ORF that encodes the large polyprotein is separated into P1, P2 and P3 domains, as seen in **Figure 1.1**. P1 is the domain that encodes four structural capsid proteins and is highly conserved across picornaviruses. The P2 - P3 domains code for seven non-structural proteins that have several functions, such as host translational shutoff and replication. Some functions of these non-structural proteins are genus-specific, while others are conserved in function, such as viral RNA-dependent RNA polymerases (Cathcart et al., 2015). Several picornaviruses belonging to the aphthoviruses and cardioviruses encode a leader protein (L) located upstream on the 5' end. The role of this protein is also genus-specific. For example, it is proteolytically active only in aphthoviruses (Cathcart et al., 2015). In cardioviruses, it regulates host cell antiviral immune responses by inhibiting interferon production (Freundt et al., 2018). The three domains are cleaved by viral encoded proteases, including 3C/3CD. The use of the Hsp90 chaperone to facilitate efficient cleavage of the P1 domain has been recognised in several picornaviruses, such as PV (Geller et al., 2007; Mutsvunguma et al., 2011).

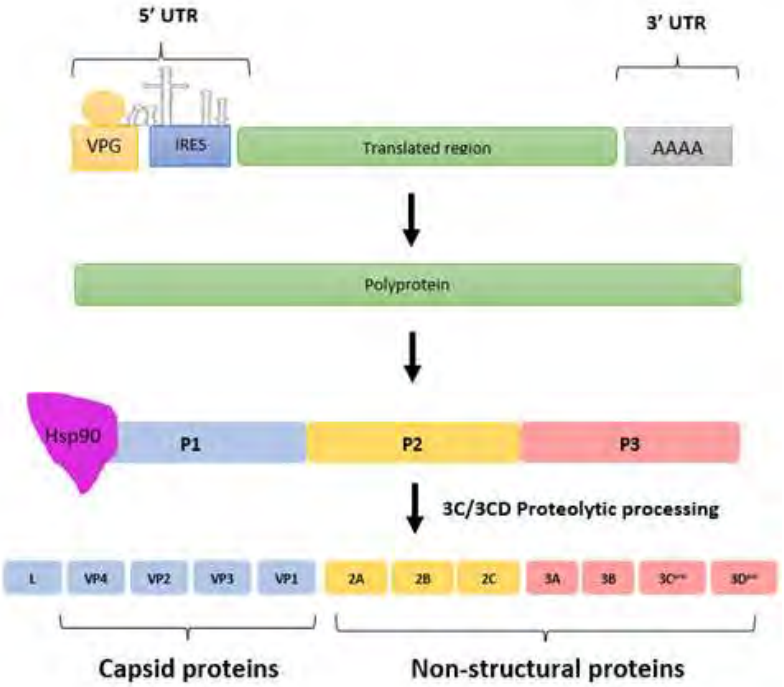

Figure 1.1 Picornavirus genome organisation. The picornavirus genome consists of a single open reading frame (ORF) that encodes a large polyprotein. The ORF is flanked on the 5' end with a 5' UTR that consists of an IRES (cloverleaf structure) and a VPg. The 3' UTR consists of a polyadenylated tail. The polyprotein is processed into three domains, namely P1, P2 and P3. Cleavage of each domain into its specific proteins is facilitated by proteases such as 3C/3CD with the help of chaperones such as Hsp90. The P1 domain encodes for the capsid proteins VP4, VP2, VP3 and VP1. Whereas the P2 and P3 domains encode for the seven non-structural proteins. Some picornaviruses, such as the aphthoviruses and cardioviruses, encode a leader protein (L) that is upstream on the 5' end. Adapted from Louten, (2016).

1.3 Picornavirus capsid structure

Mature virions in the picornavirus family have a non-enveloped icosahedral capsid with an approximate size of 30 nm. The capsid structure consists of 60 protomers organised in a pseudo-T=3 symmetry, enclosing the viral RNA genome (Sherry et al., 2020). A single protomer is comprised of three key surface capsid proteins, VP1, VP2 and VP3 (**Figure 1.2**) and one internal capsid protein, VP4. The surface proteins, VP1, VP2 and VP3, are arranged in a pentameric structure resulting in five VP1 proteins meeting at the five-fold axis and the VP2 and VP3 proteins meeting at the two-fold and three-fold axes, as seen in **Figure 1.2** (Jiang et al., 2014). The N-

termini of these three proteins are internal, while the C-termini are on the surface. Therefore, the VP4 protein located on the inside of the capsid forms a network with the N-termini and functions to stabilise the virion particle (Rossmann, 2002). Generally, the N-termini of VP4 proteins are located close to the five-fold axis, where they are bonded to a myristic acid group. The myristoylated VP4 capsid protein is associated with transporting the RNA into the host for replication and stabilising the pentameric subunits (Panjwani et al., 2014).

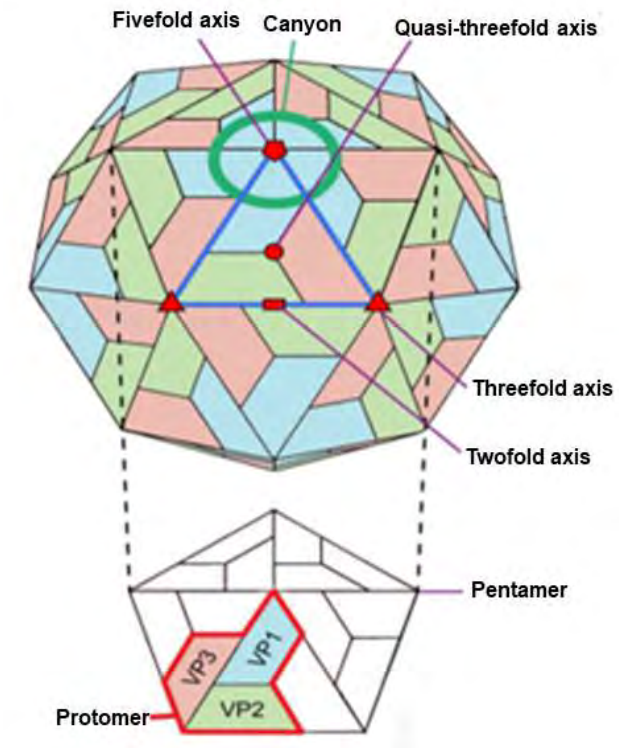

Figure 1.2 Picornavirus capsid structure and axes. Representation of a picornavirus capsid structure. The capsid consists of 60 protomers organised in a pseudo-T=3 symmetry enclosing the RNA genome. One protomer is comprised of the three surface proteins, VP1, VP2 and VP3, which are arranged in a pentameric structure. This pentameric structure results in an asymmetric unit. The different axes of symmetry consist of five VP1 proteins meeting at the five-fold axis and the VP2 and VP3 proteins meeting at the two-fold and three-fold axes. Adapted from Baggen et al., (2018).

1.4 Infectious cycle of picornaviruses

Picornaviruses generally have a short infectious cycle. The cycle begins with attachment to the host cell and ends with the virion being released. This is further discussed below.

1.4.1 Attachment, entry and uncoating

Picornavirus infection initiates when the virus binds to the host cell receptor (**Figure 1.3**). Specific cellular receptors are a crucial component in viral tropism and pathogenesis, meaning that the virus is incapable of infecting cells that lack the corresponding receptor (Whitton et al., 2005; Baggen et al., 2018). This family of viruses has diverse receptors; however, the most common picornavirus receptors are often within the immunoglobulin family, integrin receptor family, low-density lipoprotein receptor (LDLR) family, and complement control family (Tuthill et al., 2010). These receptors play a vital role in attachment, endocytosis, and inducing conformational changes in the capsid, which facilitate the uncoating of the virus (Tuthill et al., 2010; Baggen et al., 2018).

Once attachment to the receptor has occurred, the next step in the picornavirus life cycle is entry and uncoating of the capsid to release the viral RNA. Entry into the host cytoplasm usually takes place using endocytosed vesicles. Viruses are known to hijack several endocytic pathways to enter the cell. These include the clathrin-mediated and caveolin-mediated endocytic pathways (Pelkmans et al., 2001). Once the virus has entered, the single-stranded RNA needs to be released. Genome release is not well studied in picornaviruses; nevertheless, there are a few examples in the literature. Enteroviruses such as PV sustain the icosahedral capsid structure even after the VP4 and RNA release, leaving behind an empty 80S capsid intermediate (Levy et al., 2010). In contrast, cardioviruses and aphthoviruses disassemble their capsids into the pentameric subunits once they enter acidic conditions such as the endosome environment. This causes the externalisation of the VP4 subunit and RNA (Johns et al., 2009). Even though this process differs among picornaviruses, a successful infection is achieved when the genome is released and delivered to the cytoplasm in a complete and undamaged form.

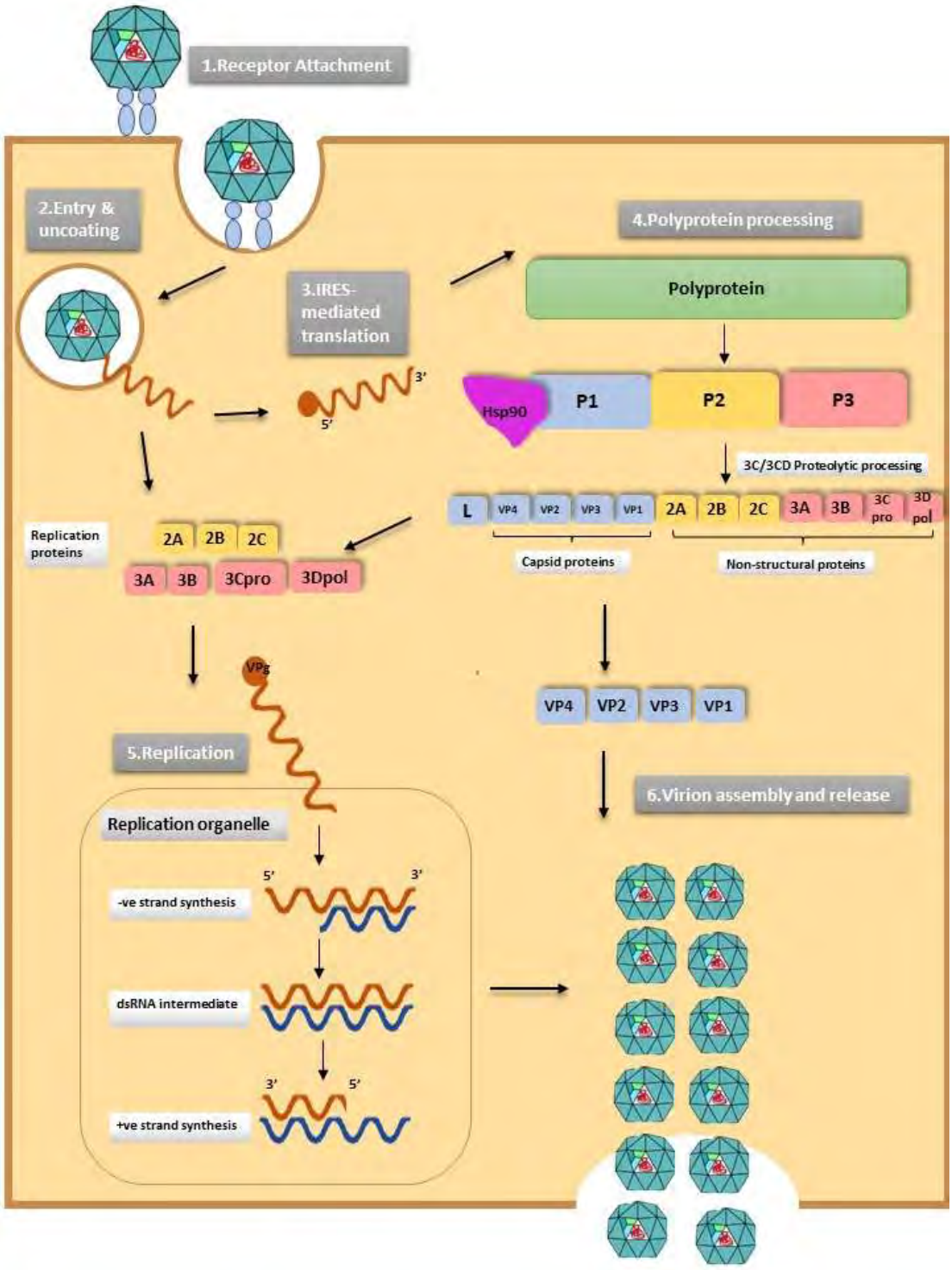

Figure 1.3 Overview of a typical picornavirus infectious cycle. 1. Receptor and attachment 2. Entry and uncoating 3. IRES-mediated translation 4. Polyprotein processing 5. Replication 6. Assembly and release. Adapted from Whitton et al., 2005 and Baggen et al., 2018.

1.4.2 Translation and polyprotein processing

Once the viral RNA is released into the cytosol, the genome is directly translated by the cellular ribosomes. Picornavirus translation is initiated in a cap-independent manner as they lack the usual 7-methyl guanosine cap at the 5' terminal. This mechanism is mediated by an IRES found on the 5' end of the genome (Baggen et al., 2018)**.** Host proteins are usually modified during the early phases of infection such that cellular mRNA translation is shut down and viral mRNA translation can proceed. As discussed above, translation of picornavirus viral mRNA occurs through a single ORF to produce a single polyprotein that is proteolytically processed (**Figure 1.1; Figure 1.3**).

Proteinases encoded by the virus involved in processing include $2A_{pro}$, $3C_{pro}$ and $3CD_{pro}$ in EVs, L_{pro} and $3C_{pro}$ in aphthoviruses, $3C_{pro}$ and $3CD_{pro}$ in cardioviruses and kobuviruses. Once the protein has been processed, an L protein (aphthoviruses, kobuviruses and cardioviruses) and the polyproteins P1, P2, and P3 are generated (Jackson and Belsham, 2021). The P1 domain, which is released by proteinase 2A (EVs) or 3C (other picornaviruses), is further cleaved into the capsid proteins VP0, VP3 and VP1. In comparison, the P2 and P3 domains are cleaved into non-structural proteins. P2 proteins such as 2BC and 2C play a role in the formation of membranous vesicles where RNA replication occurs. P3 proteins are involved in the replication process and have distinct functions, for example, 3D is the RNA-dependant RNA polymerase (Palmenberg, 1990).

1.4.3 Replication

After the initial translation of viral proteins and sufficient non-structural proteins are produced, replication can occur. Firstly, virus-induced membranous vesicles, also known as replication organelles (ROs), are formed as sites of replication (**Figure 1.3**). They are generated from remodelling the endoplasmic reticulum (ER) and Golgi apparatus membranes. Generally, the viral proteins 2BC and 3A and specific host proteins are required for RO formation (Steil and Barton, 2009; Baggen et al., 2018). Once the ROs are formed, replication is initiated by the uridylation of VPg. The RNA-dependant RNA polymerase $3D_{pol}$ is responsible for this process. $3D_{pol}$ uses the cis-acting replication element (Cre), a secondary RNA structure that acts as a template for the uridylylation of VPg to form VPgpUpU, a primer of replication (van der Linden et al., 2015). $3D_{pol}$ elongates uridylylated VPg to generate a negative-strand intermediate which serves as a template to produce more positive-strand RNAs. Positive strand RNAs can either be used for further rounds

of translation, replication or packaged to create infectious virus particles (Steil and Barton, 2009; van der Linden et al., 2015; Jackson and Belsham, 2021).

1.4.4 Virion assembly and release

After replication of the positive-strand RNA, encapsidation follows to produce new infectious viral particles (**Figure 1.3**). This complex oligomerisation process begins with the capsid precursor P1 undergoing myristoylation (absent in hepatoviruses and parechoviruses) (Jackson and Belsham, 2021). The Hsp90 chaperone protein will then associate and fold the myristoylated P1 domain, which also assists in the proteolytic processing by $3CD_{pro}$ to produce capsid proteins VP0, VP1 and VP3 (Geller et al., 2007). These proteins spontaneously form a protomer, and five of these protomers form a pentameric structure. They then assemble around the positive-strand RNA to form the provirion. The last step is the maturation process of VP0 into VP2 and VP4, producing the mature virion particle (Basavappa et al., 1994) (**Figure 1.4**). Typically, picornavirus virions are released via cell lysis, killing the host cell. However, studies have suggested that they could also be released by non-lytic mechanisms associated with releasing the mature virion in vesicles (van der Grein et al., 2019).

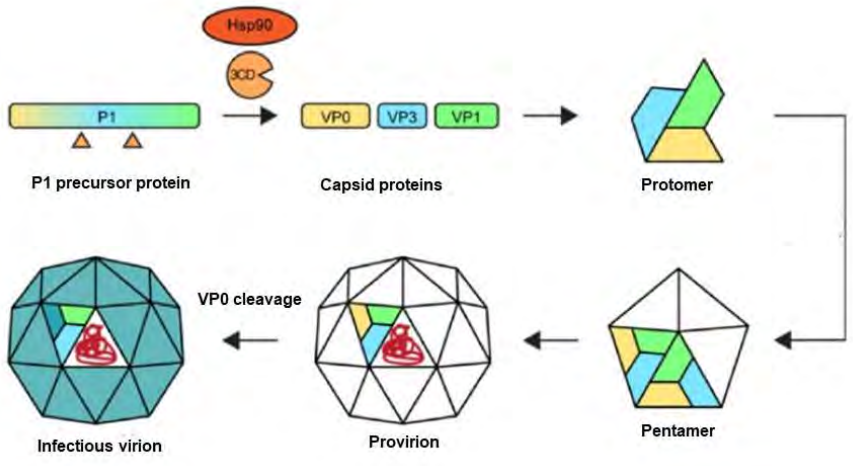

Figure 1.4 Picornavirus capsid assembly process. Once the P1 domain is separated from the P2/3 domains, the Hsp90 chaperone will stabilise it for proteolysis by the 3C/3CD proteases. Once it is cleaved into the three subunits, they will immediately form a 5S protomer. Five of these protomeric structures will combine to create a 14S pentamer, followed by twelve pentamers forming a 150S provirion which encloses the RNA genome. The last step is the maturation process, where VP0 is cleaved into VP2 and VP4, creating a 160S mature infectious virion. Adapted from van der Linden et al., (2015).

1.5 Disease prevention and control

1.5.1 Vaccination

Vaccination is one of the most effective methods for protecting against virus infections (Kinobe et al., 2022). Recently, the severe acute respiratory syndrome coronavirus type 2 (SARS-CoV-2) virus pandemic broke the vaccine research and development record as numerous vaccines were developed for the fight against this virus. The vaccines are known to provide sufficient protection against severe disease and death. However, there are drawbacks, as with many other RNA viruses (Yang et al., 2023). Picornaviruses cause significant diseases, yet only a few vaccines are available due to many challenges, which will be discussed. Current human-related vaccines against HAV, PV, and EV-A71 are approved for use by the public. Additionally, an animal-related vaccine against FMDV is also approved. Briefly, the most used commercial FMD vaccines are inactivated monovalent, bivalent or multivalent vaccines. The main drawback is that since FMDV contains numerous serotypes, the vaccine must also incorporate these several serotypes. Furthermore, the vaccines need to be temperature controlled as FMDV is heat sensitive. Lastly, these vaccines were found not to prevent primary infection resulting in a high possibility that more than 50 % of vaccinated animals will become carriers (Hardham et al., 2020).

HAV infection is highly contagious and is one of the foremost causes of acute viral hepatitis globally. Effective and safe vaccines have been accessible since the 1990s. Nevertheless, epidemic outbreaks still occur in various parts of the world (Migueres et al., 2021). Two types of HAV vaccines are available, including eight formaldehyde-inactivated vaccines commonly used in most countries and two live attenuated vaccines (LAV) commercialised and used in China (WHO, 2019). The LAVs are a single-dose subcutaneous injection that is generated by decreasing the virulence of the virus until it is harmless but still retains its antigenicity and ability to replicate (Wang et al., 2007). The benefit of this type of vaccine is that it elicits long-lasting immunity with both humoral and cellular immune responses without booster shots. The main disadvantage of LAVs is the safety concern, as the live virus has the ability to revert back to the virulent strain. Thus, the genetic stability of the vaccine needs to be guaranteed before its clinical use (Zhao et al., 2000). Another drawback is that the LAVs should not be administered to immunocompromised individuals (Faridi et al., 2009). In contrast, viral replication cannot occur with inactivated vaccines and is considered safer. However, the challenge with formaldehyde-inactivated vaccines is that

they require two doses instead of one for a significant cellular and humoral response (Jiang et al., 2008). It has been reported that a 60- 80 % decrease in T-cell and B-cell responses after 24 weeks post-HAV vaccination is reversed with a booster shot, resulting in an increase in humoral and cellular immunity (Shen et al., 2008; Cui et al., 2014).

PV contains three types, 1, 2 and 3, responsible for the disabling disease known as polio. The WHO held a meeting in 1988 intending to eradicate polio globally through vaccination. The generation of two different types of polio vaccines is considered one of the most significant medical breakthroughs of the 20th century (WHO, 2023). Wild PV types 2 and 3 have been confirmed to be eradicated globally, whereas type 1 is endemic to Afghanistan and Pakistan. Incidences of paralytic poliomyelitis are predominantly caused by rare cases of vaccine-associated paralytic poliomyelitis (VAPP) or recently due to circulating vaccine-derived polioviruses (cVDPV) (Erdem et al., 2023). There are two types of vaccines, including a live attenuated oral polio vaccine (OPV) and a killed or inactivated polio vaccine (IPV). Firstly, the OPV vaccine is composed of live strains of all three types that are weakened with a low possibility of spreading to the central nervous system (CNS). This type of vaccine is known to generate antibodies in the bloodstream against all three types, known as a humoral response, whereby it will inhibit the spread to the CNS in the event of infection with the wild type. Additionally, antibodies are produced in the mucous lining of the intestines, which are the site for PV replication (Bandyopadhyay et al., 2015). A significant challenge in administering OPVs is that, in rare cases, VAPP can occur where the vaccine strains revert back to their neurovirulent properties. This can lead to the transmission and infection of the paralytic disease (Bigouette et al., 2021). Secondly, IPVs are created by inactivating the wild-type PV strains with formalin. Typically, three doses are administered however, a booster dose is often required for an adequate immune response. It has been reported that the level of intestinal mucosal immunity is significantly lower compared to the OPV resulting in most countries administering the live vaccine. Another drawback is that substantial quantities of the virus are required to produce the IPV, leading to increased production costs and safety risks where the live virus is handled (Hampton et al., 2016).

EV-A71 is the causative agent of HFMD, creating a global threat. Several vaccine development methods have been published, including but not limited to the LAV, subunit vaccine, DNA vaccine, and mucosal vaccine (Lin et al., 2019; Li et al., 2021). However, recently three inactivated

whole virus vaccines against EV-A71 have completed clinical trials, have been approved and are commercially available in China with a recommendation by WHO that one of them could be used globally (Lei et al., 2020; Li et al., 2021). Inactivated vaccines are considered safe as they do not replicate. Additionally, the EV-A71 vaccines were shown to induce high levels of immunogenicity and neutralisation titres, with the efficacy of the three vaccines ranging between 90 % - 97 % (Li et al., 2021). Although the vaccines are effective, there are several drawbacks. These include the insufficient level of cellular immunity required for long-term protection as the virus is inactivated and does not replicate. Furthermore, a study showed that even though the vaccines induced neutralisation against other genotypes, it was found that the EV-A71 vaccines could not protect against other strains responsible for HFMD outbreaks, such as CV-A16 and CV-A10 (Lim and Poh, 2019).

Another limitation in developing these vaccines is the conformational instability of virus particles as they are heat sensitive. The maintenance of antigenicity will depend on the stability of the viral capsid, as unstable capsids result in different antigenic conformations. Thus, to preserve antigenicity and efficacy, the vaccines need to be refrigerated at 2 - 8 ºC, which may not always be achievable in developing countries with limited infrastructure (Wang et al., 2013). Due to several challenges as mentioned, only a few vaccines are available against picornaviruses. This has led to a focus on alternative strategies to control these viruses, such as antiviral compounds.

1.5.2 Control using antivirals

Due to vaccine limitations, a wealth of information and intensive research has been placed into developing and identifying antiviral agents against significant RNA viruses. For example, the Food and Drug Administration (FDA) has approved drugs against influenza, such as amantadine, oseltamivir, zanamivir, peramivir, laninamivir and baloxavir marboxil (Świerczyńska et al., 2022); SARS-CoV-2 such as remdesivir (Chera and Tanca, 2022) and dozens of drugs against HIV such as AZT, Maraviroc and Raltegravir (Adamson and Freed, 2009). In contrast, currently, there are no commercially available antivirals against picornaviruses. There are many limitations in vaccine development, as discussed above. Therefore, more attention and research are being conducted on anti-picornavirus drug identification. A range of compounds have been recognised to target picornaviruses; however, none have been approved for clinical use (van der Linden et al., 2015). As previously discussed, the infectious cycle of picornaviruses begins with binding to the host cell

receptor and ends with mature virions being released. Each stage of the lifecycle represents a potential target for antiviral compounds, either by targeting viral proteins directly or host factors involved in the virus life cycle. A summary of the significant picornavirus antiviral compounds that have been published are discussed below.

1.5.2.1 Direct-acting antivirals (DAAs)

Direct-acting antivirals are compounds that target the virus or its proteins. This has been the classical strategy to combat viral infections with the advantage of limited side effects (Baggen et al., 2018). However, the main drawback of this approach is that the virus is more likely to develop resistance against the drug. Nevertheless, there have been numerous compounds that have been identified to target specific viral proteins. EVs are the most extensively studied picornavirus genus; thus, there is more research on EV antiviral compounds.

1.5.2.1.1 Attachment inhibitors

The first step in the picornavirus life cycle is attaching to the host cell via the receptor. Several attachment inhibitors have been reported for EVs. Three compounds, pleconaril, BTA798 and pocapavir, have been shown to bind to the EV receptor binding site and prevent viral attachment to the host receptor (**Table 1.2; Figure 1.5**). Pleconaril was shown to exhibit broad-spectrum activity against the majority of EVs (Hayden et al., 2002; Hayden et al., 2003; Egorova et al., 2020); however, it was rejected by the FDA for treatment of the common cold due to safety concerns and adverse side effects (Senior, 2002). Since pleconaril only binds to the canyon in the capsid, it cannot be used to inhibit viruses such as HPeVs, which have a shallower canyon (Jackson et al., 2000). BTA798, also called vapendavir is still being tested in asthma patients that have been infected with RV. A clinical phase IIb trial was performed by Biota and reported substantial decreases in cold-like symptoms in asthmatic patients. Another phase IIb trial will be carried out to confirm these results (Biota, 2015). Pocapavir is another compound that binds to the EV capsid and was initially developed to use against PV infections; however, there has been a case where pocapavir treated neonatal enteroviral sepsis caused by CV-B3 (Torres-torres et al., 2015). Capsid binders or attachment inhibitors have the disadvantage of the virus developing resistance, making it difficult for these compounds to reach commercialisation. Additionally, they are genus-specific due to differences in the receptor binding site across the family (Jackson et al., 2000).

Table 1.2 Overview of selected inhibitors of the picornavirus life cycle

Group	Compounds	Viral target	Mechanism or Target
Direct-acting antivirals			
Attachment inhibitors	Pleconaril, BTA798, pocapavir, pirodavir	Broad spectrum EVs, RVs	Capsid binders
Translation and polyprotein inhibitors	Peptide conjugated phosphodiamidate morpholino oligomers (PPMO), Quinacrine, kaempferol, amantadine	PV1, CV-B2, RV-14, EV-A71	IRES – preventing ribosome attachment
	Rupintrivir, AG7404, fisetin, rutin	Broad spectrum RVs and EVs	$3C_{pro}$
Replication inhibitors	Nucleoside analogues-Ribavarin, NITD008, gemcitabine	Broad spectrum anti-picornaviral	$3D_{pol}$
	Non-nucleoside analogue-Amiloride	CV-B3	$3D_{pol}$
	Dibucaine, fluoxetine, pirlindole	EV-A71, CV-B3, EV-D68, EV-B, EV-D	2C
	Dipyridamole	PV, cardioviruses	RNA synthesis
Host-targeting antivirals			
Replication inhibitors	Enviroxime, GW5074, BF738735	Broad spectrum anti-picornaviral	P14KB
	Itraconazole, OSW-1, 25-hydroxycholestrol	Broad spectrum EVs, cardioviruses, HAV	OSBP
Assembly inhibitors	Geldanamycin, 17-AAG	Broad spectrum antiviral	Hsp90
	Buthionine sulfoximine, TP219	Broad spectrum antiviral	Glutathione

1.5.2.1.2 Translation and polyprotein inhibitors

As discussed above, picornavirus translation is initiated in a cap-independent mechanism using the IRES region on the genome. Without the initiation of translation, the ORF cannot be translated into proteins, resulting in the halting of the virus's life cycle. This makes the IRES a suitable drug target. Peptide-conjugated phosphodiamidate morpholino oligomers (PPMO) are ss-DNA like anti-sense agents, whereby a study demonstrated that it targets the IRES region, preventing ribosome attachment (**Table 1.2; Figure 1.5**). This study produced encouraging results illustrating the inhibition of PV1, CV-B2 and RV type 14 (Stone et al., 2008). Numerous compounds that inhibit EV-A71 translation by targeting the IRES site have been identified. For example, the compound quinacrine hinders the interaction between the IRES and polypyrimidine-tract-binding protein (PTB) (Wang et al., 2013). Kaempferol, which is a flavonoid, disrupts IRES activity by modifying the IRES trans-acting factors (ITAFs) (Tsai et al., 2011). Lastly, amantadine, a tricyclic amine, also prevents translation initiation of EV-A71 via the IRES (Chen et al., 2008).

Once the polyprotein has been translated, numerous polyprotein processing events occur, as mentioned previously. Therefore, many antiviral targets are created, such as protease inhibitors. The 3C protease ($3C_{pro}$) is a chymotrypsin-like cysteine proteinase that is accountable for the bulk of polyprotein processing and is present in all picornaviruses. Thus, the majority of research has been towards the identification of $3C_{pro}$ inhibitors. The proteases 2A of RV and EV and L of FMDV are only responsible for one cleavage event on their polyprotein. Hence, research has been minimal on drugs that target $2A_{pro}$ and $L_{pro.}$ (Neubauer et al., 2009). The $3C_{pro}$ inhibitor rupintrivir is one of few protease inhibitors that have made it to clinical studies. Rupintrivir is an irreversible peptidomimetic with an α, β-unsaturated ester. This compound imitates the protease substrate inhibiting the $3C_{pro}$. Studies have shown that this drug displays broad-spectrum *in vitro* antiviral activity against various RV serotypes and related picornaviruses (Patrick et al., 2005). However, clinical trials have been halted due to its poor oral bioavailability and inability to decrease disease severity against natural RV infections (Patrick et al., 2005). A recent study described the combination of rupintrivir and pleconaril showing a synergistic effect against EV-1 infections and suggested that it should be further investigated in clinical trials (Ianevski et al., 2022). Furthermore, rupintrivir analogues were developed, such as AG7404, which offered better oral bioavailability, exhibited antiviral *in vitro* activity, and was safe to use *in vivo* against CV-B3

(Dragovich et al., 2003; Kankam et al., 2021). Other $3C_{pro}$ inhibitors, such as the flavonoids fisetin and rutin, have been identified to inhibit picornaviruses such as EV-A71 (Lin et al., 2012).

1.5.2.1.3 Replication inhibitors

Once the translation of the initial viral proteins has taken place, replication of the genome can occur. A potential replication target is the RNA-dependant-RNA polymerase $3D_{pol}$, as this enzyme is crucial in the replication process. Polymerase inhibitors are divided into two categories: nucleoside analogues and non-nucleoside analogues. Nucleoside analogues resemble endogenous nucleosides, and the integration of these nucleosides by $3D_{pol}$ will result in chain termination or erroneous incorporation of nucleosides which could lead to high mutation rates (Crotty et al., 2000). An example of a compound is ribavirin, a synthetic purine analogue with broad-spectrum antiviral activity (**Table 1.2; Figure 1.5**). Studies have shown that it displays lethal activity against RNA viruses such as PV as it is highly mutagenic and forces the virus into 'error catastrophe' or the lethal accumulation of mutations within the nascent genome (Crotty et al., 2002). Gemcitabine is another nucleoside analogue that has been shown to display broad-spectrum inhibitory effects against EVs such as CV-B3 and EV-A71. A study was conducted whereby the authors proposed that gemcitabine causes mutations by being integrated into the RNA and that it directly binds to $3D_{pol}$, disrupting nucleotide incorporation (Kang et al., 2015). Recently, the nucleoside analogue 2'-C-methylcytidine was identified as an *in vitro* replication inhibitor of HPeV1 and HPeV3 targeting $3D_{pol}$ and established a foundation for further HPeV studies to be performed (Lanko et al., 2019).

The second class of polymerase inhibitors, known as non-nucleoside analogues, have diverse mechanisms of action. An example is the compound amiloride which enhances the error rate of $3D_{pol}$. A study was carried out that described the molecular mechanism against CV-B3. Amiloride inhibited $3D_{pol}$ of CV-B3 by competing with incoming nucleoside triphosphates and Mg^{2+} whereby, preventing VPg uridylylation and RNA elongation (Gazina et al., 2011). GPC-N114 is also a non-nucleoside analogue shown to exhibit broad-spectrum activity against EVs through the RNA-binding channel of $3D_{pol}$ (van der Linden et al., 2015). $3D_{pol}$ inhibition studies have been performed *in vitro*; however, no clinical trials have been conducted. Additionally, dipyridamole (DIP) was tested in this study, which will be further discussed in chapter 4. DIP is described as a

modified purine known to be an antiplatelet drug. However, antiviral activity was reported against a broad spectrum of viruses, such as PVs and cardioviruses, making it a suitable drug to test against TMEV GDVII (Tonew and Dzeguze, 1977; Fata-Hartley and Palmenberg, 2005).

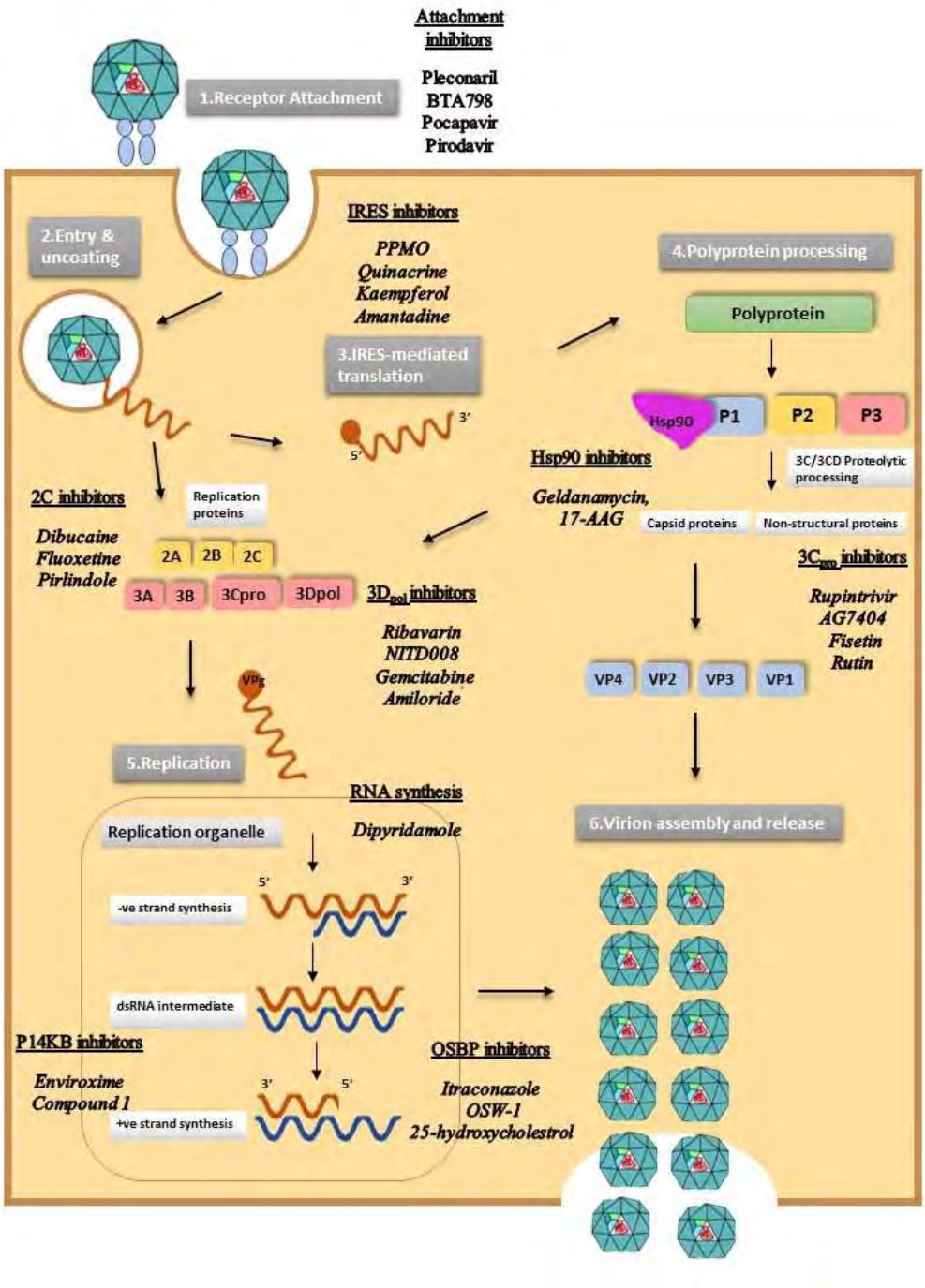

Figure 1.5 Schematic overview of selected inhibitors of the picornavirus lifecycle. The infectious cycle of picornaviruses initiates with host cell receptor attachment (1) and ends in mature virions exiting the cell (6). Theoretically, each stage of this virus lifecycle can be inhibited by antivirals. A few examples of compounds that have been published are listed.

1.5.2.2 Host-targeting agents

The most prevalent approach in antiviral research is directed towards inhibitors of viral proteins; however, there are high risks of the virus developing resistance to these compounds. Therefore, an alternative strategy targeting host factors involved in the replication cycle has emerged. The advantage of this approach is that it minimises viral resistance and could offer broad-spectrum activity against different viruses (Mahajan et al., 2021). Several compounds that target host factors involved in the picornavirus life cycle have been published.

For example, the lipid phosphatidylinositol 4-kinase type IIIB (P14KB) is a potential drug target as this host factor is essential in forming the RO in replication initiation. The compound enviroxime was identified as a P14KB inhibitor (**Table 1.2; Figure 1.5)** (van der Linden et al., 2015). However, the unsatisfactory *in vivo* efficacy in clinical trials and side effects prevented further research on enviroxime (Lamarche et al., 2012). Another crucial host factor in RO formation is oxysterol-binding protein (OSBP) which is responsible for cholesterol transport into the RO. The compound itraconazole (ITZ) is a well-studied, FDA-approved drug with anti-fungal and anti-cancer properties. Studies have identified ITZ as a broad-spectrum EV, cardiovirus, and Hepatitis C virus inhibitor. ITZ binds to the OSBP or OSBP-related protein 4 whereby it disrupts the shuttling of cholesterol into the RO (Strating et al., 2015; Shim et al., 2016; Lee et al., 2017; Bauer et al., 2018; Rhoden et al., 2018; Lanko et al., 2019). This significantly prevents RNA replication, and further research is needed for clinical development. This drug was tested as a potential control inhibitor of TMEV GDVII and will be further discussed in chapter 4.

The final step in the picornavirus life cycle is assembling and releasing the virion. A critical host factor that is involved in the assembly of the capsid is the Hsp90 chaperone. Hsp90 ensures that the P1 domain is correctly folded such that it can be successfully cleaved by $3CD_{pro}$ into the capsid proteins (Geller et al., 2007; Mutsvunguma et al., 2011). Geldanamycin or its analogue 17-allyamino-17-demethoxygeldanamycin (17-AAG) are compounds that have been shown to target Hsp90 and prevent the P1 precursor from being processed. An *in vivo* study was conducted

whereby SCARB2-transgenic mice were infected with C2, C4 and B4 genotypes of EV-A71. Geldanamycin and 17-AAG were also administered, and the results showed that the inhibitors displayed similar antiviral activity, protecting the mice from infection (Tsou et al., 2013). Thus, targeting Hsp90 is another possible therapeutic approach.

1.5.3 Resistance and toxicity

Over the last decade, numerous antivirals against picornaviruses have been discovered and tested *in vitro*. Despite the abundance of information published, little success has been accomplished as no commercialised drugs against any picornavirus exist. The main reasons for this are the high mutation rates of RNA viruses leading to resistance and toxicity of host-targeting agents. Other challenges include the shortage of broad-spectrum antivirals that could be used across the family and the difficulty of replicating results from *in vitro* studies to *in vivo* studies (Tammaro et al., 2023). RNA viruses are known to mutate rapidly, leading to antiviral resistance against drugs that directly target viral proteins (Ruiz and Russell, 2012). RNA viruses, including picornaviruses, present extraordinary abilities to adapt to new environments (Glanville and Johnston, 2015). This is because the replication process is error-prone, meaning incorrect nucleotides are inserted into the RNA copies by the RNA polymerase (Castro et al., 2005). Furthermore, picornaviruses do not possess a proofreading mechanism. Consequently, many of these mutations are maintained in the nascent genomes resulting in a heterogeneous population of viruses termed quasi-species. Quasi-species is a term that describes a population of closely related genomes in which they constantly undergo the process of genetic variation, selection, and competition resulting in a continuous evolution of the virus (Domingo et al., 2014). As such, it increases the heterogeneity and number of serotypes of each virus, making it extremely difficult not only for effective antiviral identification but also for vaccine development. For example, RVs have over 100 serotypes making it problematic when identifying those that establish disease for vaccine design (Papi and Contoli, 2011; Glanville and Johnston, 2015). It has also been reported that resistant mutations in EV-A71 have been identified against nearly all DAA *in vitro*, creating the concern that EV-A71 antivirals might rapidly develop resistance when commercialised (Wang et al., 2022). Additionally, capsid binders are the most advanced type of antiviral against picornaviruses in clinical trials. Unfortunately, resistant strains have appeared, limiting further development (Tammaro et al., 2023).

The rise in resistance has made host-targeting agents a more attractive strategy to focus on. However, several drawbacks are introduced when cellular components in the host are targeted, as this could lead to toxicity or adverse side effects. A high safety profile is required when testing drugs in clinical trials. For example, another reason that the clinical trials of the capsid binders against EV-A71 and RVs were halted was because of severe side effects. Vapendavir caused headaches, and pleconaril resulted in menstrual irregularities in females consuming an oral contraceptive (Hayden et al., 2003). Even though host-targeting agents display broad-spectrum activity across the family and other families, toxicity levels are demonstrated when transitioning to testing in human cells. For example, P14KB inhibitors were identified against HCV and were not found to be toxic to primary fibroblast cell lines. On the contrary, when tested in bone marrow cells and lymphocytes, it inhibited proliferation directly (Lamarache et al., 2012). Therefore, the antiproliferative function prohibits using P14KB as a target in HCV infection. Additionally, the strong responses to bone marrow proliferation would affect the prevention of transplant rejection (Lamarache et al., 2012).

1.6 Drug discovery and antiviral assays

Drug discovery research is a wide-ranging process through which new drugs are developed or identified. Essential factors to consider in drug discovery include developing therapeutically safe and non-toxic drugs that are efficacious against diseases of concern. Drug development is a complex process which can take approximately 12 – 15 years to reach commercialisation costing an average of $1 billion (Hughes et al., 2011). Generally, the process is divided into early drug discovery, pre-clinical phase, clinical phase and regulatory or FDA approval. The antiviral industry has evolved immensely throughout the last decade however, the consistent challenge of resistance and toxicity to the host cell, as described above, has hampered successful drug discovery, especially against picornaviruses. Therefore, the prediction of toxicity in humans by utilising *in vitro* cell-based assays has become an increasingly attractive method (Green et al., 2008) and will be focused on. The primary step in determining the efficacy of possible antivirals is to develop simple yet economical methods to evaluate whether the target is inhibited or not. Modern drug discovery consists of two approaches: phenotypic drug discovery, also known as classical pharmacology, and target-based drug discovery, also called reverse pharmacology (Zheng et al.,

2013). Different types of antiviral cell-based assays within these categories are also described below.

1.6.1 Target-based and phenotypic drug discovery

Target-based drug discovery is initiated with target identification in disease, typically discovered by doing basic research involving clinical observations of patient phenotypes or animal models (Zheng et al., 2013). For instance, a gene that codes for a protein associated with causing disease is identified, followed by assay development targeting that gene. Finally, compounds are screened to identify hits against the target (Lage et al., 2018). For the past two decades, target-based screening has been the leading technique in drug discovery; however, it does pose some limitations, such as restricting the identification of a new mechanism of action for the drug. Additionally, assays can only be developed once the molecular target is known and may be less biologically worthy (Arrowsmith, 2011).

As such, phenotypic drug discovery has gained more interest and will be focused on more in this study. This approach does not require the identification of the protein target or mechanism causing disease. Instead, it takes advantage of distinguishing traits of a disease, such as cytopathic effects (CPE), to develop an assay that can screen large compound libraries and identify hits that alter the disease phenotype (Zheng et al., 2013). CPE refer to infected cells which display degenerative changes in the monolayer. These changes can range from shrinking to clustering or even lysis of the monolayer (Agol, 2012). In a viral context, phenotypic screening examines the effect of all molecules in a viral replication cycle, which can unlock novel mechanisms of host-pathogen interaction. Another advantage is that both viral and cellular targets can be identified, broadening the spectrum of antiviral contenders.

1.6.2 Virus-specific antiviral assays

1.6.2.1 Reporter viruses/cell assays

Reporter probes are used to monitor viral replication directly, either by a reporter virus or a reporter cell assay. A reporter virus assay utilises a reporter gene that is introduced into a non-essential section of the genome in a live virus. Therefore, the reporter gene will also be expressed when the virus undergoes replication (Zuck et al., 2004). On the other hand, a reporter cell assay inserts the

reporter gene into the host cell, which is then activated when infected with the virus. Consequently, when drugs inhibit viral replication, the expression and activity of the reporter protein are also halted, indicating whether a drug possesses antiviral activity (Cao et al., 2005). A disadvantage of this system is that the decrease in signal endpoint can result in many false positives caused by certain molecules in the cell disrupting reporter activity resulting in performing additional counter screens simultaneously (Westby et al., 2005). An example of a newly synthesised reporter virus is a Senecavirus A picornavirus carrying a foreign reporter gene (SVA GD05/2017) that expresses green fluorescent protein (GFP), red fluorescent protein (RFP) or NanoLuc luciferase (Nluc). This reporter virus has the potential to screen for inhibitors against this virus (Wang et al., 2021).

1.6.2.2 Viral replicon assays

Reporter viruses utilise live viruses, creating a safety risk as these microorganisms cause severe diseases. Thus, they can only be cultured under high containment levels, which increases the cost and reduces the efficiency of the assay (Green et al., 2008). To overcome this problem, viral replicons can be used. Replicons are recombinant RNA molecules that comprise an in-frame deletion of the capsid protein region, resulting in RNA retaining its ability to replicate without generating infectious progeny virions (Hannemann, 2020). The advantages of replicons are that they can replicate efficiently in cultured cells, allowing quick high-throughput screening of potential replication, transcription and translation inhibitors (Xiong et al., 2017). The drawbacks of this technique are similar to those encountered with reporter viruses. Since luminescent and fluorescent probes are also inserted into replicons such as GFP and RFP, as mentioned above, hit compounds are characterised through a reduction of luminescent or fluorescent signal. This also introduces the disadvantage of loss-of-signal endpoints and requires counter screens such as cytotoxicity assays to remove any false positives (Emerson et al., 2004). An example worth mentioning is the hepatitis C virus (HCV) replicon. HCV only requires the expression of non-structural proteins NS2-NS5B to replicate efficiently in cell culture (Lohmann et al., 1999). Therefore, other proteins were replaced with a neomycin resistance cassette and expression of the non-structural proteins was driven by the EMCV IRES site, creating a bicistronic HCV replicon. This replicon initiated the development of first-generation DAAs boceprevir and telaprevir, resulting in the treatment and curing of patients infected with HCV (Kwong et al., 2011; Venkatraman, 2012).

1.6.3 Cytotoxic and cell viability CPE-based assays

Cytopathic viral effects on the host cell can be assessed with cytotoxic or viability assays that are used for screening potential drugs against the CPE-inducing virus. CPE-based assays are well recognised and are based on infected cells displaying virus-induced degenerative changes. These assays offer several advantages, such as achieving a high throughput when luminescent and fluorescent assays are performed on a microplate reader. This allows numerous libraries of compounds to be screened efficiently without being time-consuming. Additionally, CPE viability assays rely on a gain-of-signal compared to the loss-of-signal mentioned above. A gain-of-signal decreases the number of false positives in a high-throughput screen (HTS) during the early testing stages (Green et al., 2008). Since CPE assays allow potential inhibitors that can disrupt one of many stages in the viral life cycle to be examined, it results in additional costs when identifying the mechanism of action of hit compounds. Another drawback is that infectious virus particles are used, whereby the safety risk is enhanced, and further costs need to be employed for containment facilities. Numerous cytotoxic and viability assays exist to measure the percentage of viable cells in a population. However, four assays characterised according to their measurement endpoints will be described below (Aslanturk, 2018).

1.6.3.1 Dye exclusion

One of the simplest methods is the dye exclusion assay, whereby viable cells exclude the dyes, and dead cells take up the dyes (Yip and Auersperg, 1972). Trypan blue dye is commonly used as it is a negatively charged molecule. Therefore, the principle is based on viable cells with intact and strong cell membranes, excluding the dye, whereas dead cells cannot (Strober, 2001). The viability of cells is visually observed and measured under a microscope as viable cells retain their clear cytoplasm, and dead cells possess a blue cytoplasm (Johnston, 2010). The benefits of this method are that it is simple, quick as non-viable cells become blue within seconds, cost-effective, and a good measure of membrane integrity (Stone et al., 2009). Several disadvantages include the use of a haemocytometer to count cells. This introduces counting errors caused by inadequate dispersion of cells, cells lost during mixing, and incorrect chamber filling. In addition, trypan blue fails to distinguish healthy cells from cells losing functions as it is not sufficiently sensitive. Trypan blue can also be toxic to specific mammalian cells thus, dyes such as eosin, Congo red and erythrosine B can be alternatively used (Aslanturk, 2018).

1.6.3.2 Colourimetric assays

Colourimetric assays are based on the principle that biochemical markers are used to assess the metabolic activity of cells. Substances are used to generate a colour response in viable cells, allowing the quantification using a spectrophotometer (Präbst et al., 2017). An example is the tetrazolium compound 3-(4,5-dimethyl-2-yl)-5-(3-carboxymethoxyphenyl)-2-(4-sulfophenyl)-2H-tetrazolium, known as MTS. The MTS assay is a colourimetric method that can quantify the viability of cells. The principle is based on converting the tetrazolium salt into a coloured formazan dye in the mitochondria of viable cells. The quantity of formazan is proportional to the number of viable cells, which can be measured using a spectrophotometer at 492 nm (Berg et al., 1994; Tominaga et al., 1999). The advantage of MTS cytotoxicity assays is that they are sensitive, inexpensive, and provide a rapid signal of compound toxicity (Riss and Moravec, 1992). Several studies have been carried out using the MTS assay as an antiviral screen. A few examples include a rapid MTS assay that was developed for the detection of anti-HIV compounds (Pauwels et al., 1988), the identification of natural compounds with antiviral activity against SARS-associated coronavirus (Li et al., 2005), the development of a high through-put (HTP) screen for inhibitors against SARS-CoV (Severson et al., 2007) and antiviral activity of selected flavonoids against Chikungunya virus was investigated (Lani et al., 2016). Like any assay, MTS has a few drawbacks, including parameters such as incubation time, cell line and number affecting the absorbance levels. Therefore, these factors need to be optimised to yield a reliable assay (Rotter et al., 1993). Several other colourimetric assays include additional tetrazolium compounds such as, the MTT assay, the XTT assay, the WST-1 assay and the LDH assay, neutral red uptake assay and crystal violet assay (Aslanturk, 2018).

1.6.3.3 Luminometric assays

Luminometric assays are based on measuring luminescence signals with a microplate reader and are often convenient to use in HTSs. A common example is the adenosine triphosphate (ATP) assay. ATP is an essential energy reserve in cells used in several biological processes. This makes cellular ATP levels an attractive endpoint to measure cell viability (Duellman et al., 2015). The principal is based on the conversion of luciferin to oxyluciferin catalysed by the enzyme luciferase in the presence of ATP, yielding a luminescent signal. Therefore, the intensity of the signal is proportional to the ATP content representing viable cells. ATP viability assays are the most rapid

and sensitive and produce the least background noise. The signal is known to reach a stable glow within 10 minutes after addition, as there is no incubation step for the conversion to occur (Maehara et al., 1987). A drawback is that pipetting errors are exemplified due to the assay's high sensitivity (Aslanturk, 2018). Numerous antiviral studies have been reported on the use of ATP assays, such as the identification of antivirals against bluetongue virus (Li et al., 2009; Gu et al., 2013), the development of a HTS against dengue virus (Che et al., 2009) and influenza virus (Noah et al., 2007).

1.6.3.4 Fluorometric assays

The last category of viability assays that will be discussed is fluorometric assays. Fluorescence can be easily quantified using a fluorometer or a microplate reader and is often used in HTSs. Fluorometric assays are more beneficial compared to dye-exclusion and colourimetric assays as they offer more sensitivity (O'Brien et al., 2000). An example is the resazurin or Alamar blue assay. This technique involves the reduction of the non-fluorescent blue dye resazurin to a bright pink-fluorescent dye called resorufin and only occurs in the mitochondria of viable cells (Rampersad, 2012). The resazurin assay was selected as the most suitable assay format for the development of an *in vitro* assay to screen compounds for inhibition of TMEV GDVII-induced CPE. This is discussed in detail in chapter 3.

1.7 A biosafe picornavirus replication system using Theiler's murine encephalomyelitis virus (TMEV)

Specialised biosafety facilities are needed to study many highly infectious picornaviruses in humans and livestock. However, since picornaviruses share similar genome organisation and various lifecycle characteristics, a virus can be used which causes CPE in cell culture but is not infectious to humans handling it (Palmenberg, 1990). An example of a biosafe picornavirus is the Theiler's murine encephalomyelitis virus (TMEV), part of the genus cardiovirus (**Table 1.1**). Firstly, TMEV is known to cause neurological and intestinal infections in rodents and consists of two major subgroups described above (Oleszak et al., 2004). TMEV GDVII can infect BHK-21 cells, but it is not hazardous to human health. It can thus be used as a biosafe reference to study picornaviruses in conventional BSL 2 tissue culture facilities.

The Virus Research Group at Rhodes University has spent years developing a robust picornavirus replication system using the TMEV GDVII strain as a biosafe model. This virus has been optimised to readily infect BHK-21 cells, and infection at a high MOI results in full CPE of the cell monolayer after 8 hours. This system has been used to investigate several aspects of TMEV GDVII biology. Jauka et al. (2010) developed polyclonal antibodies against TMEV GDVII 2C protein, making it possible to proceed with techniques such as immunofluorescence and western blotting. Jauka et al. (2010) concluded that 2C, and therefore virus replication, is localised to the Golgi apparatus. Upfold et al. (2018) generated neutralising antibodies against the TMEV GDVII capsid that recognise the VP1 C-terminal of the capsid, thereby neutralising the infection by preventing the receptor's binding to the capsid. These studies have provided essential tools to detect TMEV GDVII infection by Western analysis or immunofluorescence.

1.8 Motivation

The *Picornaviridae* family cause a variety of harmful infections to both humans and animals. These diseases range from severe infections to mild illnesses and are a circulating global threat. Outbreaks of EV-A71, HPeV-A3 and the more recent PV outbreaks in the UK and FMDV in South Africa (Solomon et al., 2010; Pons-Salort et al., 2015; Orabi, 2022) have intensified the pressure to control these viruses. Currently, only three human-related vaccines against PV, HAV and EV-A71 and an animal-related vaccine against FMDV have been commercialised for public use. Vaccine development poses many limitations, especially for RNA viruses. Therefore, the substitute is to focus on drug discovery and antiviral compounds. A plethora of studies have been conducted, generating an immense amount of information regarding the inhibition of picornaviruses. However, none of these drugs is commercialised due to problems regarding resistance and toxicity. This amplifies the need for alternative strategies, such as screening novel compounds that have not been tested. Picornaviruses that are non-hazardous to humans can be used as a model virus, and TMEV GDVII was used in this study as the replication system was fortunately available. This presented an opportunity to develop a CPE-based resazurin assay to screen novel compounds against TMEV GDVII. Two libraries consisting of novel coumarin and quinoline compounds were acquired and were not tested on picornaviruses which created a knowledge gap and a possibility to screen them using a TMEV GDVII antiviral assay.

1.9 Aims, objectives and overview of chapters.

The overall aim of this study was to develop and optimise an antiviral screening assay using TMEV GDVII which infects BHK-21 cells in culture. The first objective aimed to validate the TMEV GDVII replication system that was required for developing the antiviral assay (chapter 2). Once the replication system was confirmed, the second objective was to identify the optimal parameters of a medium-throughput TMEV GDVII antiviral assay to produce one that was robust and reproducible (chapter 3). Subsequently, chapter 4 described the identification of a suitable control inhibitor against TMEV GDVII when screening compounds using the previously identified parameters of the assay. The final objective was to screen two libraries of compounds for antiviral activity using the optimised TMEV GDVII assay (chapter 5).

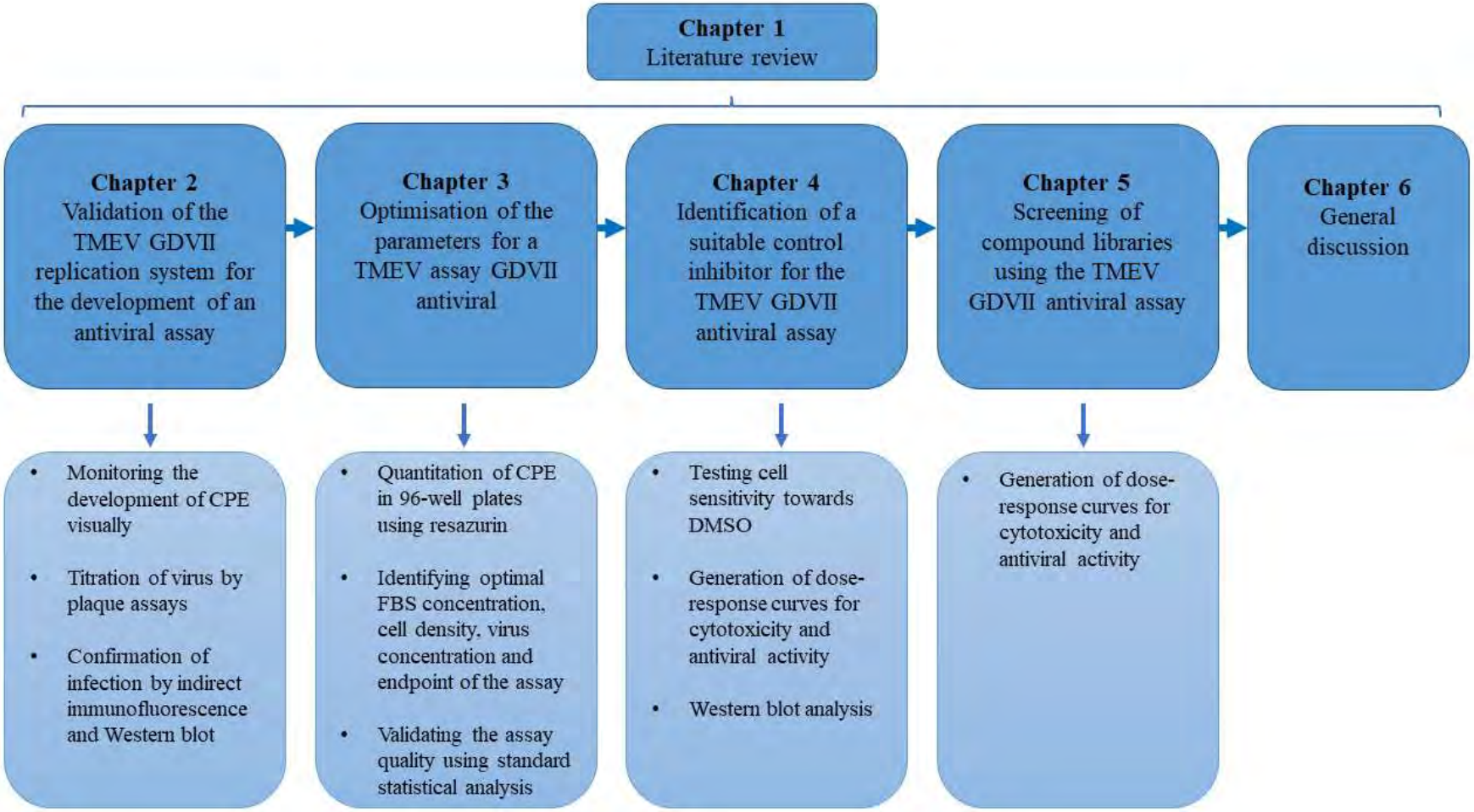
Chapter 1
Literature review
Chapter 2
Validation of the TMEV GDVII replication system for the development of an antiviral assay
Chapter 3
Optimisation of the parameters for a TMEV assay GDVII antiviral
Chapter 4
Identification of a suitable control inhibitor for the TMEV GDVII antiviral assay
Chapter 5
Screening of compound libraries using the TMEV GDVII antiviral assay
Chapter 6
General discussion
• Monitoring the development of CPE visually
• Titration of virus by plaque assays
• Confirmation of infection by indirect immunofluorescence and Western blot
• Quantitation of CPE in 96-well plates using resazurin
• Identifying optimal FBS concentration, cell density, virus concentration and endpoint of the assay
• Validating the assay quality using standard statistical analysis
• Testing cell sensitivity towards DMSO
• Generation of dose-response curves for cytotoxicity and antiviral activity
• Western blot analysis
• Generation of dose-response curves for cytotoxicity and antiviral activity

Chapter 2 Validation of the TMEV GDVII replication system for the development of an antiviral drug assay

2.1 Introduction

Before developing an antiviral assay, it was necessary to perform preparatory experiments to validate the TMEV GDVII replication system to be used. TMEV GDVII can infect BHK-21 cells and can be handled under conventional BSL-2 conditions as it does not pose a risk to human health. For this reason, it was chosen for the purpose of this study.

TMEV GDVII causes CPE in BHK-21 cells. CPE refers to infected cells which display degenerative changes in the monolayer. These changes can range from shrinking to clustering or even lysis of the monolayer (Agol, 2012). A CPE assay was performed in this chapter to monitor the onset and development of CPE in TMEV GDVII-infected cells compared to mock-infected cells at a high virus concentration. It was essential to confirm that cell death was caused by virus-induced CPE, not senescence, as the antiviral assay in the following chapters utilised a CPE-based antiviral assay for compound screening. Thus, this experiment allowed a further understanding of the virus's effects on the host cell.

Virus quantification assays are critical tools in virus research, and plaque assays remain a popular and gold standard method to quantify the concentration of infectious virus particles (Mendoza et al., 2020). The principle is based on individual virions infecting a cell, replicating then producing progeny infectious particles. These virions only infect closely surrounding cells as they are immobilised with an overlay such as methocel, generating a plaque or zone of clearance in the cell monolayer (Payne, 2017). Serial dilutions of the virus stock are made to attain a countable number of plaques in the monolayer. If there are too many infectious virions, individual cells will be infected with multiple virus particles resulting in individual plaques merging and clearing the monolayer. As the dilutions increase, plaques become more prominent and countable (Hu et al., 2022). Adapting the plaque assay in the TMEV GDVII replication system was important as accurate virus counts were required to calculate the multiplicity of infection (MOI). MOI refers to

the ratio of infectious virions to cells. For example, if 50 infectious particles are incubated with 50 cells, the MOI would be 1 (100/100 = 1). Optimising the MOI was critical in developing the TMEV GDVII antiviral assay, which is further discussed in chapter 3.

As mentioned in section **1.7**, the TMEV GDVII system has not only been used to investigate several aspects of TMEV GDVII biology but also to develop tools to detect virus replication and assembly. For example, Jauka et al. (2010) developed polyclonal antibodies against the TMEV 2C replication protein, and Upfold et al. (2018) generated neutralising antibodies against the TMEV GDVII capsid that recognised the VP1 C-terminal of the capsid. Therefore, it is possible to detect the expression of TMEV GDVII viral proteins by Western analysis or indirect immunofluorescence using both sets of antibodies, which will further confirm the infection of BHK-21 cells.

This chapter aimed to validate TMEV GDVII replication and perform preliminary experiments required for developing the antiviral assay. The specific objectives were to monitor the onset and development of CPE induced by TMEV GDVII infection; to culture and titrate TMEV GDVII stocks for the antiviral assay; and to confirm infection of cells by TMEV GDVII using immunological methods such as Western blot analysis indirect immunofluorescence.

2.2 Methods and materials

2.2.1 BHK-21 cell culture

2.2.1.1 Cell maintenance

Baby hamster kidney cells, strain 21 (BHK-21) (kindly provided by M. Ryan, University of St Andrews, UK) were cultured in a BSL-2 safety hood and maintained in complete media that consisted of Dulbecco's modified eagle medium (DMEM) (HyClone, USA) supplemented with 5 % [v/v] heat-inactivated foetal bovine serum (FBS) (Gibco, USA) and 1 % [v/v] mixture of antibiotics [100 U penicillin ml^{-1}, 10 mg streptomycin ml^{-1} and 25 µg Amphotericin B ml^{-1} (PSA)] (Gibco, USA), in 25 cm^2 vented flasks incubated at 37 °C with 5 % CO_2.

Once cells reached 70 - 80 % confluency, the medium was discarded, and cells were rinsed with pre-warmed phosphate-buffered saline (PBS) [137 mM NaCl, 2.7 mM KCl, 10 mM Na_2HPO_4 and

1.8 mM KH_2PO_4: pH 7.4]. Cells were overlayed with 2 ml pre-warmed trypsin (Lonza, USA) and incubated for 5 - 10 minutes (min). Trypsin was poured off as soon as the cells started to detach, and the flask was gently tapped to lift off all cells. Cells were resuspended in 5 ml complete medium and were seeded into 25 cm^2 flasks containing fresh complete media at a ratio between 1:3 and 1:10, dependent on when the cells were needed.

2.2.1.2 Cell cryopreservation

An 80 % confluent 25 cm^2 flask was subcultured into a 75 cm^2 flask, and once cells reached optimal confluency, they were trypsinised and resuspended in 4 ml complete media. Cells were collected by centrifugation at 300 x g for 3 min, and pellets were resuspended in 2 ml cryopreservation media [29 % DMEM, 60 % FBS, 10 % DMSO and 1 % PSA]. Resuspended cells were aliquoted into cryovials and stored at -80 °C or in liquid nitrogen.

2.2.1.3 Cell counting

Cell viability was tested by mixing an equal volume of trypan blue [0.4 % trypan blue and PBS] into an aliquot of trypsinised cells. Cells were counted using the Neubauer improved counting chamber and seeded in complete media at specific cell densities, depending on the experiment.

2.2.2 Preparation of TMEV GDVII viral stocks

TMEV strain GDVII (kindly provided by M. Ryan, University of St Andrews, UK) was used to infect BHK-21 cells in subsequent experiments. Confluent 75 cm^2 flasks were rinsed three times with pre-warmed PBS and infected with 500 µl of a TMEV GDVII stock diluted in serum-free DMEM. Infected cells were gently agitated at room temperature (RT) for 1 hour (h) to allow the virus to adsorb. Additional serum-free DMEM was added, and infected cells were incubated at 37 °C with 5 % CO_2. Following 24 h of incubation, infected cells were freeze-thawed three times, aspirated, and then centrifuged to remove cell debris. Supernatants were aliquoted into cryovials, and viral stocks were stored in 1 ml aliquots at -80 and titrated by plaque assay.

2.2.3 CPE assay

CPE was monitored by counting and seeding cells into a 6-well plate containing complete media at a density of 5.75 x 10^5 per well. Following 24 h or once cells reached 80 % confluency,

monolayers were rinsed twice with pre-warmed PBS. Cells were infected with 1 ml of TMEV GDVII virus stock, and control cells were mock-infected with serum-free DMEM containing no virus. The plate was gently agitated for 1 h at RT to allow virus adsorption before aspirating virus inoculum and rinsing with PBS. 1.5 ml of serum-free DMEM was added to each well and incubated for 7 h at 37 °C with 5 % CO_2. Microscopic images were captured between 0 - 8 hours post-infection (hpi) to monitor the development of CPE.

2.2.4 Titration of TMEV GDVII by plaque assay

A plaque assay determined the quantity or concentration of infectious virus particles as plaque forming units per ml (PFU/ml). Cells were counted and seeded into a 12-well plate containing complete media at a density of 1.75 x 10^5 per well. Following 24 h or until cells reached 80 % confluency, a 10-fold serial dilution of the TMEV GDVII stock was made in serum-free DMEM in a total volume of 1 ml. Cell monolayers were rinsed with pre-warmed PBS, followed by adding 0.25 ml of virus dilutions 10^{-3} – 10^{-7} into individual wells. Infected cells were gently agitated at RT for 1 h to allow virus adsorption. Virus inoculum was aspirated from each well without disturbing the monolayer and overlayed with 1.5 ml of methocel overlay solution [60 mM NaCl, 1.25 % methocel (Sigma-Aldrich, USA), ddH_2O and 50 % DMEM]. Infected cells were incubated at 37 °C with 5 % CO_2 for 48 h or until visible plaques (zones of clearance on monolayer) formed. The overlay solution was aspirated off the monolayers before rinsing the cells with pre-warmed PBS. Cells were fixed with 4 % paraformaldehyde solution for 15 min with gentle agitation before rinsing with PBS. The monolayers were stained overnight at RT with Coomassie solution [45 % methanol, 45 % ddH_2O, 10 % glacial acetic acid and 0.002 % [w/v] Coomassie Brilliant Blue R-250]. Stained cells were rinsed with PBS, and the number of plaques was counted for each dilution. Plaque assay was performed in triplicate, and virus titre was calculated in terms of PFU/ml using the formula:

$$\text{PFU per ml} = \frac{average\ no.of\ plaques}{dilution\ factor * volume\ plated}$$

2.2.5 Indirect immunofluorescence and microscopy

Cells were seeded and grown to 80 % confluency on ethanol-sterilised 13 mm coverslips in a 24-well plate containing complete media before being rinsed with pre-warmed PBS. Cells were

infected with 0.1 ml of TMEV GDVII virus stock diluted in serum-free DMEM at MOI of 25 per well. Control cells were mock-infected with serum-free DMEM. The plate was gently agitated at RT for 1 h before removing virus inoculum and rinsing with PBS. Cells were incubated in 0.15 ml serum-free DMEM for a further 4 h at 37 °C with 5 % CO_2. Virus inoculum was aspirated, and cells were rinsed with PBS before being fixed with 4 % paraformaldehyde for 15 min.

Following fixation, cells were rinsed three times with PBS and incubated with polyclonal rabbit primary antibodies against TMEV GDVII 2C (1:500) (Jauka et al., 2010) or anti-TMEV capsid antibodies (1:5000) (Upfold et al., 2018) diluted in 2 % BSA block buffer that contained permeabilisation buffer (PB) [10 % sucrose and 0.15 % Triton X-100 in PBS] for 2 h with gentle agitation at RT. Cells were washed three times with wash buffer [PBS containing 0.1 % Tween-20] for 15 min each before incubating with anti-rabbit Alexa Fluor 546 or 488 conjugated secondary (2 °) antibodies (Invitrogen, USA) (1:500) for 20 min. Cells were washed three times with wash buffer for 15 min each, followed by incubating the cells with 4′,6-diamino-2 phenylindole dihydrochloride (DAPI) (Sigma, USA) (0.8 µg/ml) for 15 min to stain the cell nuclei. Cells were washed twice with PBS before mounting the slides using Dako fluorescence medium (Dako Inc., USA). Images were captured using the EVOSTM FL Auto 2 Imaging System and microscope (Invitrogen, USA). Immunofluorescent experiments were performed in duplicate.

2.2.6 Preparation of TMEV GDVII-infected cell lysates

Cell lysates were produced for Western Blot analysis as described in section **2.2.3** however, cells were only incubated for 6 hpi before being rinsed with PBS, trypsinised and resuspended in serum-free DMEM. Pellets were collected by centrifugation at 1000 x g for 2 min and were resuspended in PBS. Cell lysates were stored at -20 °C for sodium dodecyl-sulfate polyacrylamide gel electrophoresis (SDS) and Western analysis.

2.2.7 SDS-PAGE

Samples for SDS-PAGE analysis were resuspended in 4 x SDS loading buffer [62.5 mM Tris-HCl (1 M stock, pH 6.8), 10 % glycerol, 0.02 % bromophenol blue, 0.5 % β-mercaptoethanol and 2 % SDS] and boiled at 95 °C for 5 min. Denatured samples were resolved on a 12 % polyacrylamide resolving gel [12 % [v/v] acrylamide/bisacrylamide (Sigma-Aldrich, USA), resolving gel buffer [37.5 mM Tris-HCl (1.5 M stock), (pH 8.8), 0.1 % [w/v] SDS, 0.1 % [w/v] ammonium persulphate

and 0.2 % TEMED] which were prepared using a Mini-Protean 3 gel casting system (Bio-Rad, USA). The gels were electrophoresed in 1 x SDS running buffer [25 mM Tris, 190 mM glycine and 0.1 % [w/v] SDS] at 100 V for 1.5 h. Protein molecular weights were estimated using the PageRuler™ Prestained Protein Ladder (10 - 170 kDa) (Thermo Scientific, USA). The gel was stained with Coomassie solution overnight at RT and destained in destain solution [40 % methanol, 10 % glacial acetic acid and 50 % ddH_2O] until protein bands were visible.

2.2.8 Western blot analysis

Samples were resolved by SDS-PAGE and transferred onto nitrocellulose membranes (Bio-Rad, USA) in ice-cold transfer buffer [25 mM Tris, 192 mM glycine, 20 % methanol and 70 % ddH_2O] at 100 V for 1 h. The membrane was stained with Ponceau [0.5 % [w/v] Ponceau and 1 % glacial acetic acid] for 1 min, then washed with ddH_2O to confirm protein transfer. Membranes were incubated overnight at 2 °C in 1 % block solution [1 % blocking reagent (B.M. Chemiluminescence western blotting kit (mouse/rabbit) (Roche, Germany) (cat. no. 11 520 709 001)) and Tris-buffered saline (TBS; 100 mM Tris, 300 mM NaCl)]. Followed by incubation in 0.5 % block solution that contained the polyclonal rabbit primary antibodies against TMEV GDVII 2C (1:200) (Jauka et al., 2010) or anti-TMEV capsid antibodies (1:2500) (Upfold et al., 2018) for 1 h at RT while shaking. Membranes were washed three times in Tris-buffered saline with Tween (TBS-T) [100 mM Tris, 300 mM NaCl and 0.1 % Tween-20] for 5 min each. Secondary anti-mouse/rabbit IgG-POD labelled antibodies (B.M. Chemiluminescence western blotting kit) diluted 1:20 000 µl in 0.5 % block solution were added to the membranes for 20 min while shaking at RT, followed by three wash steps in TBS-T for 10 min each. Membranes were then incubated for 1 min in a protein detection reagent (B.M. Chemiluminescence western blotting kit), and proteins were visualised using the ChemiDoc Molecular Imager XRS + (Bio-Rad, USA). Images were analysed using Image Lab™ software, version 5.1 (Bio-Rad, USA).

2.3 Results

2.3.1 Development of CPE in TMEV GDVII-infected cells

A CPE assay (**Figure 2.1**) was performed to visually monitor the development of CPE in TMEV GDVII-infected cells by infecting 80 % confluent monolayers with TMEV GDVII or with serum-free DMEM containing no virus (mock). The cells were incubated and monitored until full CPE

occurred. Images captured under the microscope illustrate that mock-infected monolayers remained fully confluent even after 8 hpi. In contrast, TMEV GDVII-infected cells presented the onset of CPE at 5 hpi, and by 8 hpi, the cells were all rounded, dead and had reached full CPE.

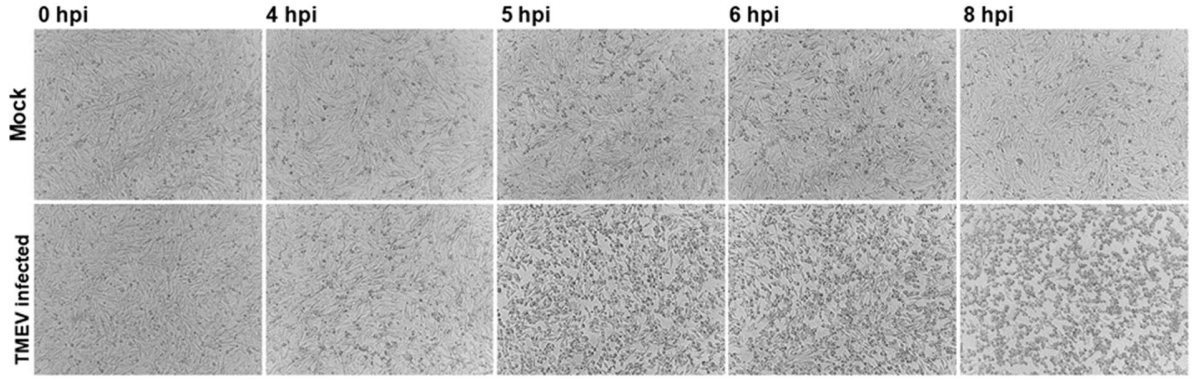

Figure 2.1 Development of CPE in TMEV GDVII-infected cells. CPE assay illustrating TMEV GDVII and mock-infected cells over 8 hpi. Full CPE was observed at 8 hpi in TMEV GDVII-infected cells, in contrast, mock-infected cells remained confluent.

2.3.2 Titration of TMEV by plaque assay

To perform a plaque assay, confluent cell monolayers were infected with TMEV GDVII at dilutions between 10^{-3} and 10^{-7}. Plaques were quantifiable at dilution $10^{-6,}$ which yielded a mean pfu/ml of 1.08 x 10^{8} (**Figure 2.2**) of the prepared virus stock. Dilutions 10^{-3} and 10^{-4} produced a clear monolayer, 10^{-5} resulted in too many plaques to count, and 10^{-7} remained a confluent monolayer with no plaques. In subsequent experiments, the virus titre in pfu/ml was used to determine the MOI.

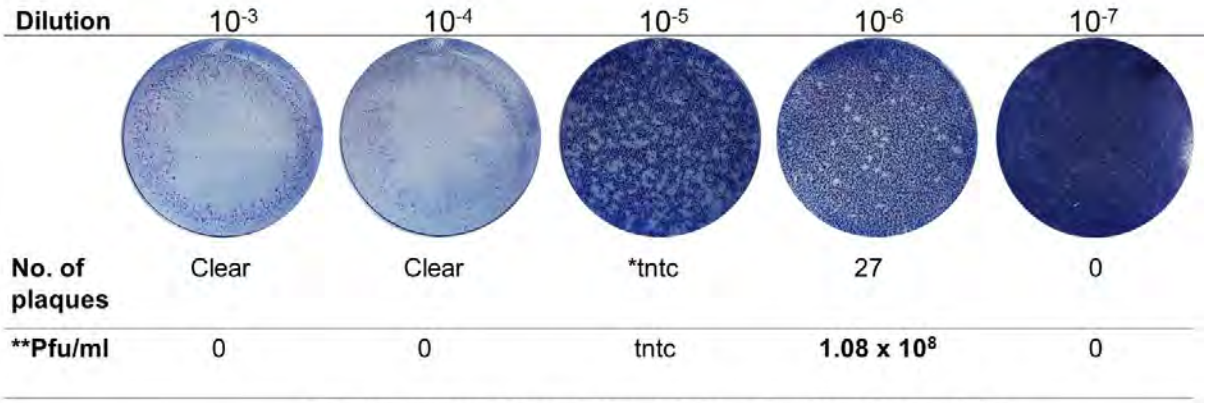

Figure 2.2 Titration of TMEV GDVII stock by plaque assay. BHK-21 cells grown to 80 % confluency were infected with 10-fold serial dilutions of a TMEV GDVII stock between 10^{-3} and 10^{-7}. Infected monolayers were overlayed with methocel and incubated for 48 h or until plaques formed. Cells were stained with Coomassie, and plaques were quantifiable at dilution 10^{-6}, yielding an average pfu/ml of 1.08 x 10^{8} of the TMEV GDVII stock. Values are the average of three independent experiments.

2.3.3 Detection of TMEV GDVII by indirect immunofluorescence and Western analysis

Infection of BHK-21 cells was confirmed using virus-specific antibodies by indirect immunofluorescence and Western analysis. The results are presented in **Figure 2.3.A and B**. No signal was detected in the control cells, including mock-infected cells and TMEV GDVII-infected cells probed with secondary antibody alone (**Figure 2.3.A panels B and F**). The anti-VP1 capsid antibodies generated a signal detecting TMEV GDVII VP1 capsid proteins in infected cells (**panels J and K**) with a cytoplasmic distribution but an increased concentration in the juxtanuclear region (**panel L**). Similarly, a signal was detected using anti-2C antibodies (**panels N and O**) with slight cytoplasmic staining and intense concentration in the perinuclear region (**panel P**).

Cell lysates were collected at 6 hpi for Western analysis. Polyclonal primary antibodies against TMEV GDVII capsid (1:2500) were used for detecting TMEV GDVII viral proteins. A single protein band of approximately 37 kDa was detected in TMEV GDVII-infected cells corresponding to the TMEV GDVII VP1 protein, and bands were absent in mock-infected cells (**Figure 2.3.B**). Similarly, antibodies against TMEV GDVII 2C (1:200) were used, and a band of approximately

37 kDa was also detected. Again, no protein bands were visible in the lysates of mock-infected cells.

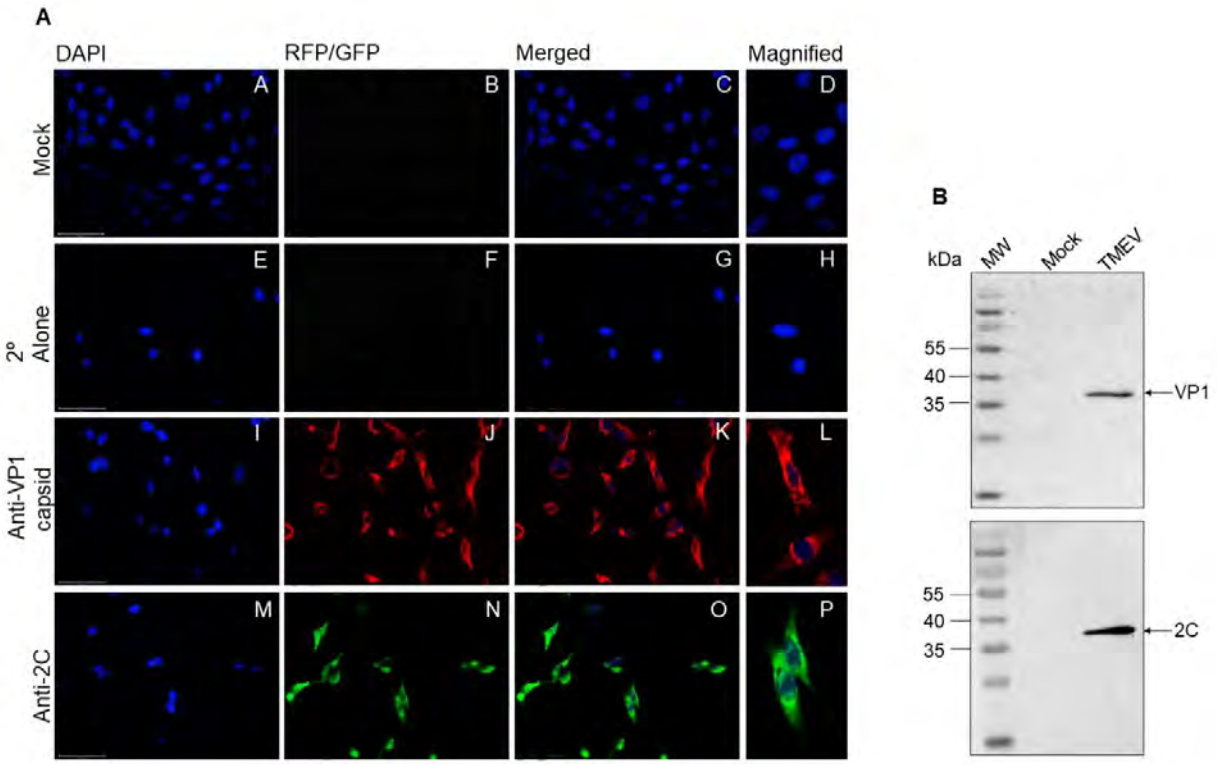

Figure 2.3 Detection of TMEV GDVII viral proteins. A) Cells were infected with TMEV GDVII (Panels E-P) or mock-infected (panels A-D) with serum-free DMEM and fixed with paraformaldehyde after 5 hpi. Cells were stained with primary antibodies against TMEV GDVII 2C (1:500) (Panels M-P) or anti-TMEV GDVII capsid VP1 antibodies (1:5000) (Panels A-D; I-L). Primary antibodies were probed using species-specific Alexa Fluor 546 (RFP) or 488 (GFP) conjugated secondary antibodies. DAPI was used to stain cell nuclei. Scale bars = 50 µM. B) Western analysis of 6 h TMEV GDVII-infected and mock-infected cell lysates. Polyclonal primary antibodies against TMEV GDVII 2C (1:200) and capsid VP1 (1:2500) were also used to detect TMEV GDVII. MW (molecular weight marker in kDa).

2.4 Discussion

This chapter aimed to validate the TMEV GDVII replication system in BHK-21 cells by monitoring CPE, determining the infectious viral titre, and detecting viral proteins using indirect immunofluorescence and Western analysis. These preliminary experiments were necessary for the development of the antiviral assay in subsequent chapters.

A CPE assay was performed to distinguish mock from TMEV GDVII infected monolayers visually and to monitor the development of CPE in infected cells. Mock-infected cells remained confluent and displayed the typical BHK-21 fibroblast morphology even after 8 hpi. In comparison, TMEV GDVII-infected monolayers started exhibiting signs of CPE at 5 hpi accompanied by cell detachment, rounding-up and clumping by 8 hpi. This result confirmed that the observed changes in cell morphology were caused by TMEV GDVII infection and not cell senescence. It was also noted that the onset and development of CPE within 8 hpi was consistent with studies by Upfold et al. (2018) and Upfold, (2019).

The next experiment was to perform plaque assays to quantify the concentration of infectious virus particles in the TMEV GDVII stock. This was necessary to calculate the MOI, which is an important parameter to optimise when developing an antiviral assay and will be further discussed in chapter 3. It should be noted that the $TCID_{50}$ was not used to calculate the MOI as plaque assays were previously optimised in this replication system, which was validated in this chapter. Plaque assays are also considered to be more accurate than $TCID_{50}$ assays. Plaques were prominent and countable at dilution 10^{-6} and were averaged from three independent experiments yielding a pfu/ml of 1.08×10^{8}. These results are consistent with those reported in previous studies where plaque assays to titre TMEV GDVII stocks were performed (Jauka et al., 2010; Mutsvunguma et al., 2011).

Previously generated polyclonal primary antibodies against the TMEV GDVII capsid VP1 and 2C protein were utilised as tools to detect the presence of TMEV GDVII and confirm that it was responsible for the infection of BHK-21 cells. Mock-infected cells and cells probed with secondary antibodies alone were used as controls and generated no signal as expected. However, capsid VP1 proteins were detected after 5 hpi in TMEV GDVII-infected cells and had similar cytoplasmic distribution with increased concentration in juxtanuclear regions as in previous experiments (Ross et al., 2016; Upfold et al., 2018). Furthermore, 2C proteins were detected in TMEV GDVII-infected cells and accumulated in the perinuclear region after 5 hpi. Jauka et al. (2010) described similar results and concluded that 2C localises to the Golgi apparatus at later stages of infection. Cell lysates collected from the CPE assay after 6 hpi and analysed using Western blots produced protein bands detected using anti-capsid VP1 and anti-2C primary antibodies in TMEV GDVII-infected cells but were absent in mock-infected cells confirming that it was a viral protein. 37 kDa

protein bands were consistent with the size of the VP1 capsid and 2C proteins reported previously (Upfold et al., 2018; Jauka et al., 2010, respectively). The detection of the expression of viral proteins VP1 and 2C using indirect immunofluorescence and Western analysis in TMEV GDVII-infected cells confirms that TMEV GDVII was present and caused CPE.

In conclusion, the CPE assay visually confirmed virus infection of BHK-21 cells. Secondly, plaque assays accurately quantified infectious virus particles. Finally, indirect immunofluorescence and Western experiments detected TMEV GDVII viral proteins confirming infection. Therefore, the replication system was used in subsequent experiments to develop the antiviral assay.

Chapter 3 Optimisation of the parameters for the TMEV GDVII resazurin antiviral assay

3.1 Introduction

The ability to develop and run robust, sensitive, and reproducible assays is critical for antiviral drug discovery. Typically, there are two drug screening approaches, including target-based or phenotypic screening, which was previously discussed. For this study, a phenotypic cell-based assay was developed to test compounds against TMEV GDVII. Phenotypic screening does not require the identification of a specific protein target or a complete understanding of the mechanism causing disease. Instead, distinctive traits of the disease are selected, and appropriate model systems, such as cell lines, are chosen to develop an assay that can screen compounds and identify those that alter the disease phenotype (Zheng et al., 2013). In the previous chapter, TMEV GDVII was shown to infect BHK-21 cells causing CPE and cell death. This confirmed the replication system and presented the opportunity to develop a CPE-based cell viability antiviral assay. CPE antiviral assays form part of the phenotypic approach, and compounds are assessed on their ability to inhibit virus-induced cell death by quantifying cell viability.

A range of assays exist to measure cell viability, but resazurin was selected as an indicator for the TMEV GDVII antiviral assay. Resazurin (7-hydroxy-10-oxidophenoxazin-10-ium-3-one) acts as an electron acceptor in the electron transport chain, and it is believed that NADPH dehydrogenase is responsible for the transfer of electrons from NADPH to resazurin which is reduced to resorufin. This reduction assay is both colourimetric and fluorometric as resazurin is a non-fluorescent blue dye that is reduced to bright pink, highly fluorescent resorufin in the mitochondria of metabolically active cells. Viable cells continuously reduce the dye, thereby increasing the levels of fluorescent resorufin and the pink colour of the cell culture medium (O'Brien et al., 2000). Thus, it is possible to observe the colour change visually and quantify the fluorescence using a microplate reader set to an excitation and emission wavelength of 560 nm and 590 nm, respectively (Aslanturk, 2018). Resazurin has been used for the detection of microbial contamination in food products over the last 70 years (O'Brien et al., 2000; Travnickova et al., 2019) but has gained interest in drug

discovery against microbial pathogens in the last 20 years, with it being one of the most highly referenced reagents used for viability and cytotoxic assays (Rampersad, 2012). These assays have not only been developed to screen compounds against bacteria such as Mycobacterium (Taneja and Tyagi, 2007; Webster et al., 2010); parasites such as Trypanosoma brucei (Sykes and Avery, 2009); fungi such as Aspergillus fumigatus (Monteiro et al., 2012); cancer cell lines (Uzunoglu et al., 2010) but also against numerous viruses. Several publications describe the use of resazurin in cytotoxic and CPE inhibition assays against but not limited to Zika virus (Rausch et al., 2017; Zhu et al., 2019; Pettke et al., 2020); Chikungunya virus (Cruz et al., 2013; Archila et al., 2022); SARS-CoV-2 virus (Tietjen et al., 2020; Uemura et al., 2021) and FMDV (Willems et al., 2011). Resazurin possesses various advantages over other metabolic indicators, such as MTS, including the low cost of the reagent, and the short incubation period, which is usually 1 - 4 hours, depending on the assay parameters. It can be used in numerous cell models as it is non-toxic, non-radioactive and involves no cell lysis, as resorufin diffuses outside cells after being formed, making it possible for post-measurement assays and continuous observation of cells. Resazurin reduction can be measured qualitatively as a colour change to pink but also quantitively as colourimetric absorbance readings or fluorometric fluorescence readings (Page et al., 1993; O'Brien et al., 2000). Fluorescence readings have higher sensitivity and were chosen as the detection method in the TMEV GDVII assay. Another benefit of resazurin is that it is water soluble and easily permeable through cell membranes resulting in an assay with no extra wash or incubation steps. As with any assay, resazurin has disadvantages as a viability indicator. Firstly, it is photosensitive, and handling or incubations should be carried out in the dark. The optimum pH and temperature are between 7-7.4 and 37 °C, respectively, meaning that the culture medium should have a buffering capacity and plates should be incubated at this specific temperature. Another drawback of the reduction resazurin assay is the bleaching or quenching of the pink colour caused by the production of the colourless product dihydroresorufin (Erb and Ehlers, 1950; Goegan et al., 1995). This usually occurs after extended incubation times, which is an essential consideration when designing these assays. The suitability of the parameters used in the assay, such as incubation times, cell density, and negative and positive controls, should be optimised to produce a resazurin assay that does not result in false positives or artefact signals (O'Brien et al., 2000).

The parameters focused on in this chapter include FBS concentration, cell density, virus concentration and the endpoint of the assay. BHK-21 cells were readily susceptible to infection

with TMEV GDVII, which induced pronounced CPE at high virus concentrations, as shown in the previous chapter. Developing a medium-throughput screen (MTS) for antiviral testing against TMEV GDVII requires the quantitation of CPE in a 96-well plate or larger to allow multiple compounds to be tested. The approach chosen to measure viral-induced CPE was based on determining cell viability by quantifying resazurin reduction to the highly fluorescent resorufin in viable and metabolically active cells. Once the quantification of CPE with resazurin was confirmed in a pilot assay, the parameters were optimised to produce a robust and reproducible assay.

FBS promotes rapid cell growth, and traditional cell culture media contains 5 % or higher concentrations (Li et al., 2009). In this study, 5 % FBS was used for maintenance and seeding; however, the risk of overgrowth could lead to over-confluent cell monolayers, which could affect assay sensitivity. Therefore, an FBS concentration that yields a confluent monolayer was essential at the end of the assay. Similarly, cell seeding density was also optimised to obtain high fluorescent signals without cell overgrowth. Monolayers should be confluent with cells in the exponential growth phase to prevent the possibility of false negatives or positives when screening compounds.

Additionally, identifying the optimal virus concentration in terms of MOI and the endpoint of the assay was critical in developing an accurate assay. A high infectious titre would be too potent for a compound to inhibit in cell culture, and a low concentration would not cause CPE, resulting in a false positive compound. Thus, the lowest possible MOI yielding full CPE (lowest cell viability) was identified at the end of the chosen incubation time. Selecting a low MOI to allow multiple viral replication cycles was important as it allowed the identification of compounds that can affect each stage of the life cycle. The optimal parameters were also determined and confirmed using standard assay statistics.

The main aim of this study was to develop a medium-throughput compound screening assay of high quality and preciseness. An acceptable assay generates a distinct difference between the positive and negative control without high variability. This is measured using metrics such as Signal/Background (S/B) ratios and Z'- factors (Zhang et al., 1999). These standard statistics were used to evaluate the TMEV GDVII assay as it effectively measures its overall performance, quality and robustness. The S/B ratio is a simple measure to compare the mean signal to the mean background and is beneficial in the initial stages of assay development. Unfortunately, this method

does not consider the variability of the controls. Instead, a different statistical analysis called the Z'- factor is used, which compares the variability of both controls to the difference in means. A Z' value between 0.5 - 1 suggests a statistically significant difference between the positive and negative control indicative of robust assay performance (Sui and Wu, 2007).

The overall aim of this chapter was to optimise the parameters of a medium-throughput TMEV GDVII antiviral assay to produce a sensitive, robust, and high-quality assay. The quantitation of CPE in 96-well plates was first confirmed, followed by identifying the optimal FBS concentration, cell density, virus concentration and endpoint of the assay. Once the suitable parameters were chosen, the assay quality was validated using standard statistical analysis.

3.2 Methods and materials

3.2.1 Cell culture and plating

BHK-21 cells were maintained as described in section **2.2.1**. For assay optimisation, cells were counted and then seeded in 96-well clear flat bottom plates (Sigma-Aldrich, USA) in 100 µl complete media [DMEM, 5 % [v/v] FBS, 1 % [v/v] PSA]. Cells were incubated for 24 h at 37 °C with 5 % CO_2.

3.2.2 Quantitation of CPE using resazurin

A pilot assay was conducted to determine whether or not viral-induced CPE in BHK-21 cells could be quantitated in 96-well plates with resazurin by seeding 7500 cells, as described in section **3.2.1**. Following the 24 h incubation, cells were infected with TMEV GDVII at a 10-fold dilution ranging from an MOI of 0.5 - 0.00005 in assay media [DMEM, 2 % [v/v] FBS and 1 % [v/v] PSA] in a total volume of 200 µl/well. Background controls included wells with only assay media (no cells), and cells were also mock-infected with only assay media (no virus) as a positive control. Infected cells were incubated for 72 h at 37 °C with 5 % CO_2. Cell viability was measured by adding 20 µl of resazurin (0.54 mM) (Sigma-Aldrich, USA) per well, followed by a 3 h incubation at 37 °C with 5 % CO_2. Fluorescence signals were detected using the Synergy MX microplate reader (BioTek Instrumentd, Inc) at excitation wavelength 560 nm and emission wavelength 590 nm. Microscopic images were also captured after 72 hpi using an inverted light microscope (10 X

magnification). Three independent experiments were performed with three technical replicates for each treatment in each plate.

3.2.3 Optimisation of FBS concentration

The optimal FBS concentration was determined by seeding cells, as described in section **3.2.1**. After the 24 h incubation, the media was replaced with fresh media containing varying concentrations of FBS ranging from 0 – 8 % in a total volume of 200 µl/well. Background controls included wells with only assay media (no cells). Cells were then incubated for 72 h at 37 °C with 5 % CO_2, and cell viability was measured by adding 20 µl of resazurin per well. Microscopic images were captured for each FBS concentration. The assay was performed in independent triplicates, with each plate containing four technical replicates per treatment.

3.2.4 Optimisation of cell density

The cell density was optimised by seeding cells in 5 % FBS at varying cell densities between 5000 - 35 000 cells/well, as described in section **3.2.1**. Following 24 h, the media was replaced with fresh assay media containing 2 % FBS in a total volume of 200 µl/well, and cells were incubated for a further 72 h at 37 °C with 5 % CO_2. Background controls included wells with only assay media (no cells). Cell viability was quantified by adding 20 µl/well resazurin. Furthermore, microscopic images were taken for each density after 72 hpi. Three independent experiments were performed, each including four technical replicates.

3.2.5 Optimisation of TMEV GDVII MOI and endpoint of the assay

The optimal MOI and endpoint of the assay were identified by seeding 15 000 cells/well in 5 96-well plates as described in section **3.2.1**. After the 24 h incubation, cells in all plates were identically infected with TMEV GDVII at a 2-fold dilution ranging from an MOI of 0.1 - 0.00039. The TMEV GDVII stock was first diluted in assay media, followed by a 2-fold serial dilution of the virus. The media was replaced with virus dilutions in a total volume of 200 µl/well. Background controls included wells with only assay media (no cells), and positive controls consisted of cells mock-infected with assay media (no virus). Cells were incubated at 37 °C with 5 % CO_2, and 20 µl/well of resazurin was added to a plate at varying hpi, including 10, 24, 34, 48

and 72 hpi. The assay was performed in three independent experiments, with each plate containing four technical replicates.

3.2.6 Validation of the parameters of the TMEV GDVII assay

15 000 cells/well were seeded as described in section **3.2.1**. Once the cells were incubated for 24 h, Rows 2-4 in a 96-well plate were infected with TMEV GDVII, diluted in 2 % FBS assay media, at an MOI of 0.00625. Rows 5-7 were mock-infected (no virus) with 2 % FBS assay media, and rows 8-10 included the background control with assay media only (no cells) in a total volume of 200 µl/well. The cells were incubated for 72 h at 37 °C with 5 % CO_2, followed by the addition of 20 µl/well of resazurin to measure cell viability. Microscopic images were captured, and two independent experiments were performed.

3.2.7 Data normalisation and statistical analysis

Fluorescence readouts were analysed in Microsoft Excel by subtracting the mean no-cell background control from all treatments. Fluorescence signals were either reported as relative fluorescence units (RFU) representing the mean ± SD fluorescence for each treatment or cell viability (%). The measured RFU values were normalised as cell viability (%) using the formula:

$$\text{Cell viability (\%)} = \left(\frac{RFU_{sample}}{\mu RFU_{mock}}\right) \times 100$$

where RFU_{sample} represents fluorescence values of each treatment and μRFU_{mock} represents the mean value of the mock-infected (no virus) positive control. Unpaired t-tests were performed where a p-value less than 0.05 was considered statistically significant. * p-value < 0.05, ** p-value < 0.005, *** p-value < 0.0005, **** p-value < 0.00005. Graphs were created and analysed using GraphPad Prism (version 9.4.1 for Windows 64-bit). Statistical validation of the TMEV GDVII assay was determined and calculated using S/B ratios, and Z'-factors using the following formulas:

$$\text{S/B} = \left(\frac{\mu RFU_{sample}}{\mu RFU_{NC\ control}}\right)$$

where μRFU_{sample} represents the mean fluorescence values of each treatment and μRFU_{NC} *control* represents the mean fluorescence of the no-cell background control.

$$\text{Z'-factor} = 1 - \left(\frac{(3\sigma_{mock}+3\sigma_{virus})}{(\mu_{mock}-\mu_{virus})}\right)$$

where μ_{mock}, μ_{virus}, σ_{mock}, and σ_{virus} represent the mean (μ) and standard deviations (σ) of the mock-infected positive control (*mock*) and virus only (*virus*) negative control.

3.3 Results

3.3.1 Quantitation of CPE induced by TMEV GDVII infection in BHK-21 cells

In order to establish whether viral-induced CPE in BHK-21 cells can be quantitated in 96-well plates with resazurin, cells were infected with TMEV GDVII at a 10-fold dilution starting with an MOI of 0.5, followed by detecting fluorescence signals using resazurin after a 72 h incubation. Cells were also mock-infected with assay media (no virus) as a positive control which was used to normalise RFU values to cell viability (%). **Figure 3.1.A** shows that cell viability decreases as MOI increases. TMEV GDVII infected cells were also compared to mock-infected cells and yielded decreases in cell viability (S/B) as MOI decreased (**Figure 3.1.B**) illustrating that cells infected at higher MOIs produced larger S/B ratios. Additionally, all virus-infected cells showed a significant difference compared to the mock ($P < 0.05$).

A

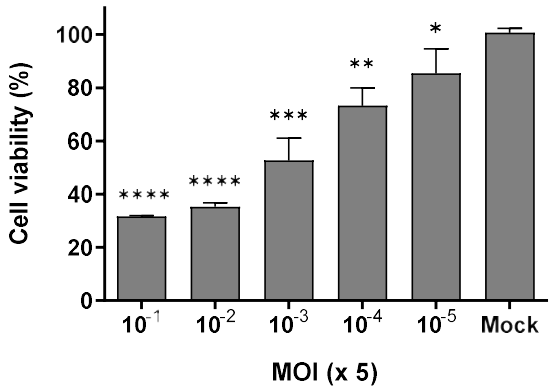

B

MOI (X 5)	10^{-1}	10^{-2}	10^{-3}	10^{-4}	10^{-5}
S/B	3.19	2.86	1.91	1.37	1.18

Figure 3.1 Quantitation of TMEV GDVII induced CPE in BHK-21 cells. 7500 cells/well were seeded in 96-well plates and incubated for 24 h at 37 °C before being infected with TMEV GDVII at a 10-fold

dilution. A) Fluorescence signals were detected after 72 hpi with resazurin, and data were normalised to the means of mock-infected cells and represented cell viability. Unpaired t-tests were performed whereby statistically significant values were represented as * ($P < 0.05$). Each data point represents the mean value ± SD of 3 replicates. B) S/B ratios were calculated for each MOI relative to the mock control. Three independent experiments were performed, and one representative experiment is presented.

A step-by-step approach is described below to identify the optimal assay conditions, including FBS concentration, seeding cell density, virus concentration and endpoint of the assay.

3.3.2 Optimisation of FBS concentration

The optimal FBS concentration that yields a confluent monolayer at the end of the assay was selected by replacing the media with fresh media containing varying concentrations of FBS between 0 - 8 %. After 72 hpi, fluorescence signals were measured using resazurin and expressed as relative fluorescence units (RFU). Cell viability is represented as these RFU values and **Figure 3.2.A** shows that viability increases as the FBS concentrations increase. A statistically significant difference is observed between no cells (NC) and 0 % FBS ($P < 0.05$). However, both treatments produced relatively lower signals than the rest of the concentrations. There was no significant difference between 4 % and 8 % FBS-treated cells, whereas 2 % FBS-treated cells showed a strong fluorescent signal with a significant difference between both 1 % and 4 % FBS-treated cells ($P < 0.05$). As the FBS concentrations increased, so did the S/B ratios, showing that 2 - 8 % FBS-treated cells yielded good S/B ratios greater than 5 (**Figure 3.2.B**). Microscopic images were captured at 72 hpi and illustrated that 0 % and 1 % FBS-treated cells produced a non-confluent cell monolayer (**Figure 3.2.C**), coinciding with the low RFU values and S/B ratios. Cells treated with 4 % and 8 % FBS started aggregating, which is a sign of overgrowth. Finally, the 2 % FBS-treated cells produced high fluorescent signals and a suitable S/B ratio of 9.96 but also resulted in evenly distributed confluent monolayers. As such, 2 % was chosen as the optimal FBS concentration in subsequent experiments.

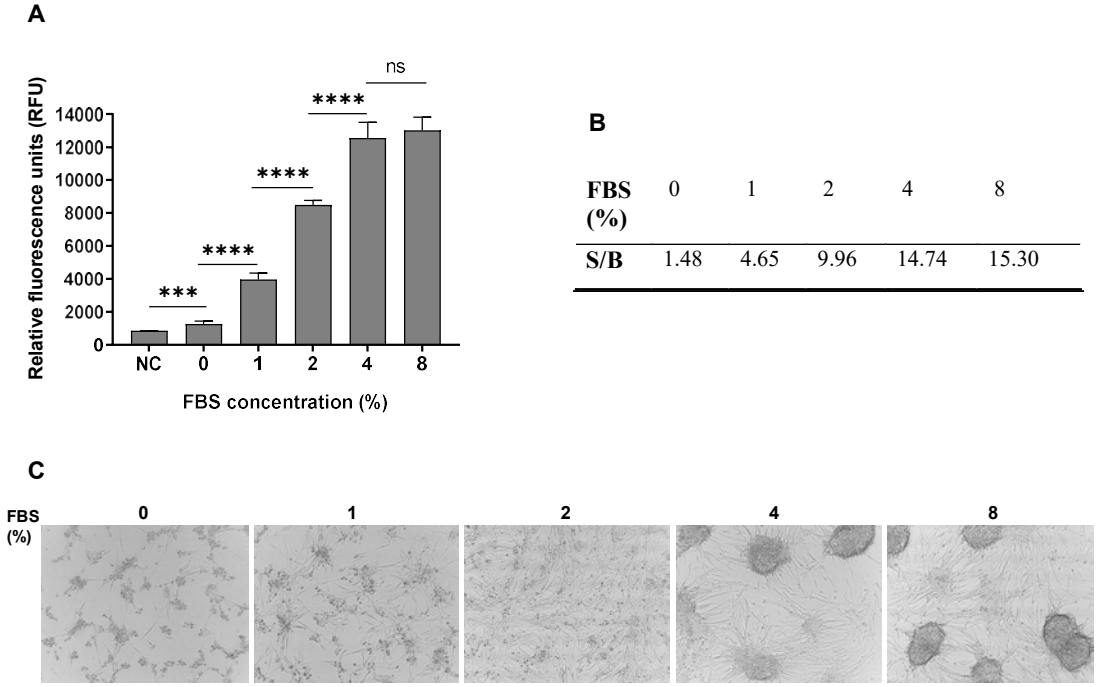

Figure 3.2 The effect of varying FBS concentrations on BHK-21 cells. 7500 cells/well were seeded in 96-well plates and incubated for 24 h at 37 °C before replacing media with fresh media containing varying FBS concentrations. A) Cell viability was expressed as relative fluorescence units which were detected after 72 hpi with resazurin. Unpaired t-tests were performed whereby statistically significant values were represented as * ($P < 0.05$). Each data point represents the average value of 4 replicates ± SD. B) S/B ratios were calculated for each FBS concentration, where the signal represented the mean value of each FBS concentration and background the mean value of the no-cell (NC) control. C) Microscopic images of cells treated with varying FBS concentrations were captured after 72 hpi. Independent experiments were performed in triplicate, with one representative experiment being presented.

3.3.3 Optimisation of seeding cell density

Cell seeding density in a 96-well plate was optimised to obtain high fluorescent signals without cell overgrowth by the end of the assay. Cells were seeded at varying cell densities between 5000 – 35 000 cells/well and were incubated for 24 h before replacing media with new assay media containing 2 % FBS, as chosen from the previous experiment. Cell viability was assessed by adding resazurin and detecting fluorescence readings after 72 hpi. **Figure 3.3.A** demonstrates that fluorescence intensity increased proportionally to cell density and produced S/B ratios greater than 5 from 10 000 cells and above (**Figure 3.3.B**). When observed under the microscope after 72 hpi,

5000 cells per well did not grow to a confluent monolayer, coinciding with low RFU values and S/B ratios, and cells started aggregating from densities of 20 000 onwards, even though they produced high RFU values (**Figure 3.3.C**). Lastly, not only did 15 000 cells/well grow to a confluent monolayer with no cell aggregation, but it also yielded high RFU values with an acceptable S/B ratio of 10.74. For these reasons, it was chosen as the optimal cell density.

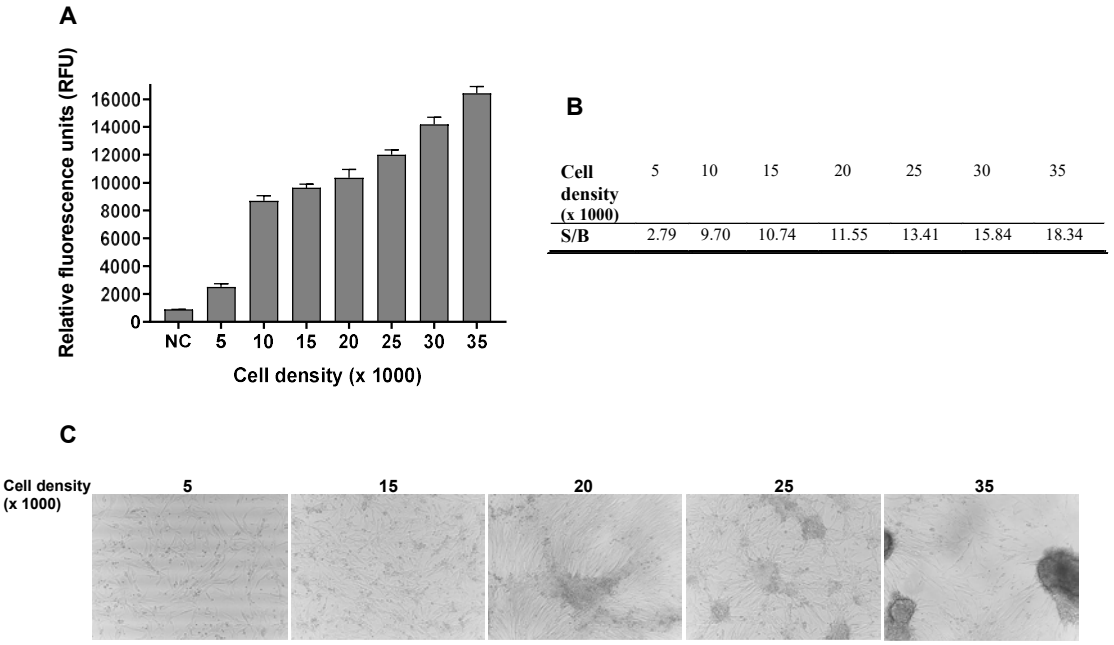

Figure 3.3 Optimisation of seeding cell density. BHK-21 cells were seeded in 96-well plates at varying densities and incubated for 24 h at 37 °C, followed by replacing media with fresh assay media containing 2 % FBS. A) Cell viability was expressed as relative fluorescence units (RFU) which were measured after 72 hpi with resazurin. Each data point represents the average value of 4 replicates ± SD. B) S/B ratios were calculated for each cell density, where the signal represented the mean value of each density and the background the mean value of the no-cell (NC) control. C) Microscopic images of cell monolayers at different densities were captured after 72 hpi. Independent experiments were performed in triplicate, and one representative experiment is presented.

3.3.4 Optimisation of TMEV GDVII MOI and endpoint of the assay

In order to identify the optimal virus concentration and endpoint of the assay, seeded cells were infected with TMEV GDVII at a 2-fold dilution series ranging from an MOI of 0.1 - 0.00039.

Background controls included wells with only assay media (no cells), and positive controls consisted of cells mock-infected with assay media (no virus). Cells were incubated for 10, 24, 34, 48 and 72 hpi after which resazurin was added to each plate. **Figure 3.4.A** illustrates that at 10 hpi, cell viability values were high at all MOIs, and Z'-factors were inadequate for an acceptable assay (**Figure 3.4.B**). Cell viability decreased for all MOIs except 0.00078 and 0.00039 as the incubation times became longer, between 24 - 48 hpi. However, 72 hpi yielded the lowest viability for MOIs between 0.1 - 0.00156 compared to the rest of the incubation times. Again, MOIs of 0.00078 and 0.00039 produced high viability signals after 72 hpi, which coincides with their unsuitable Z'-factors. Z'- factors ranging between 0.89 - 0.93 were calculated for MOIs 0.1 - 0.00156 after 72 hpi. Cells infected with an MOI of 0.00625 was the lowest MOI that yielded acceptable Z'-factors between 34 - 72 hpi with a score of 0.93 at 72 h. As such, 0.00625 and 72 h were chosen as the assay's optimal MOI and the endpoint as the Z'-factors were indicative of a robust assay.

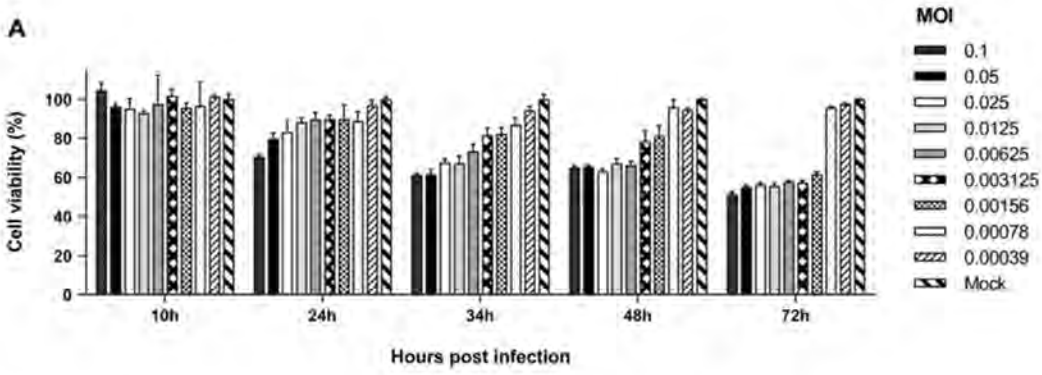

B

Z'-factors

	0.1	0.05	0.025	0.0125	0.00625	0.003125	0.00156	0.00078	0.00039
10h	5.44	-2.47	-3.99	-0.65	-19.21	12.93	-2.61	-12.52	9.32
24h	0.76	0.38	-0.24	0.20	-0.33	0.04	-1.48	-0.61	-2.43
34h	0.76	0.64	0.63	0.45	0.35	0.04	0.07	-0.37	-1.24
48h	0.89	0.90	0.85	0.76	0.81	0.24	0.13	-1.98	0.31
72h	0.91	0.93	0.91	0.89	0.93	0.92	0.90	0.42	0.29

Figure 3.4 Optimisation of TMEV GDVII MOI and endpoint. 15000 cells/well were seeded in 5 96-well plates and incubated for 24 h before infecting them with TMEV GDVII at a 2-fold dilution. A) Fluorescence signals were detected with resazurin at various time points, and data were normalised to the means of mock-infected cells and represented cell viability. Each data point represents the mean value ± SD of 4 replicates. B) Z'- factors were calculated for each MOI at varying times relative to the mock-

infected cells. Independent experiments were performed in triplicate, with one representative experiment shown.

3.3.5 Validation of the chosen parameters of the TMEV GDVII assay

In order to validate that the chosen parameters resulted in a robust, reproducible and reliable assay, 15 000 cells/well were seeded and incubated for 24 h at 37 °C, followed by infecting rows 2 - 4 with TMEV GDVII at an MOI of 0.00625 diluted in 2 % FBS assay media. Rows 5 - 7 of the plate were mock-infected with assay media (no virus), and finally, rows 8 - 10 of the plate consisted of the background control no-cells (media only). Plates were incubated for 72 h before the addition of resazurin. The experiment was repeated in independent duplicates. All replicate RFU values from both experiments are presented in **Figure 3.5.A**, demonstrating low variability between replicates and a Z'- factor of 0.74 between the mock positive control and virus-negative control. A statistically significant difference ($P < 0.05$) between the mean cell viabilities of mock and virus-infected cells is presented in **Figure 3.5.B**, which corresponds to images captured on the microscope illustrating confluent mock-infected monolayers and rounded-up cells exhibiting signs of full CPE in virus-infected cells.

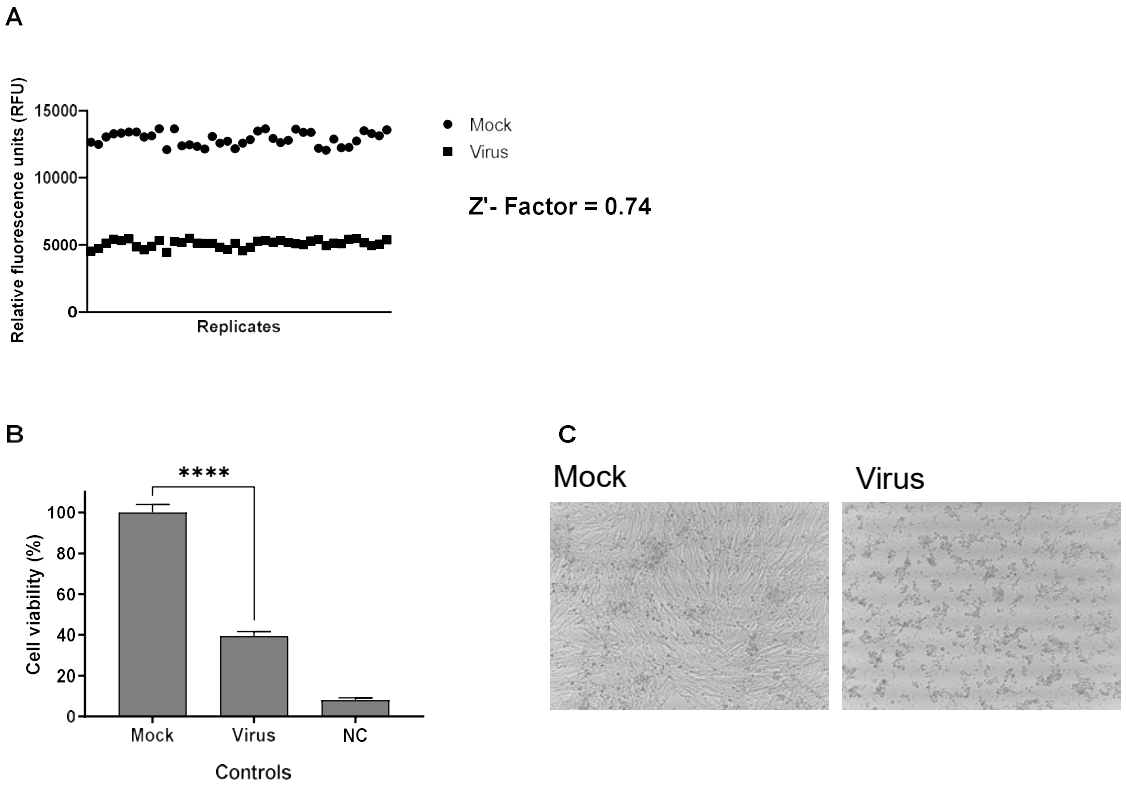

Figure 3.5 Validation of the parameters chosen in the TMEV GDVII assay. 15 000 cells/well were seeded and incubated for 24 h. The 96-well plate was divided into cells being infected with TMEV GDVII at an MOI of 0.00625, cells being mock-infected with assay media (no virus) and lastly, wells that only contained assay media (no cells). All media contained 2 % FBS and plates were incubated for 72 h. A) Fluorescence signals were detected using resazurin, and RFU values for each replicate were plotted. B) RFU values were normalised to the mean mock control to represent cell viability and unpaired t-tests were performed whereby statistically significant values were represented as * ($P < 0.05$). Each data point represents the average value of 40 replicates ± SD calculated from two independent experiments. C) Microscopic images were captured distinguishing mock-infected from virus-infected monolayers after 72 hpi.

3.4 Discussion

This chapter aimed to identify suitable parameters, including FBS concentration, cell density, virus concentration and the assay endpoint. Once optimal conditions were selected, the assay was validated using standard assay development statistics to confirm that the chosen parameters resulted in a clear difference between the positive and negative controls. CPE-based antiviral

assays are considered one of the most common and reliable assays for screening compounds. Therefore, this approach was taken when developing a TMEV GDVII resazurin-based antiviral assay. Numerous studies have reported the development of CPE-based assays against viruses such as influenza, SARS-CoV-2, arenavirus, bluetongue, dengue, yellow fever, EVs and HPeVs (Bolken et al., 2006; Noah et al., 2007; Severson et al., 2007; Gong et al., 2008; Severson et al., 2008; Li et al., 2009; Rhoden et al., 2015; Rhoden et al., 2018; Lanko et al., 2019; Zhang et al., 2019; Jeon et al., 2020).

The replication system that was confirmed in the previous chapter demonstrated that BHK-21 cells were susceptible to TMEV GDVII-induced CPE at high MOIs. This study aims to develop an assay that can screen numerous compounds with medium throughput. As such, it was essential to test whether viral-induced CPE could be quantitated in a 96-well plate using resazurin as a viability indicator in a preliminary experiment. Cell viability decreased as the virus concentration increased; similarly, S/B ratios relative to the mock-infected cells were reduced as virus concentration decreased, suggesting a correlation between CPE and fluorescent signals. This indicated that TMEV GDVII-induced CPE could be quantitated in BHK-21 cells using resazurin. Subsequently, the assay parameters were further optimised to produce a more robust assay.

FBS is the most commonly used supplement in cell culture media, typically at 5 - 15 % concentrations, as it promotes division and rapid cell growth (Baker, 2016). Most antiviral assays need longer incubation times to allow the virus to replicate multiple times, which creates the risk of cell overgrowth and over-confluent cell monolayers (Li et al., 2009). When varying concentrations of FBS were tested on BHK-21 cells, cell viability was shown to increase as the FBS concentration increased. Cells treated with 0 % and 1 % generated low viability and S/B values corresponding to the microscopic images showing non-confluent monolayers. Additionally, there was no significant difference between 4 % and 8 % FBS-treated cells suggesting that the viability of cells reached a plateau and cell growth was stunted. This concurred with the microscopic images illustrating over-confluent and aggregated cells concluding that these FBS concentrations were not suitable for the assay. Finally, cells treated with 2 % FBS yielded high viability readings, an S/B ratio of 9.96, and a confluent monolayer was observed under the microscope. Therefore, 2 % FBS was chosen as the optimal concentration in the assay media. Several studies have also used 2 % or less FBS when conducting cell-based antiviral activity assays

against RNA viruses, such as dengue (Che et al., 2009; Qing et al., 2010; Zou et al., 2011; Nobori et al., 2018; Sanaki et al., 2019; Uemura et al., 2021), zika (Han et al., 2018; Li et al., 2018), and SARS-CoV-2 (Jeon et al., 2020; Runfeng et al., 2020; Damme et al., 2021; Uemura et al., 2021). Most importantly, supplementation with a 2 % FBS concentration was used in numerous assays testing for viral inhibition against other picornaviruses, such as but not limited to EMCV, HAV, PV, EV-A71, EV-D68, CV-A24, CV-B3, and HPeV-1 (Debing et al., 2013; Rhoden et al., 2013; Strating et al., 2015; Smee et al., 2016; Hao et al., 2019; Zhang et al., 2019; Li et al., 2022). It has also been reported that some viruses replicate more efficiently at lower FBS concentrations, between 0 - 2 % and that viral replication is suppressed in host cells at higher concentrations above 10 % (Tobita et al., 1997; Tmizutani et al., 1999; Iki et al., 2005; Hossain et al., 2007 and Qin et al., 2013). It is speculated that FBS contains fetuin-like factors that inhibit virus replication by preventing virus attachment to the host cell (Hossain et al., 2007; Qin et al., 2013).

The next experiment optimised the seeding cell density to verify that the cells were not overgrown when the resazurin readings were measured. It was important that confluent monolayers were grown and that cells were still in the exponential log phase of growth to prevent false negatives from occurring when testing compounds for antiviral activity. The fluorescence intensity was shown to increase proportionally to cell density and did not reach a plateau. However, microscopic examination illustrated that seeding 5000 cells/well did not grow to a confluent monolayer, and cells seeded at 20 000 cells/well and above had become over-confluent after 72 hpi. Therefore, 15 000 cells/well was identified as the optimal density for the antiviral assay as the cells grew to a confluent monolayer with a high fluorescence reading and an S/B ratio of 10.74.

The endpoint of the assay for the initial experiments was 72 hpi which was chosen based on previous studies where similar experiments were carried out using other picornaviruses (Palma et al., 2007; Oberste et al., 2009 Strating et al., 2015; Smee et al., 2016; Zhang et al., 2019; Li et al., 2022). However, an MOI - time matrix experiment was conducted to confirm that 72 hpi was the optimal endpoint and to identify the most suitable virus concentration for the TMEV GDVII assay. Typically, virus concentration, in terms of MOI, is optimised to avoid the infection being too potent or weak for the compound to inhibit. When varying MOIs of TMEV GDVII were used to infect BHK-21 cells, all MOIs at 72 hpi yielded the lowest cell viability readings compared to the rest of the time points and confirmed that it was the most appropriate endpoint for the assay. The

exceptions were MOIs 0.00078 and 0.00039, generating high viability readings at all time points, meaning that these concentrations were too low to cause CPE in cells. Therefore, the optimal MOI was chosen based on the calculated Z'- factors. The lowest MOI that yielded consistently good scores with a Z'-factor greater than 0.5 of 0.93 at 72 hpi was 0.00625. For this reason, an MOI of 0.00625 and an endpoint of 72 hpi were decided as the optimal parameters.

Any assay developed should be reproducible and robust, especially if the purpose is to screen numerous compounds. Hence, the parameters chosen above for the TMEV GDVII assay were validated by performing the assay with multiple replicates on a plate (intra-plate) and independently repeating the experiment (inter-plate). An assay of high quality should have a distinctive difference between the positive control (mock-infected with assay media and no virus) and the negative control (infected with virus causing full CPE) with low variability. The TMEV GDVII assay produced a Z'- factor greater than 0.5 of 0.74, and a statistically significant difference ($P < 0.05$) is demonstrated between the two controls. Furthermore, microscopic images were captured, visually illustrating a clear difference between the monolayers. Mock-infected cells displayed the typical fibroblast morphology and were confluent, whereas virus-infected cells were all rounded and presented signs of full CPE. This further indicated that the assay was robust and reliable for compound screening.

In conclusion, the parameters chosen for the TMEV GDVII antiviral assay included adding 2 % FBS to the assay media, seeding the cells at a density of 15 000 cells/well, infecting the cells with TMEV GDVII at an MOI of 0.00625 and an endpoint of 72 hpi at which resazurin will be added. These parameters were optimal as they resulted in a significant difference between the mock-infected positive control and virus-infected negative control yielding an acceptable Z'- factor above 0.5. The next chapter involves utilising the TMEV GDVII antiviral assay to test potential control inhibitors for antiviral activity.

Chapter 4 Identification of a suitable control inhibitor for the TMEV GDVII antiviral assay

4.1 Introduction

When the screening of compounds is performed, a principal factor to consider is the selection and inclusion of experimental controls. The previous chapter optimised the mock and virus-alone non-biological controls to develop a robust and reproducible assay. However, a control drug that can potentially inhibit CPE in TMEV GDVII infected cells is also needed so that it can be compared to newly screened compounds. A known inhibitor can be used to identify hit compounds that exhibit a higher inhibitory effect than the control compound in terms of IC_{50} values, which will be further discussed below (Chai et al., 2015; Amanat et al., 2020). To date, no studies have been reported on a drug capable of inhibiting CPE induced by TMEV GDVII infection in cell culture. Nevertheless, optimising the parameters of the TMEV GDVII antiviral assay created an opportunity to test for potential inhibitors that could not only be used to screen other compounds but would also contribute to research on TMEV GDVII.

Since there are currently no approved antiviral therapies against picornaviruses, the repurposing of FDA-approved drugs that have succeeded in clinical trials is an emerging substitute for developing novel antivirals (Bauer et al., 2018). Itraconazole (ITZ) is a well-recognised triazole antifungal agent that has been repurposed and shown to exert anticancer and, more importantly, antiviral activity. It inhibits the CYP51 fungal enzyme, an essential catalyst in the sterol biosynthesis pathway, thus weakening the fungal cell membrane (Lestner and Hope, 2013). Additionally, drug-repurposing screens found that ITZ exhibits anticancer activity through the prevention of angiogenesis by inhibiting the functions of mTOR and vascular endothelial growth factor receptor (VEGFR2) (Kim et al., 2010; Xu et al., 2010; Nacev et al., 2011). More relevantly, previous studies have shown that ITZ possesses broad-spectrum antiviral activity against picornaviruses, including EVs, HPeVs, and cardioviruses (Gao et al., 2015; Strating et al., 2015; Shim et al., 2016; Lee et al., 2017; Bauer et al., 2018; Rhoden et al., 2018; Lanko et al., 2019). It has been reported to inhibit viral replication in a broad spectrum of EVs and cardioviruses by

targeting the oxysterol-binding protein (OSBP) (Strating et al., 2015). Picornaviruses are known to form membranous replication organelles (ROs) through virus-induced alterations of the secretory pathway membranes (Belov et al., 2012). The viral non-structural proteins 2BC and 3A are thought to be responsible for recruiting vital host proteins to the RO (Gao et al., 2015). For example, EVs recruit phosphatidylinositol 4-kinase type III β (PI4KB), whereas the cardiovirus EMCV uses a different isoform, PI4KA. These are Golgi-localised lipid kinases that generate phosphatidylinositol-4 phosphate (PI4P), which in turn recruits OSBP to ROs (Hsu et al., 2010; Dorobantu et al., 2015; Strating et al., 2015). OSBP functions to transport lipids at membrane contact sites (MCSs) which are defined as sites between two organelles that are in close proximity to each other, such as the ER and trans-Golgi apparatus (Mesmin et al., 2013). OSBP contains an OSBP-related domain (ORD) that attaches cholesterol and PI4P to its lipophilic pocket, thereby facilitating the shuttling of cholesterol from the ER to the Golgi apparatus. For viral RO formation, cholesterol is transported to the RO instead (Mesmin et al., 2013). A novel mechanism of action of ITZ has been reported against EVs and cardioviruses whereby the drug directly binds to OSBP, inhibiting cholesterol from being shuttled to the RO, thereby hindering the formation of ROs and viral replication (Strating et al., 2015). This suggested that ITZ had the potential to possess antiviral activity against TMEV GDVII, which is also a cardiovirus, and was selected as a possible control compound to use in the TMEV GDVII antiviral assay.

Dipyridamole (DIP) is a modified purine (Fata-Hartley and Palmenberg, 2005) that was first introduced in 1959 as a coronary vasodilator agent (Gibbs and Lip, 1998) and is known to be an orally administered antiplatelet drug. DIP reduces platelet aggregation by inhibiting platelet phosphodiesterase, resulting in cyclic adenosine monophosphate (cAMP) accumulation, thereby preventing platelet prostaglandin synthesis (Kim and Liao, 2008). Additionally, DIP elevates tissue adenosine levels by hindering its reuptake into cells and further increasing cAMP concentrations (Kim and Liao, 2008). However, the administration of DIP for coronary artery disease has become outdated as more modern antiplatelet drugs have emerged (Allahham et al., 2021). DIP has been repurposed and screened for antiviral activity whereby several studies have described broad-spectrum activity against viruses such as PV, RV, influenza virus A, herpes simplex virus, SARS-CoV-2 and HIV (Tonew and Dzeguze, 1977; Tonew et al., 1977; Oehring and Schmidt, 1978; Tonew et al., 1982; Szebeni et al., 1989; Tenser and Gaydos, 2001; Fata-Hartley and Palmenberg, 2005; Liu et al., 2020). More appropriately, DIP has been reported to

demonstrate effective inhibition of the cardiovirus EMCV in cell culture using the Krebs-2 system (Fata-Hartley and Palmenberg, 2005). This study confirmed that DIP did not affect viral translation and polyprotein processing. Instead, viral RNA synthesis was inhibited in an unknown reversible mechanism of action. DIP was shown to decrease the formation of both minus and positive-strand RNA when added at early stages in the replication cycle. Therefore, it was concluded that the drug disrupts a stage in the initiation of EMCV RNA synthesis (Fata-Hartley and Palmenberg, 2005). DIP was thus chosen as another potential control compound against TMEV GDVII for the antiviral assay.

As mentioned in chapter 2, neutralising polyclonal antibodies that recognise the 37 kDa VP1 protein were generated by Upfold et al. (2018). TMEV GDVII particles were utilised as an antigen for immunisation, resulting in the serum consisting of antibodies that specifically recognise the VP1 capsid protein (Upfold et al., 2018). The study also showed that the antibodies significantly reduced plaque formation, and the prevention of receptor binding was suggested to be the neutralisation mechanism. The anti-TMEV GDVII capsid antibodies recognised epitopes inside the VP1 C-terminal loop, which extends over a pit that is thought to be the receptor binding site in TMEV GDVII (Grant et al., 1992; Luo et al., 1992). Thus, the antibodies neutralise viral infection by preventing attachment and entry into the host cell (Upfold et al., 2018). These results created an opportunity to investigate whether the anti-TMEV GDVII capsid antibodies could also be used as an effective antiviral control for the screening assay.

Typically, compounds that are screened are first dissolved or stored in the organic solvent dimethyl sulfoxide (DMSO). ITZ, DIP and the compound libraries to be assayed in the next chapter were also solubilised in DMSO. However, high concentrations above 1 % are known to become toxic to cells (Tomeczkowski et al., 1993; Irvine et al., 1999). As such, before the antiviral effects of the compounds can be tested in the TMEV GDVII assay, it is important to investigate what concentrations of DMSO are toxic to BHK-21 cells. Once this is established, the antiviral efficacy of the potential inhibitors will be examined using a dose-response analysis. When a possible antiviral agent is identified, usually dose-response curves are generated by testing the compound at ten doses to reveal the range of cellular cytotoxicity and antiviral efficacy (Gu et al., 2013). Cytotoxicity is represented as 50 % cytotoxicity concentration (CC_{50}), i.e., the dose of a drug that exhibits 50 % cytotoxicity to cells between the minimum and maximum. Similarly, antiviral

efficacy is denoted by the 50 % inhibitory concentration (IC_{50}), which is the half-maximal inhibitory concentration of a drug that inhibits virus-induced CPE. These values are essential in selecting an effective antiviral inhibitor and are used to compare the potencies and toxicities of potential compounds that are screened (Hughes et al., 2011). Therefore, dose-response curves were generated for ITZ, DIP and the anti-TMEV GDVII capsid antibodies to determine and identify the most suitable inhibitor to use as a control in the TMEV GDVII assay.

The overall aim of this chapter was to select a suitable control inhibitor of TMEV GDVII that could be used to compare to when screening compounds for antiviral activity using the TMEV GDVII assay. Firstly, the sensitivity of the cells to DMSO was investigated, followed by the generation of dose-response curves to test for cytotoxicity and antiviral activity of ITZ, DIP and the anti-TMEV capsid antibodies. Lastly, the antiviral effects of the potential inhibitors were assessed using Western blot analysis.

4.2 Methods

4.2.1 Cell culture and plating

BHK-21 cells were maintained as described in section **2.2.1**. Cells were counted and seeded in 96-well clear flat bottom plates (Sigma-Aldrich, USA) at a cell density of 15 000 cells/well in a total volume of 100 µl complete media [DMEM, 5 % [v/v] FBS, 1 % [v/v] PSA]. Cells were incubated for 24 h at 37 °C with 5 % CO_2.

4.2.2 DMSO sensitivity analysis

All compounds were dissolved in DMSO. Therefore, the effect of DMSO on BHK-21 cell growth was evaluated by firstly seeding cells, as described in section **4.2.1**. After the 24 h incubation, the media was replaced with fresh assay media [DMEM, 2 % [v/v] FBS, 1 % [v/v] PSA] containing a range of DMSO (Thermo Scientific, USA) concentrations between 0.02 - 2.56 % in a total 200 µl/well volume. Positive controls included mock-treating cells with only assay media (no DMSO), and background controls consisted of wells with only assay media (no cells). Cells were then incubated for 72 h at 37 °C with 5 % CO_2 before adding 20 µl of resazurin (0.54 mM) to detect fluorescence readings. The cells were incubated for 3 h at 37 °C with 5 % CO_2. Fluorescence signals were detected using the Synergy MX microplate reader (BioTek Instrumentd, Inc) at

excitation wavelength 560 nm and emission wavelength 590 nm. Each treatment had three technical replicates.

4.2.3 Compound and antibody preparation

Potential reference compounds ITZ and DIP were purchased from Acros Organics (USA) and Alfa Aesar (USA), respectively. Compounds were dissolved in DMSO, yielding stock solutions of 10 mM for ITZ and 100 mM for DIP. The neutralising anti-TMEV GDVII capsid antibody (Upfold et al., 2018) was also tested as an antiviral inhibitor. The antibody's concentration (µM) was measured using a Nanodrop ND-1000 spectrophotometer (Thermo Scientific, USA). Samples were prepared by performing a 10-fold dilution of the antibody in PBS between 1:1000 and 1:10 before measuring the concentration. The spectrophotometer was blanked with 1 µl of sterile water before each sample was measured. The final concentration was the average of 18 readings. The compounds and antibodies were stored at -20 °C.

4.2.4 Cytotoxicity assays to generate dose-response curves

The toxicity of the compounds and the anti-TMEV GDVII capsid antibodies on BHK-21 cells was assessed by firstly seeding cells as described in section **4.2.1**. Following the 24 h incubation, ITZ, DIP, and the antibody were each prepared by performing a 10-point 3-fold serial dilution in assay media. Media was replaced with fresh assay media containing the prepared dilutions yielding final concentrations between 100 - 0.005 µM for ITZ and DIP and 30 - 0.002 µM for the antibody in a total volume of 200 µl/well. Background controls included wells with assay media only (no cells), and positive controls included cells mock-treated with assay media (no compound). Respective dilutions for each compound/antibody had four technical replicates. Cells were then incubated for 72 h at 37 °C with 5 % CO_2 before adding 20 µl of resazurin (0.54 mM) to detect fluorescence signals for the generation of dose-response curves and CC_{50} values. Three independent experiments were performed for each compound/antibody.

4.2.5 Antiviral assays to generate dose-response curves

ITZ, DIP and the anti-TMEV GDVII capsid antibodies were tested for antiviral activity against TMEV GDVII simultaneously and similarly to the cytotoxic assay described in section **4.2.4**. The only addition is that after treating cells with the compounds/antibody in a total volume of 100

µl/well, they were infected with TMEV GDVII at an MOI of 0.00625 in a total volume of 100 µl/well, resulting in the final volume being 200 µl/well. Background controls consisted of wells with assay media only (no cells). Positive controls included cells mock-treated with assay media (no compound or virus) and negative controls comprised of cells infected with TMEV GDVII (no compound). The 10 dilutions for each compound/antibody had three technical replicates. After a 72 h incubation, 20 µl of resazurin (0.54 mM) was added to each well to detect fluorescence for the generation of dose-response curves and IC_{50} values. The experiment was performed independently in triplicate for each compound/antibody. Microscopic images were captured after 72 hpi.

4.2.6 Antiviral assays with varying MOIs and endpoints

Various parameters of the assay were tested, such as MOI and endpoint, to confirm that the previously selected parameters were optimal. Cells were seeded as described in section **4.2.1**. followed by replacing media with new assay media consisting of varying concentrations of compounds in a total volume of 100 µl/well. Final concentrations included 1, 0.5, 0.25 and 0.0125 µM for ITZ and 30, 20, 13 and 9 µM for DIP (each surrounding their CC_{50} value). Additionally, cells were treated with the anti-TMEV GDVII capsid antibody at a concentration of 3.3 µM. Next, the cells were infected with TMEV GDVII at three MOIs, 0.00625, 0.00312 and 0.00156, in a total volume of 100 µl/well, resulting in the final volume being 200 µl/well. Background controls consisted of no cells and only assay media, positive controls included cells mock-treated with assay media (no compound/virus) and negative controls comprised of cells infected with the virus alone (no compound). The cells were incubated at 37 °C with 5 % CO_2, followed by the addition of 20 µl of resazurin (0.54 mM) at two endpoints, 48 and 72 hpi, to measure fluorescence. Each treatment was repeated in triplicate.

4.2.7 Western blot analysis of cell lysates

Potential antiviral effects of ITZ, DIP and the anti-TMEV GDVII capsid antibody were assessed by detecting viral proteins through Western blot analysis. Cells were counted and seeded in 24-well plates at a density of 95 000 cells/well in a final volume of 500 µl/well complete media. Following a 24 h incubation at 37 °C with 5 % CO_2, the media was replaced with fresh assay media containing the compounds/antibody in a total volume of 250 µl/well. The cells were then infected

with TMEV GDVII at an MOI of 0.00625 in a total volume of 250 µl/well, yielding a final volume of 500 µl/well with final concentrations of 0.6 µM, 16 µM and 3.3 µM for ITZ, DIP and the antibody respectively. Positive controls consisted of cells mock-treated with assay media (no compound/virus), and negative controls included cells infected with the virus alone (no compound). Cells were incubated at 37 °C with 5 % CO_2 before collecting cell lysates using trypsin at 30, 48 and 72 hpi. Samples were analysed by SDS-PAGE and Western blot as described in section **2.2.8**.

4.2.8 Data analysis and normalisation

Fluorescence readouts were analysed in Microsoft Excel by subtracting the mean no-cell background control from all treatments. The values were normalised to the mean mock-infected controls (no virus/compound) representing 100 % cell viability (%) using the formula:

$$\text{Cell viability (\%)} = \left(\frac{RFU_{sample}}{\mu RFU_{mock}}\right) \times 100$$

where RFU_{sample} represents fluorescence values of each treatment and μRFU_{mock} represents the mean value of the mock-infected positive control. Unpaired t-tests were performed where a p-value less than 0.01 was considered statistically significant. * p-value < 0.01, ** p-value < 0.001, *** p-value < 0.0001, **** p-value < 0.00001. Graphs were created and analysed using GraphPad Prism (version 9.4.1 for Windows 64-bit).

For the dose-response curves, results were expressed as the percent inhibition of CPE by comparing the fluorescence intensity of experimental wells to the intensities of mock-infected cells (representing 100 % inhibition of CPE) and TMEV GDVII-infected control wells (0 % inhibition of CPE) on the same plate using the formula:

$$\text{Inhibition of CPE (\%)} = \left(\frac{RFU_{sample} - \mu RF\ _{virus}}{\mu RFU_{mock} - \mu RFU_{virus}}\right) \times 100$$

where RFU_{sample} represents fluorescence values of each treatment, μRFU_{mock} represents the average of the mock-infected (no virus/compound) control, and μRFU_{virus} are the mean values of TMEV GDVII-infected control wells (no compound). Compound toxicity was presented as cell

viability and calculated using the formula above. Curves represented the mean and standard deviation from 3 or 4 technical replicates and were generated using a four-parameter curve fitting function on GraphPad Prism (version 9.4.1 for Windows 64-bit) to calculate IC_{50} and CC_{50} values.

4.3 Results

4.3.1 DMSO sensitivity analysis

The effect of DMSO on the growth of BHK-21 cells was assessed since all compounds were dissolved in this reagent. Varying final concentrations of DMSO were used to treat cells ranging between 0.02 - 2.56 %. Following the 72 h incubation, resazurin was added to detect fluorescence signals which were then normalised to the mock-treated positive control (no DMSO) representing cell viability (%). **Figure 4.1** illustrates that when cells were treated with DMSO at 0.64 % or lower concentrations, cell viability remained high with no significant differences compared to the mock-treated cells ($P < 0.01$). In contrast, when concentrations of 1.28 % or higher were tested, there was a considerable decrease in cell viability, with a significant difference compared to mock-treated cells ($P < 0.01$).

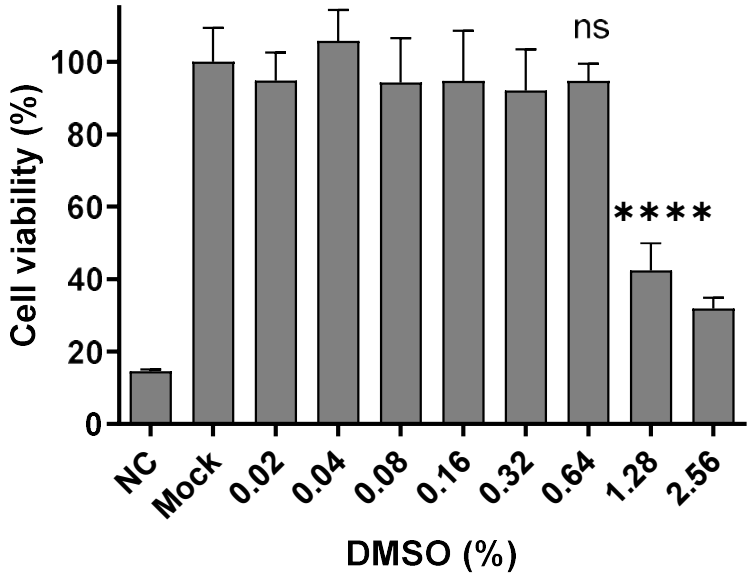

Figure 4.1 The effect of DMSO on the viability of BHK-21 cells. 15000 cells/well were seeded and incubated for 24 h before replacing media with new assay media containing various DMSO concentrations between 0.02 - 2.56 %. Fluorescence signals were measured after 72 hpi with resazurin, and data were normalised to the average of mock-treated (no DMSO) cells and represented cell viability. Unpaired t-tests were carried out whereby statistically significant values were represented as * ($P < 0.01$), and non-significant values were abbreviated as ns. Each data point represents the mean value ± SD of 3 replicates.

4.3.2 Cytotoxicity and antiviral activity of potential control inhibitors for the TMEV GDVII antiviral assay

In order to investigate the cytotoxicity and antiviral activity of the potential control compounds, ITZ and DIP, and the anti-TMEV GDVII capsid antibodies, two simultaneous assays were performed using the parameters identified in the previous chapter. Firstly, the toxicity of the compounds/antibody on BHK-21 cells (without virus) was tested by treating cells with a 3-fold dilution ranging from 100 - 0.005 µM for ITZ and DIP and 30 - 0.002 µM for the antibody. Dose-response curves were generated (**Figure 4.2.A**) by measuring fluorescence with resazurin after 72 hpi and normalising values to the mock-infected (no virus/compound) cells to represent cell viability in blue. The compounds displayed a typical sigmoidal curve indicating that they become toxic to BHK-21 cells at 1.23 µM and above for ITZ and 33 µM and higher for DIP, yielding CC_{50} values of 0.69 µM and 16.25 µM respectively. The antibody did not exhibit toxicity at any tested concentration; therefore, the CC_{50} could not be defined as a linear response was generated. A similar assay was performed (**Figure 4.2.A**), except that antiviral activity was examined against TMEV GDVII by infecting cells at an MOI of 0.00625. Dose-response curves were created by detecting fluorescence signals and normalising the data to mock-infected (no virus/compound) and infected (no compound) cell controls to represent the inhibition of CPE in red. Neither ITZ nor DIP inhibited TMEV GDVII CPE at non-toxic concentrations resulting in IC_{50} values that could not be determined, and this coincided with microscopic images showing full CPE for all concentrations (data not shown). In contrast, the antibody potently inhibited TMEV GDVII CPE as it depicts a characteristic sigmoidal curve producing an IC_{50} of 1.62 µM, preventing CPE at concentrations of 3.3 µM and above. Additionally, when the mean values of the controls were compared to the antibody-treated cells infected with the virus (3.3 µM), a significant difference was detected compared to the virus-alone infected cells ($P < 0.01$). In contrast, no significant differences were shown relative to the mock-treated cells and the cells treated with antibody alone

(no virus) at this concentration (**Figure 4.2.B**). This correlated to microscopic images illustrating a confluent monolayer that was identical to the mock-infected and uninfected antibody-treated cells (**Figure 4.2.C**). Thus, the anti-TMEV GDVII capsid antibody was considered the most suitable control inhibitor for the assay.

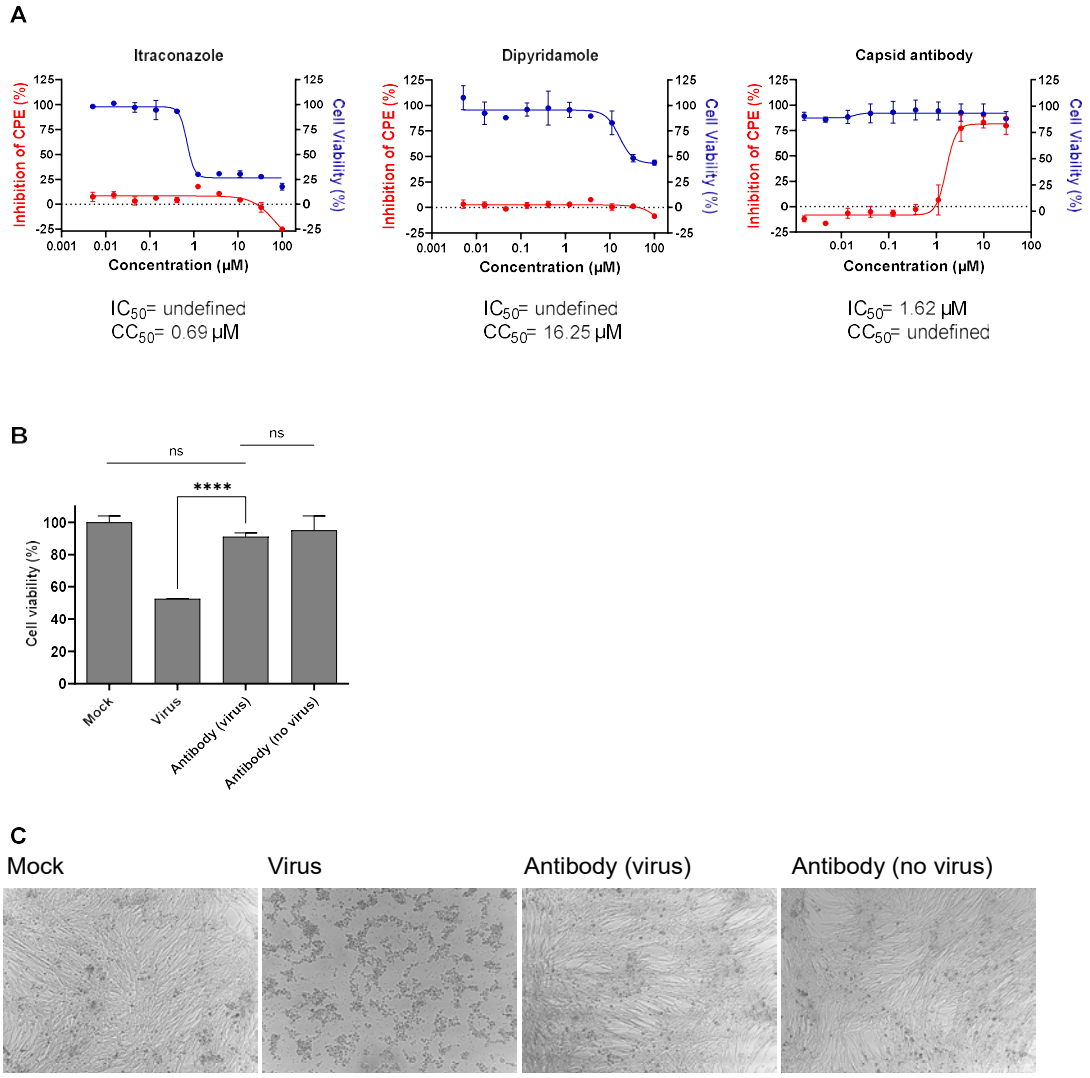

Figure 4.2 Cytotoxic and antiviral effects of potential control inhibitors for the TMEV GDVII screening assay. 15000 cells/well were seeded and incubated for 24 h before treating cells with ITZ, DIP or the anti-TMEV GDVII capsid antibody at varying concentrations between 100 - 0.005 µM for the compounds and 30 - 0.002 µM for the antibody. A) Fluorescence signals were detected after 72 hpi using resazurin, normalised to the average of mock-treated cells, and represented cell viability in blue. Each data point represents the mean value ± SD of 4 replicates. Similarly, the antiviral activity of the

compounds/antibody at those various concentrations was tested by infecting cells at an MOI of 0.00625. Fluorescence readings were measured, and data were normalised to the average of mock-treated and infected cells generating dose-response curves representing the inhibition of CPE in red. Each data point represents the mean value ± SD of 3 replicates. B) Mean values ± SD of the mock and virus alone controls compared to cells treated with the antibody (3 µM**)** with and without virus. Unpaired t-tests were performed whereby statistically significant values were represented as * ($P < 0.01$). Three independent experiments were performed, but one representative experiment is presented. C) Microscopic images of control cells and antibody-treated (3 µM**)** cells with and without the virus were captured after 72 hpi.

4.3.3 Confirmation that ITZ and DIP do not effectively inhibit TMEV GDVII and that the chosen assay parameters are optimal

Since the previous experiment showed that ITZ and DIP could not inhibit TMEV GDVII-induced CPE, various assay components, including MOI and endpoint, were tested to confirm that the previously chosen parameters were optimal and that the compounds failed to inhibit CPE. Seeded cells were treated with 4 concentrations of each compound, ranging from 1 - 0.0125 µM for ITZ and 30 - 9 µM for DIP (each surrounding their CC_{50} values). Cells were then infected at three MOIs, 0.00625, 0.00312 and 0.00156, followed by measuring fluorescence using resazurin at two endpoints, including 48 and 72 hpi. **Figure 4.3** illustrates that when cells were treated with ITZ and infected at an MOI of 0.00625, none of the concentrations effectively inhibited TMEV GDVII CPE after 72 hpi as cell viability values were similar and as low as the virus alone control (no compound). There was also a significant difference compared to the positive mock-infected control ($P < 0.01$). Similar results were produced after 48 hpi where no significant inhibition was detected. There were also minimal differences when comparing the results between 48 and 72 hpi. DIP did not effectively inhibit TMEV GDVII CPE when infecting cells at 0.00625 MOI at 72 and 48 hpi. All concentrations in cells displayed low viability readings that were similar, if not lower than the virus alone control, also showing a significant difference to mock-infected cells ($P < 0.01$). Again, no significant differences were seen between 48 and 72 hpi values. In addition, when cells were infected at lower MOIs, 0.00312 and 0.00156, neither ITZ nor DIP inhibited TMEV GDVII CPE as cells treated with all compound concentrations yielded low viability readings, and most were even lower than the virus alone control. When comparing the negative virus-infected controls (no compound), cells infected at an MOI of 0.00625 produced the lowest viability values of 52 % and 45 % at 48 hpi and 72 hpi, respectively, followed by MOI of 0.00312 yielding 66 % and 50 %

viability at 48 hpi and 72 hpi, respectively and lastly, infection at an MOI of 0.00156 resulted in 72 % and 68 % viability readings confirming that an MOI of 0.00625 with an endpoint of 72 hpi was optimal. Lastly, each experiment incorporated treating cells with the anti-TMEV GDVII capsid antibody at the non-toxic concentration of 3.3 µM. The resulting viability readings were high, ranging between 80 % - 101 % showing inhibition of infection at all three MOIs, even at both endpoints.

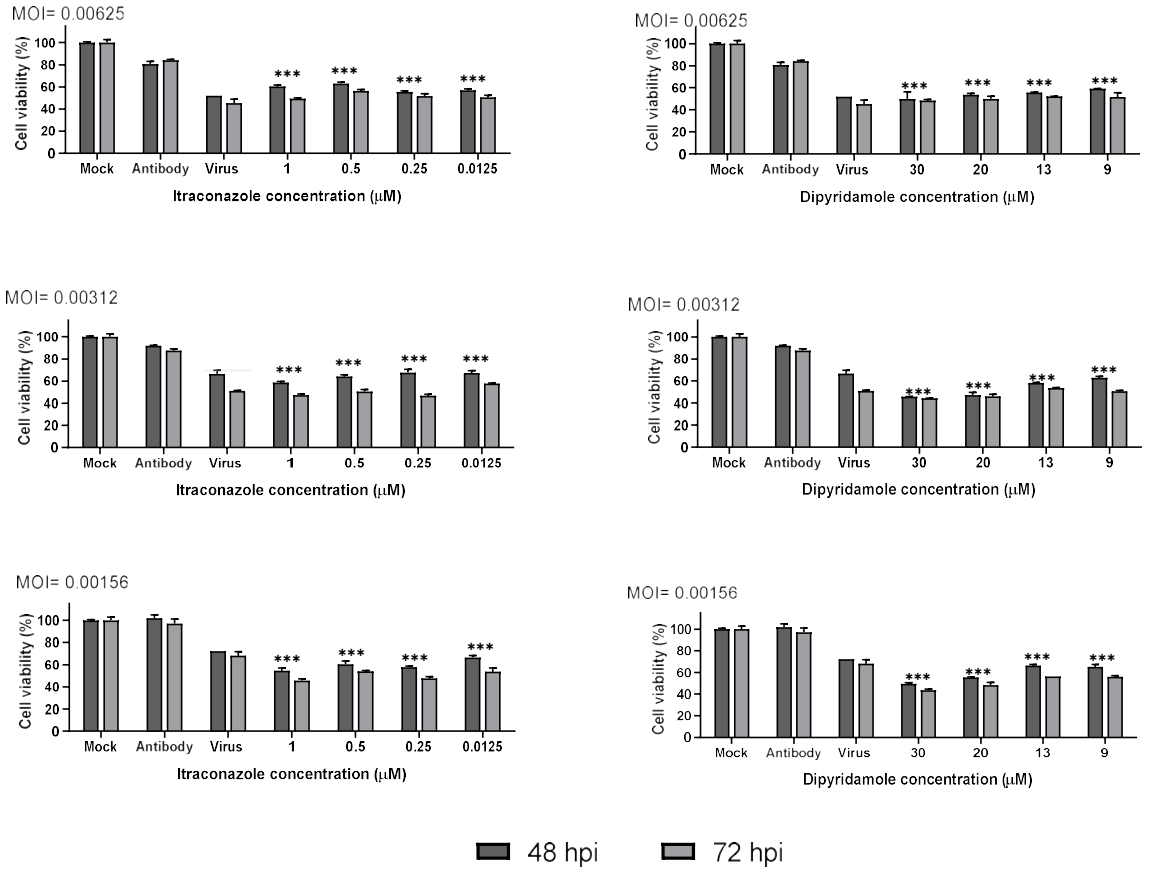

Figure 4.3 Confirmation that ITZ and DIP do not inhibit TMEV GDVII infection. 15000 cells/well were seeded, followed by treating cells with various concentrations of ITZ (1 - 0.0125 µM), DIP (30 - 9 µM) and the anti-TMEV GDVII capsid antibody (3.3 µM). Cells were then infected at three different MOIs, including 0.00625, 0.00312 and 0.00156. Fluorescence readouts were measured with resazurin at two endpoints, 48 and 72 hpi, followed by normalising the data to the mean values of mock-infected cells

representing cell viability. Unpaired t-tests were performed whereby statistically significant values were represented as * ($P < 0.01$). Each data point represents the average value ± SD of 3 replicates.

4.3.4 Detection of viral proteins after treatment with ITZ, DIP and the anti-TMEV GDVII capsid antibody

TMEV GDVII viral proteins were detected after treating cells with ITZ (0.6 μM), DIP (16 μM) and the anti-TMEV GDVII capsid antibody (3.3 μM), followed by infection at an MOI of 0.00625. Cell lysates were collected at 30, 48 and 72 hpi before TMEV GDVII proteins were detected using the primary antibodies anti-TMEV GDVII capsid (1:2500) and anti-2C (1:200). Coomassie-stained gels were presented on the left panel since internal loading controls were inaccessible (**Figure 4.4**). Western analysis showed that faint bands were detected at 30 hpi, corresponding to the TMEV GDVII VP1 protein in the virus control and ITZ-treated samples. The intensity of these two bands increased at 48 hpi and was the brightest at 72hpi, with an additional band being produced in the DIP-treated lane. Compound-treated cells generated significantly fainter bands, meaning fewer VP1 proteins, compared to the virus-infected control at 72 hpi. No proteins were detected in the DIP samples at 30 and 48 hpi. Similarly, no viral protein bands were observed for mock-infected controls and antibody-treated cells at any time point. Furthermore, viral protein bands were produced corresponding to the size of the 2C TMEV GDVII protein when the anti-2C antibody was used. A faint band was detected at 30 hpi in the virus control sample, which increased in intensity after 48 and 72 hpi. No bands were seen at 30 hpi for ITZ and DIP-treated samples. Contrastingly, faint bands developed at 48 hpi with an increase in intensity at 72 hpi. Again mock-infected controls and antibody-treated samples did not result in bands forming at any time as expected.

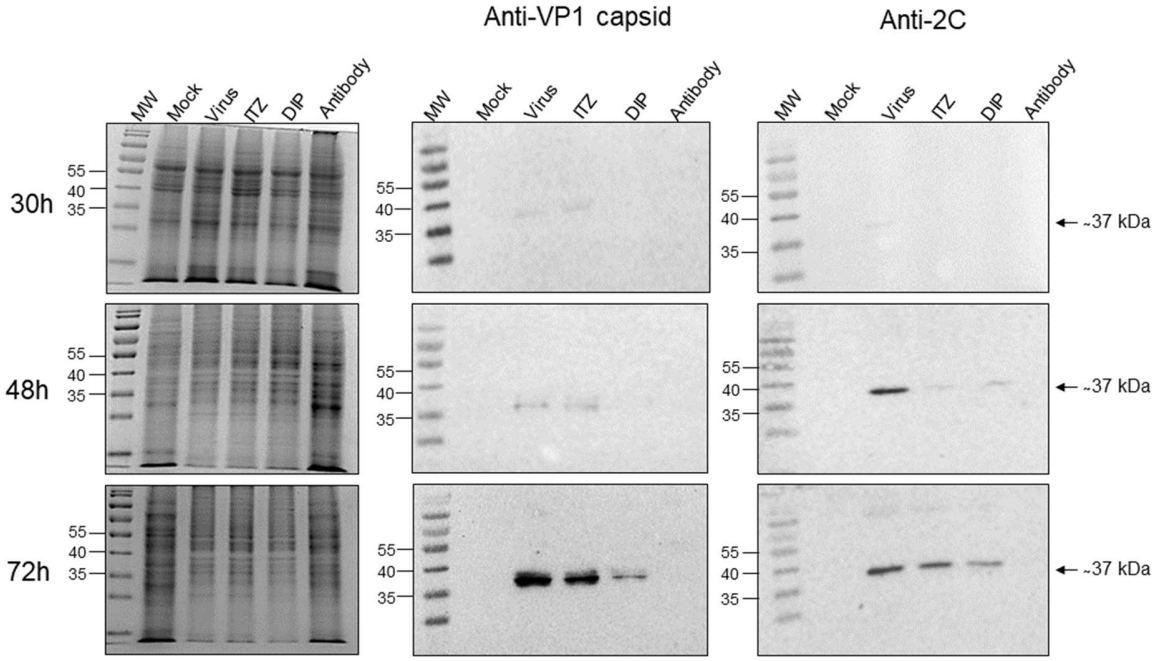

Figure 4.4 Detection of the expression of TMEV GDVII viral proteins. Cells were seeded and treated with ITZ (0.6 µM), DIP (16 µM) and the anti-TMEV GDVII capsid antibody (3.3 µM) before being infected at an MOI of 0.00625. Controls included mock-infecting cells (no virus) and infecting cells with the virus alone (no compound). Coomassie-stained gels are presented on the left panel and Western blots are on the right. Viral proteins were detected after 30, 48 and 72 hpi using the primary antibodies anti-TMEV GDVII capsid (1:2500) and anti-2C (1:200). MW (molecular weight marker in kDa).

4.4 Discussion

The overall aim of this chapter was to select a suitable inhibitor of TMEV GDVII-induced CPE that could be used in the antiviral assay as a reference control for comparison. The compounds tested in the current and following chapter were solubilised in a DMSO solution; typically, most chemical libraries are stored in this organic solvent (Hughes et al., 2011). Therefore, before the potential inhibitors were tested for antiviral activity, the sensitivity of the cells towards varying concentrations of DMSO was investigated. High concentrations above 1 % were shown to affect membrane permeability and cell viability (Irvine et al., 1999). When previously tested in BHK-21 cells, DMSO concentration-dependent damage was observed, and it was concluded that concentrations above 0.7 % become toxic (Tomeczkowski et al., 1993). These results are consistent with this study which showed that DMSO concentrations above 1.28 % are toxic to

BHK-21 cells as there was a considerable reduction in cell viability. Similar experiments were conducted in antiviral assay development against dengue and bluetongue virus, where these studies also concluded that there should be no more than 1 % DMSO added to the cell culture for the screening process, which is recommended for most standard cell-based assays (Che et al., 2009; Li et al., 2009). Therefore, when screening compounds with the TMEV GDVII antiviral assay, the final DMSO concentrations were always kept below 1 % to prevent toxicity.

The subsequent experiments focused on generating dose-response curves to compare and identify the most suitable inhibitor of TMEV GDVII-induced CPE between ITZ, DIP and the anti-TMEV GDVII capsid antibody. The results showed that ITZ did not inhibit CPE at non-toxic concentrations even after certain parameters of the assay were modified, such as MOI and the endpoint at which resazurin readings were measured. The previously mentioned study, which was used as motivation for selecting ITZ, showed that it inhibited a broad spectrum of EVs and cardioviruses (Strating et al., 2015). However, a few differences compared to the TMEV GDVII assay could be speculated as to why ITZ did not exhibit antiviral activity. Firstly, different cell lines were used in the Strating et al. (2015) study, namely HeLa R19 and Buffalo green monkey (BGM) kidney cells. ITZ did not display any cytotoxic effects in these cell lines at any concentration. In contrast, the results in this chapter showed that it was highly toxic to BHK-21 cells at concentrations of 1.23 µM and above, suggesting that a dose that could have had antiviral activity was too toxic to the BHK-21 cells. Currently, BHK-21 cells are the only cell line found to be susceptible to TMEV GDVII infection in cell culture. More importantly, the Strating et al. (2015) study investigated a different cardiovirus species, EMCV (*Cardiovirus A*). As mentioned, ITZ is believed to target the host factor OSBP, thereby preventing cholesterol shuttling to ROs and disrupting replication in EMCV (Strating et al., 2015). Since TMEV GDVII is a different species of cardiovirus and no inhibitors have been tested against this virus before, it can be hypothesised that it relies on different host factors for replication since ITZ did not have an effect. Similar results were reported demonstrating antiviral activity of ITZ against the picornavirus strain HPeV-3 but, interestingly, not against HPeV-1 (Lanko et al., 2019). Additionally, ITZ was reported to inhibit the EV-D68 strain (Strating et al., 2015) but failed to exhibit any antiviral activity towards the same strain in a different study (Rhoden et al., 2015). Therefore, it was suggested that ITZ activity might be sensitive to virus concentration even within a relatively narrow range (Rhoden et al., 2015).

DIP did not inhibit TMEV GDVII-induced CPE at non-toxic concentrations either, even when the assay parameters were changed. The previous study mentioned in the introduction showed that DIP effectively inhibited a different cardiovirus species EMCV (mengovirus) (Fata-Hartley and Palmenberg, 2005). However, various differences were highlighted when compared to the TMEV GDVII antiviral assay, which could be the cause of unsuccessful inhibition. Firstly, HeLa and mouse L929 cells were used instead of BHK-21 cells. The results in this chapter illustrated that DIP became toxic at concentrations of 33.33 µM and higher. In contrast, the mengovirus study showed inhibition in HeLa and L cells at the high DIP concentration of 80 µM (Fata-Hartley and Palmenberg, 2005), suggesting that an inhibitory dose might have been missed due to toxicity to the BHK-21 cells. Secondly, DIP was dissolved in ethanol in the mengovirus study instead of DMSO, implying that the solubility of the drug might not have been efficient enough in DMSO. Future solubility experiments could be conducted comparing whether dissolving DIP in ethanol or DMSO increases the inhibitory effect. Thirdly, different inhibition assays were performed where mengovirus plaque formation was observed (Fata-Hartley and Palmenberg, 2005) instead of quantifying CPE using a resazurin-based assay. This was similar to another study that investigated the inhibitory effects of DIP on mengovirus using an agar diffusion plaque inhibition test (Tonew and Dzeguze, 1977). The virus was only allowed to replicate for 1 replication cycle between 4 - 8 hpi in FL and L cells, after which an inhibitory action was observed (Tonew and Dzeguze, 1977). These differences compared to the TMEV GDVII assay could explain why DIP did not inhibit TMEV GDVII-induced CPE in BHK-21 cells. It should also be noted that an experiment was performed whereby ITZ and DIP were allowed to incubate with the cells for 2 h before being infected with the virus (data not shown); however, it did not make a difference as no inhibition of CPE was observed.

The anti-TMEV GDVII capsid antibody effectively inhibited TMEV GDVII-induced CPE at concentrations of 3.3 µM and above with an IC_{50} of 1.62 µM. Additionally, the antibody did not exhibit any cytotoxic effects on the BHK-21 cells. Compared to other positive and negative controls, the antibody-treated cells (infected) generated signals that were significantly different to the virus-alone infected cells but showed no significant differences to the mock-treated cells and the cells treated with antibody alone (no virus). Microscopic images coincided with these results illustrating a confluent monolayer after infected cells were treated with the antibody. Therefore,

based on the above data, the neutralising anti-TMEV GDVII capsid antibody was chosen as the most appropriate and effective anti-TMEV GDVII control among the tested three inhibitors.

The last experiment used the anti-2C and anti-TMEV GDVII capsid antibodies as tools to observe whether TMEV GDVII viral proteins were expressed after being treated with ITZ, DIP and the anti-TMEV GDVII capsid antibody, seeing that the compounds did not inhibit CPE. VP1 proteins are structural proteins of the mature capsid, and 2C is a non-structural protein involved in genome replication. VP1 was detected at 30 - 72 hpi in ITZ-treated cells, yet the intensity of the bands was much fainter than the virus control. Interestingly, VP1 proteins were not detected in DIP-treated cells at 30 and 48 hpi but were observed at 72 hpi with a fainter band compared to the virus control. Furthermore, the anti-2C antibody was used to detect the 2C replication protein. No protein was detected in both ITZ and DIP-treated cells at 30 hpi, even though a faint band was observed in the virus control lane. At 48 and 72 hpi, the intensity of the bands slightly increased but was not as bright as the virus control. No conclusion can be made from this observation, as this preliminary experiment was not quantifiable, which will be further discussed. Nonetheless, no bands appeared in mock-infected and anti-TMEV GDVII capsid antibody lanes meaning that the antibody potently inhibited virus-induced CPE and prevented viral proteins from being expressed even up to 72 hpi. This further confirmed that it was the most suitable inhibitor of TMEV GDVII of the three. A drawback of this experiment is that only the presence of the viral protein and not the amount could be examined, as no loading control was accessible at the time. The Coomassie-stained gels provided a vague indication of the amount of protein loaded. Therefore, this experiment could be improved in the future by including an appropriate loading control.

The overall aims of this chapter were achieved as it was concluded that DMSO concentrations above 1 % were toxic to BHK-21 cells, the anti-TMEV GDVII capsid antibody exhibited potent antiviral activity and displayed no cytotoxicity based on the dose-response curves. Contrary to expectation, ITZ and DIP did not inhibit virus-induced CPE. Thus, the anti-TMEV GDVII capsid antibody was selected as the most suitable control inhibitor of TMEV GDVII when screening compound libraries in the next chapter and the future.

Chapter 5 Screening of compound libraries using the TMEV GDVII antiviral assay

5.1 Introduction

The previous chapters described the optimisation and development of a TMEV GDVII antiviral assay, providing an opportunity to screen two libraries for antiviral activity containing novel compounds. Natural products from plants or other organisms are a valuable source of novel chemical compounds such as antivirals (Musarra-Pizzo, 2021). Coumarin (2H-chromen-2-one) is a compound that is naturally found in an extensive range of plants, animals, and micro-organisms. It is made up of a bicyclic system containing an α-pyrone and a benzene ring. Thus, numerous chemical substitutions are feasible, generating a range of potential medicinal compounds (Hassan et al., 2016). Coumarins and its derivatives have been shown to target various proteins, enzymes and pathways that are necessary for viral entry and successful infection, such as polymerase-related proteins, proteases, integrases, and several factors involved in interferon signalling pathways (Mishra et al., 2020). Several studies have reported that coumarins and their analogues exert antiviral activity against HIV, hepatitis B virus, HCV, herpes simplex virus, SARS-CoV-2, chikungunya virus, dengue virus, RVs, EVs and HAV (Kashman et al., 1992; Huang et al., 1994; Chang et al., 1997; Bedoya et al., 2005; Marquez et al., 2005; Conti et al., 2009; Neyts et al., 2009; Conti et al., 2010; Xu et al., 2014; Hassan et al., 2016; Kassem et al., 2019; Mishra et al., 2020; Chidambaram et al., 2021). A large group of coumarin compounds and derivatives were newly synthesised and tested for HIV integrase inhibition (Jesumoroti, 2016), and twelve of these compounds were screened against TMEV GDVII.

In recent years, antiviral activity on viruses such as influenza and hepatitis B has been described for certain quinones and other structurally related molecules with therapeutic potential (Hossan et al., 2018; Parvez et al., 2019). Quinones are a class of cyclic organic compounds that are formed from aromatic compounds by converting CH= groups into C=O carbonyl groups, producing a fully conjugated cyclic dione structure (Skancke and Skancke, 1988). Quinones are located in a wide

variety of plants, bacteria and some fungi and animals (O'Brien, 1991). Quinones have shown antiviral activities against DNA and RNA viruses by inhibiting viral entry, replication, and genome transcription, as well as affecting the function of important enzymes for the viral replicative cycle (Da Costa et al., 2013; Liu et al., 2013; Pinto et al., 2014; Yiu et al., 2014; Alam et al., 2015; Chi et al., 2015). For the purpose of this study, a Marine Natural Product (MNP) library was screened to assess the viral activity against the TMEV GDVII virus (Kalinski et al., 2021). A total of twelve pure compounds from the MNP library were tested, where two compounds were orthoquinones while the rest of the compounds were pyrroloiminoquinones.

Thus, this chapter aimed to examine whether the novel compounds supplied in the coumarin and MNP library possessed any antiviral activity against TMEV GDVII using the newly optimised antiviral assay from the previous chapters. This was achieved by generating dose-response curves to test for cytotoxicity against BHK-21 cells and antiviral activity against TMEV GDVII, whereby IC_{50} and CC_{50} values were obtained. Additionally, Z'- factors were calculated to validate the robustness of the assay.

5.2 Methods and materials

5.2.1 Cell culture and plating

BHK-21 cells were maintained as described in section **2.2.1**. Cells were seeded in 96-well clear flat bottom plates (Sigma-Aldrich, USA) at a cell density of 15 000 cells/well in a total volume of 100 µl complete media [DMEM, 5 % [v/v] FBS, 1 % [v/v] PSA]. Cells were incubated for 24 h at 37 °C with 5 % CO_2.

5.2.2 Compound libraries

Two compound libraries consisting of 12 compounds each were screened. Prof R. Klein (Department of Chemistry, Rhodes University) kindly donated the coumarin library, and Prof R. Dorrington (Department of Biochemistry and Microbiology, Rhodes University) kindly supplied the MNP library. All compounds were dissolved in DMSO, yielding stock solutions of 100 mM and 50 mM for compounds in the coumarin and MNP libraries, respectively, which were stored at -20 °C. Stocks were made up using the calculation below:

Mass of compound (g) = $concentration\ (M) * volume\ (L) * molecular\ weight\ (\frac{g}{mol})$

5.2.3 Antiviral and cytotoxic assays to generate dose-response curves

The compound libraries were assessed for antiviral activity against TMEV GDVII by seeding cells, as described in section **5.2.1**. After the 24 h incubation, the compounds were serially diluted (3-fold) in assay media [DMEM, 2 % [v/v] FBS, 1 % [v/v] PSA]. The media was substituted with new assay media containing the prepared dilutions resulting in final concentrations between 100 - 0.005 µM for each compound in a total 100 µl/well volume. Cells were then infected with TMEV GDVII at an MOI of 0.00625 in a total volume of 100 µl/well, resulting in the final volume being 200 µl/well. Cytotoxicity was tested simultaneously on each plate for each compound by omitting the virus and adding an additional 100 µl/well of assay media instead. Background controls comprised of wells with assay media only (no cells). Positive controls included cells mock-treated with assay media (no compound/virus), and negative controls consisted of cells infected with TMEV GDVII (no compound). After incubating the cells for 72 h, 20 µl of resazurin (0.54 mM) was added to each well followed by a 3 h incubation at 37 °C with 5 % CO_2. Fluorescence signals were detected to generate dose-response curves using the Synergy MX microplate reader (BioTek Instrumentd, Inc) at excitation wavelength 560 nm and emission wavelength 590 nm. The anti-TMEV capsid antibody dose-response curves were used as a comparison control curve.

5.2.4 Data analysis and normalisation

Fluorescence readouts were analysed in Microsoft Excel by subtracting the mean no-cell background control from all treatments. For the dose-response curves, results were expressed as percent inhibition of CPE using the formula:

$$\text{Inhibition of CPE (\%)} = \left(\frac{RFU_{sample} - \mu R_{virus}}{\mu RFU_{mock} - \mu R_{virus}}\right) \times 100$$

where RFU_{sample} represents fluorescence values of each treatment, μRFU_{mock} represents the average of the mock-infected (no virus/compound) control (100 % inhibition), and μRFU_{virus} are the mean values of TMEV GDVII-infected control wells (no compound) (0 % inhibition). Similarly, compound cytotoxicity was presented using the formula:

$$\text{Cell viability (\%)} = \left(\frac{RFU_{sample}}{\mu RFU_{mock}}\right) \times 100$$

where RFU_{sample} represents fluorescence values of each treatment and μRFU_{mock} are the mean values of the mock-infected positive control (100 % viability). Curves represented the mean and standard deviation from 2 or 3 technical replicates and were generated using a four-parameter curve fitting function on GraphPad Prism (version 9.4.1 for Windows 64-bit) to calculate IC_{50} and CC_{50} values. Z'-factors were calculated on each plate using the mock-infected and TMEV-infected controls as described in section **3.2.7**.

5.3 Results

5.3.1 Screening of the coumarin and MNP libraries for antiviral activity and cytotoxicity

In order to examine the antiviral efficacy and cytotoxicity of the compounds within the coumarin and MNP libraries, two simultaneous assays were performed using the TMEV GDVII antiviral assay. The ability of the compounds to reduce virus-induced CPE was tested by treating cells with 3-fold diluted compounds with concentrations ranging from 100 - 0.005 µM. This was followed by infecting cells at an MOI of 0.00625 and detecting fluorescence after 72 hpi. Inhibitory dose-response curves are represented in red (**Figure 5.1.A and B**). The toxicity of the compounds in the same cell line was investigated simultaneously on each plate, and toxicity dose-response curves are shown in blue (**Figure 5.1.A and B**). Many of the coumarin compounds (compound A-L) were toxic to the cells at concentrations of 33 µM and above, and none of the compounds effectively inhibited CPE as most values were around 0 %. Similarly, compounds 1-12 in the MNP library were mostly toxic at higher concentrations. Compound 11 was the only non-toxic compound with high viability readings at all concentrations. However, no compound exhibited sufficient antiviral activity, and IC_{50} values could not be calculated due to the lack of dose-dependent protection (undefined) (**Figure 5.1.C**). In comparison, the anti-TMEV GDVII capsid antibody control was able to neutralise TMEV GDVII infection with an IC_{50} of 1.62 µM. Lastly, the Z'-factors were calculated for each plate using the mock-infected (no virus/compound) and TMEV GDVII-infected (no compound) cell controls and consistently produced scores above 0.5, confirming a robust and reliable assay (**Figure 5.1.C**).

A

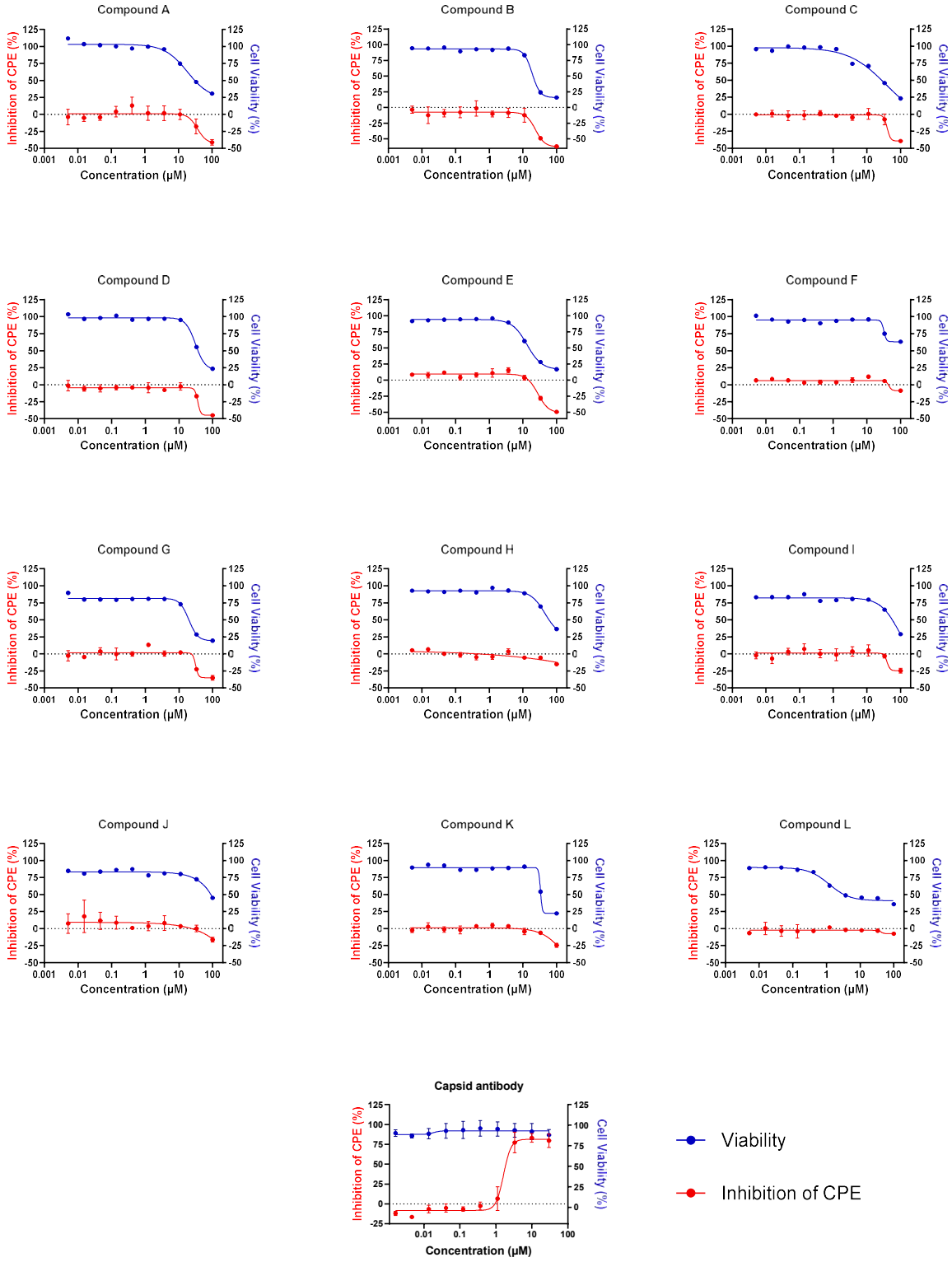
Compound A
Compound B
Compound C
Compound D
Compound E
Compound F
Compound G
Compound H
Compound I
Compound J
Compound K
Compound L
Capsid antibody
Inhibition of CPE (%)
Cell Viability (%)
Concentration (μM)
Viability
Inhibition of CPE

B

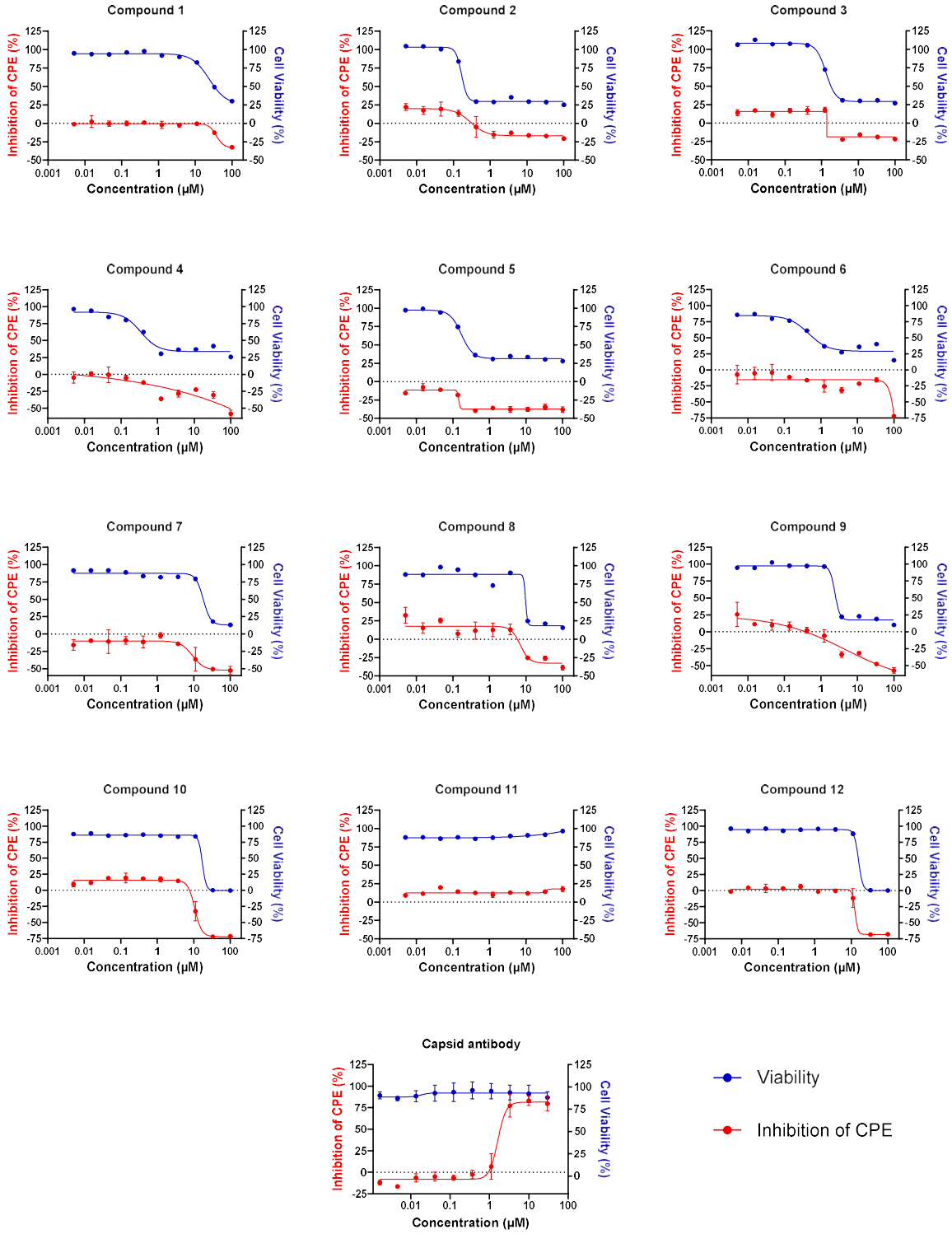
Compound 1
Compound 2
Compound 3
Compound 4
Compound 5
Compound 6
Compound 7
Compound 8
Compound 9
Compound 10
Compound 11
Compound 12
Capsid antibody
Inhibition of CPE (%)
Cell Viability (%)
Concentration (μM)
Viability
Inhibition of CPE

C

Compound	IC_{50} (µM)	CC_{50} (µM)	Z'- factor
A	Undefined	18.37	0.61
B	Undefined	18.76	0.61
C	Undefined	36.43	0.62
D	Undefined	30.87	0.62
E	Undefined	13.15	0.70
F	Undefined	31.85	0.70
G	Undefined	19.52	0.74
H	Undefined	45.47	0.74
I	Undefined	87.4	0.64
J	Undefined	Unstable	0.64
K	Undefined	33.13	0.68
L	Undefined	1.192	0.68
1	Undefined	23.97	0.76
2	Undefined	0.16	0.76
3	Undefined	1.31	0.76
4	Undefined	0.34	0.77
5	Undefined	0.17	0.77
6	Undefined	0.46	0.74
7	Undefined	18.11	0.74
8	Undefined	9.69	0.72
9	Undefined	2.42	0.72
10	Undefined	17.16	0.79
11	Undefined	Undefined	0.79
12	Undefined	15.69	0.77
Anti-TMEV capsid antibody	1.62	Undefined	0.76

Figure 5.1 Cytotoxic and antiviral effects of novel compounds in coumarin and MNP libraries. 15000 cells/well were seeded before adding the compounds at varying concentrations between 100 - 0.005 µM. Fluorescence readouts were measured after 72 hpi, normalised to the average of mock-treated cells, and represented cell viability in blue. Similarly, the antiviral activity of the compounds was examined by infecting cells at an MOI of 0.00625. Fluorescence signals were detected, and data were normalised to the average of mock-treated and infected cells generating dose-response curves representing the inhibition of CPE in red. A) Dose-response curves of the coumarin library. B) Dose-response curves of the MNP library,

including the anti-TMEV GDVII capsid antibody control curve. C) IC_{50}, CC_{50} and Z'-factors of each compound.

5.4 Discussion

The overall aim of this chapter was to screen novel compounds from two chemical libraries, consisting of coumarins (compounds A-L) and MNP (compounds 1-12) for antiviral activity using the TMEV GDVII antiviral assay. The results from the dose-response curves indicated that none of the 24 compounds effectively inhibited CPE in this assay compared to the anti-TMEV GDVII capsid antibody control, which neutralised TMEV GDVII infection with an IC_{50} of 1.62 µM.

Even though no hits were identified, the assay was still considered robust and consistent. Each 96-well plate tested two compounds simultaneously, including the positive (mock-infected) and negative controls (infected with no compound). This made it possible to calculate the Z'- factor for each plate, whereby consistent values between 0.61 - 0.79 were produced. These scores demonstrated that the assay was sufficiently robust, reproducible, and reliable.

A majority of the coumarin compounds displayed toxicity towards the BHK-21 cells at concentrations of 33 µM and higher as cell viability readings decreased at these concentrations. When compared to the results from the study that described the synthesis of these compounds and their activity against HIV, low toxicity levels against HeLa cells were reported (Jesumoroti, 2016). However, a few key similarities and differences should be noted compared to the TMEV GDVII assay. Firstly, the cell cytotoxicity assay was also resazurin based, whereby cell viability was represented based on fluorescence readings. In contrast, the HeLa cell line was used, which was shown to be more tolerable to the compounds compared to BHK-21 cells. More importantly, it should be noted that the conclusion stating that the compounds produced a low toxicity profile was based on performing the assay at only one concentration of 25 µM. This differed from the TMEV GDVII assay as varying doses with a maximum concentration of 100 µM were tested, resulting in toxicity at these high concentrations. Another key difference is that the cytotoxicity assay had an endpoint of 48 h instead of 72 h (Jesumoroti, 2016); therefore, it would be worthwhile to investigate whether 48 h improves the results. Additionally, an interesting study described the synthesis of newly developed coumarin derivatives and their antiviral activity against picornaviruses by binding to their capsids (Conti and Desideri, 2010). The picornaviruses tested

were RV serotypes 1B and 14 and EV-A71, and the compounds were shown to disrupt the replication of these picornaviruses. Cell cytotoxicity of the compounds towards HeLa and HEp-2 (human epithelioma) cells was measured using a tetrazolium-based colourimetric assay. Furthermore, a plaque reduction assay was used to examine inhibitory activity. Overall, the compounds produced low toxicity towards HeLa cells, while three compounds were toxic to the HEp-2 cells. Substantial differences were noted in the sensitivity of the viruses to each compound, as the potency was considerably lower for EV-A71 compared to the RV serotypes. The most active compounds in HeLa cells against the viruses were also the most toxic towards HEp-2 cells, indicating that the cell line greatly affects the results (Conti and Desideri, 2010). Therefore, even though no hits were identified in the TMEV GDVII assay, possibly due to toxicity towards the cells, there might be antiviral activity if tested in another cell line. This was not possible to investigate as BHK-21 cells are currently the only cell line susceptible to TMEV GDVII infection.

Similarly, compounds 2-6 and 8-9 in the MNP library were highly toxic to the BHK-21 cells as low cell viability readings were generated even at low concentrations such as 3.7 µM. Compound 11 was the only compound that possessed no cytotoxicity however, no antiviral activity was observed at these concentrations. Similar studies were performed whereby emodin, a natural anthraquinone, was investigated as an antiviral to treat infections caused by the picornavirus CV-B4 (Liu et al., 2013). The results showed that the compound decreased CV-B4 replication and entry into HEp-2 cells in a dose-dependent manner. In contrast to the TMEV GDVII assay, cytotoxicity was tested on HEp-2 cells by an MTT assay which showed that the highest non-toxic dose was 46.26 µM (Liu et al., 2013).

Another consideration when evaluating the results of these experiments is that the assay used can be described as a medium-throughput screen, as only 24 compounds were tested for antiviral activity. Placing this into perspective, the hit rate in a HTS, which screens thousands of compounds, is usually below 2 %. For example, the hit rates in HTSs against bluetongue virus were between 0.05 - 0.10 % (Li et al., 2009), influenza virus inhibition assays produced hit rates of 0.08 % and 0.022 % (Noah et al., 2007; Severson et al., 2008) and 0.01 % for a SARS-CoV HTS (Severson et al., 2007). Additionally, a study was published that described a HTS that aimed to identify quinone analogues as potential inhibitors of the picornavirus CV-B3, specifically targeting the 3C protease using a FRET assay (Jung et al., 2018). Initially, 6000 molecules were

screened, resulting in 81 molecules displaying inhibition above 64 %. After performing dose-response assays with the selected compounds, only two compounds exhibited significant antiviral activities (Jung et al., 2018). Thus, it was not unexpected that no hits were confirmed from the coumarin and MNP libraries in this study, especially since they have not been tested in picornaviruses.

The main aim of this chapter was achieved as the coumarin and MNP libraries of compounds were screened for TMEV GDVII antiviral activity. After the dose-response curves were generated, it concluded that most of the compounds were highly toxic to the BHK-21 cells, and no hits or antiviral activity against TMEV GDVII was discovered. Nevertheless, the assay was consistently robust as the Z'- factors indicated a reproducible and reliable assay. Therefore, the TMEV GDVII antiviral assay will benefit the drug discovery field as other compound libraries can now be screened for antiviral activity against this virus.

Chapter 6 General discussion and future work

Even though worldwide efforts are on their way to eradicate PV, several other picornaviruses are still a threat and are circulating globally. There have been outbreaks, accompanied by severe diseases, of PV, EV-A71 and EV-D68 in Asia, Europe, the UK and the USA and HPeV-A3 outbreaks in Australia (Solomon et al., 2010; Khatami et al., 2015; Pons-Salort et al., 2015; Sethi et al., 2022). More recently, an unexpected outbreak of FMDV occurred in South Africa, predominantly in KwaZulu-Natal, resulting in a temporary suspension of the movement of cattle in the entire country (Orabi, 2022). At present, there are no antiviral drugs against any picornavirus that the FDA has approved. Therefore, the pressure and urgency to develop and identify antivirals against these viruses have intensified. Picornaviruses share similarities in their genome structure and capsid organisation. As such, picornaviruses that are non-hazardous to humans without posing any biosafety concerns can be used as model systems, and in this case, TMEV GDVII was investigated. The overall aim of this study was to develop and optimise an antiviral screening assay using TMEV GDVII, which infects BHK-21 cells in culture.

The purpose of the first objective of this study was to validate the TMEV GDVII- BHK-21 replication system and perform preparatory experiments. Before attempting to develop the antiviral assay, it was essential to confirm that BHK-21 cells were susceptible to infection by TMEV GDVII. A CPE assay was conducted to distinguish non-infected from infected cells visually. This confirmed that the observed changes in cell morphology were triggered by TMEV GDVII infection and not cell senescence. Additionally, the onset and development of full CPE when infected at a high MOI was within 8 hpi, consistent with a study performed by Upfold et al. (2018). Furthermore, the plaque assays successfully quantified the number of infectious virus particles in the TMEV GDVII stock, making it possible to calculate the MOI that was required when optimising the parameters of the antiviral assay. The results from the plaque assays were similar to those described in previous studies that titred TMEV GDVII stocks (Jauka et al., 2010; Mutsvunguma et al., 2011). Several difficulties were encountered when performing the plaque assays before achieving acceptable results. Therefore, future experiments could investigate whether replacing the methocel with suspensions of a microcrystalline cellulose Avicel overlay

would improve the assay. It has been reported that using Avicel as an overlay medium in plaque assays is easier, more sensitive and faster than the popular methocel or agar overlays due to its low viscosity (Matrosovich et al., 2006; Yin et al., 2014). Lastly, indirect immunofluorescence and Western blot experiments using the previously generated antibodies against the TMEV GDVII VP1 capsid and 2C protein detected the presence of these viral proteins in TMEV GDVII infected cells but not in uninfected cells. This confirmed the infection of BHK-21 cells by TMEV GDVII, resulting in the utilisation of the replication system in the development of the antiviral assay.

Once the replication system was validated, the second objective was to identify the optimal parameters of a medium-throughput phenotypic CPE-based TMEV GDVII antiviral assay. In the initial stages of antiviral identification, a crucial step in antiviral drug discovery is to develop robust assays (Chai et al., 2015). Therefore, the first parameter that was examined was FBS, a traditional supplement used in cell culture generally between 5 - 15 % (Li et al., 2009). Since the assay required a relatively long incubation time, the risk of overgrowth was increased. Thus, 2 % was selected as the optimal FBS concentration as it generated a confluent monolayer without any signs of overgrowth. The subsequent experiment assessed the most suitable cell seeding density that yielded confluent monolayers with cells in the exponential log phase of growth. A 15000 cells/well density was identified as optimal since it produced confluent monolayers with a high fluorescence reading. The following two parameters, which included the MOI and endpoint of the assay, were tested simultaneously, and the most appropriate factors were chosen based on the calculated Z'-factors. The purpose of the experiment was to select the lowest MOI that yielded full CPE at the endpoint that yielded acceptable Z'- factors. Longer incubation times were included as it was necessary to choose a low MOI that would allow multiple viral replication cycles so that a variety of compounds that could potentially inhibit each stage of the lifecycle could be identified. Therefore, an MOI of 0.00625 and an endpoint of 72 hpi were the most optimal.

It should be noted that although cell-based assays are well-established tools for drug discovery as they offer data of higher value than target-based or biochemical assays, the characteristic biological complexity and variability of cells introduce drawbacks with assay design and execution (Beske and Goldbard, 2002). These include disparities when seeding cells, varying cell responses and the edge effect. The edge effect refers to a phenomenon which states that the contents in the peripheral wells of a plate evaporate quicker during longer incubations, such as 72 hpi. The thermal

gradients are highest around the edges of the plate, meaning that the outer wells reach 37 °C more rapidly than the innermost wells. This can cause a change in cell morphology, leading to a varied response in the compounds being tested (Lundholt et al., 2003). PBS was added to the peripheral wells in the TMEV GDVII assay to prevent this from occurring. However, when compounds were screened, the entire 96-well plate was utilised to maximise throughput, thereby introducing the risk of the edge effect. Instead of reducing throughput by excluding the outer wells, a study was published that described pre-incubating plates at RT for an hour after seeding cells. This allows the cells to settle to the bottom of the well, thereby reducing thermal gradients in the outer wells to control the edge effect (Lundholt et al., 2003). The phenotypic response, in this case, virus-induced CPE, determines the readout of the assay, which results in longer incubation times or endpoints compared to target-based assays. Therefore, artefacts caused by instruments such as incubators in shorter assays will be magnified with longer incubation times. The temperature, CO_2 levels and even plate positions must be closely monitored in the incubator to minimise any noise and variability that can deteriorate the assay performance (Maddox et al., 2008). Even though the TMEV GDVII antiviral assay consistently produced Z'-factors above 0.5, validating a robust assay performance, it would be worthwhile to explore whether decreasing the assay endpoint of 72 hpi would increase the hit rate from the compound libraries as suggested in a published study (Li et al., 2009). Endpoints below 72 hpi were tested when optimising the parameters of the assay, which showed that both 48 and 72 hpi produced acceptable Z'- factors, and for this reason, ITZ and DIP were also tested at these time points. However, when the compound libraries were screened, fluorescence was only measured after 72 hpi as this endpoint produced better Z'- factors. Therefore, future experiments could compare readouts taken after 48 hpi and whether decreasing the endpoint would improve the assay.

Finally, after the parameters were identified, an experiment was conducted whereby the assay robustness was validated with high reproducibility and low deviation using Z'- factors. This statistical metric compares the variability of both uninfected and infected controls to the difference in their means. Multiple replicates on a plate (intra-plate) and repeating the experiment independently (inter-plate) produced an average Z'- factor of 0.74, indicative of its high quality. This was important to perform, especially when numerous compounds were being screened. In this study, the compound libraries were only screened once, as low quantities of the compounds

were supplied. Thus, the assay needed to be robust enough to produce accurate, sensitive and reliable results.

When comparing the uninfected mock control (100 % viability) to the infected virus-alone control, it should be critiqued that the infected control yielded viability readings that were higher than expected (approximately 40 - 50 %). Upon visual examination under the microscope, the infected control generated a monolayer that illustrated 100 % CPE, where all cells appeared to be dead. Thus, lower viability readings below 50 % were expected when measured using resazurin. This could have been caused by cell debris or cells that visually appeared dead but were still metabolically active and able to take up and convert the resazurin, thereby increasing the fluorescence readouts. Future experiments could investigate whether rinsing cells with PBS before adding resazurin would reduce viability readings as dead cells would be removed (Smee et al., 2017). A study reported the antiviral activity of compounds against three unrelated RNA viruses (chikungunya, dengue and Junin) using four dyes, including resazurin (Smee et al., 2017). The study also evaluated how efficiently the dyes could distinguish the infected from the uninfected cells. It was estimated that in the dengue infection, cell viability appeared to be approximately 15 % in infected cells when examined under the microscope. Interestingly, resazurin fluorescence detected 32 % viability, almost double what was observed and similar to the results found in this study. In comparison, resazurin absorbance readings detected 16 %, which was the most accurate, and neutral red dye detected 24 % cell viability (Smee et al., 2017). Therefore, in the future, it would be interesting to compare different dyes or methods to detect cell viability, such as neutral red or measuring resazurin absorbance instead of fluorescence in the TMEV GDVII antiviral assay. Nevertheless, acceptable Z'-factors were still produced by measuring resazurin fluorescence readings confirming a robust TMEV GDVII assay.

At present, no inhibitor has been identified against TMEV GDVII. Thus, after optimising the assay parameters, the third objective involved investigating whether potential inhibitors possessed antiviral activity that could not only be used as a control when screening compounds but would also contribute to research on this virus. Before antiviral activity was tested, DMSO toxicity towards BHK-21 cells was investigated as the compounds were solubilised in this solution. The results generated were similar to other studies, which showed that DMSO concentrations above 1 % were toxic to BHK-21 cells (Tomeczkowski et al., 1993; Che et al., 2009; Li et al., 2009).

Consequently, when compounds were screened with the TMEV GDVII assay, the final DMSO concentrations were always kept lower than this concentration to prevent toxicity.

The chosen compounds, which included ITZ and DIP, were described in the literature as broad-spectrum cardiovirus inhibitors (Tonew and Dzeguze, 1977; Fata-Hartley and Palmenberg, 2005; Strating et al., 2015; Bauer et al., 2018). Therefore, after the assay parameters were optimised, it presented an opportunity to test these compounds against TMEV GDVII, another cardiovirus. Additionally, the anti-TMEV GDVII capsid antibody that was described in chapter 2 was found to neutralise the virus infection after a plaque reduction assay was performed (Upfold et al., 2018). Thus, the antibody was also examined as a possible control inhibitor for the antiviral assay. After generating dose-response curves, it was found that the anti-TMEV GDVII capsid antibody displayed potent antiviral activity against TMEV GDVII and no cytotoxicity against BHK-21 cells. Contrary to expectation, ITZ and DIP exhibited cytotoxicity at high concentrations but no inhibition of the virus. The antibody was thus selected as the most suitable control inhibitor for the antiviral assay. It should be noted that only two compounds were tested due to time constraints and logistics. Even though the antibody served as a sufficient control inhibitor, it is preferred to incorporate a control compound instead of a control antibody when screening other compounds for antiviral activity. The work performed in chapter 4 can be expanded in the future as plenty of other compounds could be examined for antiviral activity against TMEV GDVII. Compounds that have exhibited cardiovirus antiviral activity, such as pyrrolidine dithiocarbonate (PDTC), can be tested. PDTC was shown to inhibit EMCV (mengovirus) by disrupting viral RNA synthesis and polyprotein processing (Lanke et al., 2007). However, the SARS-CoV-2 pandemic resulted in a plethora of studies being published on antiviral strategies and broad-spectrum inhibitors against RNA viruses. It would be worthwhile to test whether some of these compounds would affect TMEV GDVII, which is also an RNA virus. Three nucleoside analogues stand out as remarkable broad-spectrum antivirals against RNA viruses, including remdesivir, an FDA-approved drug for the treatment of COVID-19 patients; ribavirin, an approved drug against HCV and favipiravir an approved drug in Japan against influenza T-705 (Crotty et al., 2000; Furuta et al., 2002; Graci and Cameron, 2006; Delang et al., 2018; Tchesnokov et al., 2019; Beigel et al., 2020; de Wit et al., 2020; Grein et al., 2020; Jeon et al., 2020; Geraghty et al., 2021).

The last experiment for this objective used the anti-TMEV GDVII capsid and anti-2C antibodies to detect the presence and expression of viral proteins after treating infected cells with ITZ, DIP or the anti-TMEV GDVII capsid antibody, considering that the compounds did not inhibit CPE. Western blot analysis detected viral proteins after treatment with ITZ, DIP and the infected control. As expected, no viral proteins were detected in cells treated with the anti-TMEV GDVII capsid antibody and uninfected control, supporting the conclusion that the antibody was the most appropriate control inhibitor of the three. This preliminary experiment presented a few flaws and drawbacks that could be improved in the future. The experiment could only detect whether viral proteins were present but failed to quantify the expression levels. This was due to an absence of an appropriate loading control which was not accessible at the time. When performing Western blotting experiments, the total amount of protein loaded into each well must be carefully controlled to ensure an accurate comparison of protein content between samples (Welinder and Ekblad, 2011). The most popular solution is to use antibodies that can detect housekeeping proteins that are continuously expressed as loading controls (Welinder and Ekblad, 2011; Nie et al., 2017). Common housekeeping proteins include β-actin, β-tubulin and glyceraldehyde 3-phosphate dehydrogenase (GAPDH) (Liu and Xu, 2006; Wu et al., 2012). Therefore, future experiments could include a loading control such as those mentioned above. Before using the protein as a loading control, it should be investigated whether their expression levels in BHK-21 cells are consistent when exposed to varying treatments. On another note, it would be interesting to perform immunofluorescence experiments after treating infected cells with the compounds and examining whether viral proteins could be detected at various times post-infection. This could then be compared to the results generated from the Western analysis.

Finally, the last objective of this study aimed to screen novel compounds from a coumarin and MNP library for antiviral activity against TMEV GDVII using the optimised assay from the previous chapters. No hits were determined as compounds displayed no inhibition of CPE. Considering that only 24 compounds were tested, it was not unexpected that no hits were discovered. High-throughput studies which screen thousands of compounds typically generate hit rates below 2 % (Noah et al., 2007; Severson et al., 2008; Li et al., 2009; Jung et al., 2018). Nevertheless, the current novel TMEV GDVII antiviral assay presented in this study can still be used to screen numerous relevant libraries of compounds which will benefit the drug discovery field against picornaviruses that can be FDA-approved or commercialised.

In conclusion, this study focused on developing and identifying a novel TMEV GDVII antiviral screening assay. After the TMEV GDVII-BHK-21 replication system was validated, it served as a foundation for the optimisation of the parameters of a medium-throughput TMEV GDVII antiviral assay to produce one that was robust and reproducible. Subsequently, the anti-TMEV GDVII capsid antibody was selected as the most suitable control inhibitor when screening compounds. Finally, after all the components of the assay were confirmed, it was possible to screen two libraries of novel compounds for antiviral activity. Even though no hits were discovered, this assay has great potential to screen numerous compound libraries. This is the first study to develop an assay using TMEV GDVII and provides a widespread platform for further studies and possibly high-throughput screening to be conducted. This study enhanced the current knowledge and contributed to the battle to discover and approve drugs against picornaviruses.

References

Abed, Y. and Boivin, G. (2008). New saffold cardioviruses in 3 children, Canada. *Emerging Infectious Diseases*, 14(5), pp. 834-836. doi: 10.3201/eid1405.071675.

Adamson, C. and Freed, E. (2009). Anti-HIV-1 therapeutics: From FDA-approved drugs to hypothetical future targets. *Molecular Interventions*, 9(2), pp. 70-74. doi: 10.1124/mi.9.2.5.

Agol, V. (2012). Cytopathic effects: virus-modulated manifestations of innate immunity? *Trends in Microbiology*, 20(12), pp. 570-576. doi: 10.1016/j.tim.2012.09.003.

Alam, Z., Al-Mahdi, Z., Zhu, Y., McKee, Z., Parris, D.S., Parikh, H.I., Kellogg, G.E., Kuchta, A. and McVoy, M.A. (2015). Anti-cytomegalovirus activity of the anthraquinone atanyl blue PRL. *Antiviral Research*, 114, pp. 86–95. doi: 10.1016/j.antiviral.2014.12.003.

Albulescu, L., Wubbolts, R., van Kuppeveld, F.J. and Strating, J.R. (2015). Cholesterol shuttling is important for RNA replication of coxsackievirus B3 and encephalomyocarditis virus. *Cellular Microbiology*, 17(8), pp. 1144-56. doi: 10.1111/cmi.12425.

Alhazmi, A., Nekoua, M.P., Mercier, A., Vergez, I., Sane, F., E.K. and Hober, D. (2022). Combating coxsackievirus B infections. *Reviews in Medical Virology*, 33(1), e2406. doi: https://doi.org/10.1002/rmv.2406.

Allahham, M., Lerman, A., Atar, D. and Birnbaum, Y. (2021). Why not dipyridamole: a review of current guidelines and re-evaluation of utility in the modern era. *Cardiovascular Drugs And Therapy*, 36(3), pp. 525-532. doi: 10.1007/s10557-021-07224-9.

Amanat, F., White, K. M., Miorin, L., Strohmeier, S., McMahon, M., Meade, P., Liu, C., Albrecht, R. A., Simon, V., Moran, T. and Krammer, F. (2020). An in vitro microneutralization assay for SARS-CoV-2 serology and drug screening. *Current Protocols in Microbiology*, 58(1). https://doi.org/10.1002/cpmc.108.

Archila, E. D., López, L. S., Castellanos, J. E. and Calvo, E. P. (2022). Molecular and biological characterization of an Asian-American isolate of Chikungunya virus. *Public Library of Science: ONE*, 17(4), e0266450. doi: https://doi.org/10.1371/journal.pone.0266450.

Arita, M., Kojima, H., Nagano, T., Okabe, T., Wakita, T., Shimizu, H. (2013). Oxysterol-binding protein family I is the target of minor enviroxime-like compounds. *Journal of Virology,* 87(8), pp. 4252-4260. doi: 10.1128/jvi.03546-12.

Arrowsmith, J. (2011). Trial watch: Phase II failures: 2008-2010. *Nature reviews. Drug discovery*, 10(5), pp. 328-329. doi: https://europepmc.org/article/med/21532551.

Aslantürk, O.S. (2018). In Vitro Cytotoxicity and Cell Viability Assays: Principles, Advantages, and Disadvantage. In, *Genotoxicity: A predictable risk to our actual world*, Larramendy, M.L. and Soloneski, S. (Eds.). Intech Open, Turkey, pp. 9-10.

Baggen, J., Thibaut, H. J., Strating, J. R. P. M. and van Kuppeveld, F. J. M. (2018). The life cycle of non-polio enteroviruses and how to target it. *Nature Reviews Microbiology*, 16(6), pp. 368-381. doi: 10.1038/s41579-018-0005-4.

Baker, M. (2016). Reproducibility: Respect your cells! *Nature*, 537, pp. 433–435. doi: https://doi.org/10.1038/537433a.

Bandyopadhyay, A.S., Garon, J., e Seib, K. and Orenstein, W.A. (2015). Polio vaccination: past, present and future. *Future Microbiology*, 10(5), pp. 791-808. doi: https://doi.org/10.2217/fmb.15.19.

Basavappa, R., Filman, D., Syed, R., Flore, O., Icenogle, J. and Hogle, J. (1994). Role and mechanism of the maturation cleavage of VP0 in poliovirus assembly: Structure of the empty capsid assembly intermediate at 2.9 Å resolution. *Protein Science*, 3(10), pp. 1651-1669. doi: 10.1002/pro.5560031005.

Bauer, L., Ferla, S., Head, S. A., Bhat, S., Pasunooti, K. K., Shi, W. Q., Albulescu, L., Liu, J. O., Brancale, A., van Kuppeveld, F. J. and Strating, J. R. (2018). Structure-activity relationship study of itraconazole, a broad-range inhibitor of picornavirus replication that targets oxysterol-binding protein (OSBP). *Antiviral Research*, 156, pp. 55-63. doi: 10.1016/j.antiviral.2018.05.010.

Bedard, K. and Semler, B. (2004). Regulation of picornavirus gene expression. *Microbes and Infection*, 6(7), pp. 702-713. doi: 10.1016/j.micinf.2004.03.001.

Bedoya, L.M., Beltrán, M., Sancho, R., Olmedo, D.A., Sánchez-Palomino, S., del Olmo, E., López-Pérez, J.L., Muñoz, E., San Feliciano, A. and Alcamí, J. (2005). 4-Phenylcoumarins as HIV transcription inhibitors. *Bioorganic and Medicinal Chemistry Letters*, 15(20), pp. 4447-4450. doi: 10.1016/j.bmcl.2005.07.041.

Beigel, J.H., Tomashek, K.M., Dodd, L.E., Mehta, A.K., Zingman, B.S., Kalil, A.C., Hohmann, E., Chu, H.Y., Luetkemeyer, A., Kline, S., Lopez de Castilla, D., Finberg, R.W., Dierberg, K., Tapson, V., Hsieh, L., Patterson, T.F., Paredes, R., Sweeney, D.A., Short, W.R., Touloumi, G., Lye, D.C., Ohmagari, N., Oh, M.D., Ruiz-Palacios, G.M., Benfield, T., Fätkenheuer, G., Kortepeter, M.G., Atmar, R.L., Creech, C.B., Lundgren, J., Babiker, A.G., Pett, S., Neaton, J.D, Burgess, T.H., Bonnett, T., Green, M., Makowski, M., Osinusi, A., Nayak, S. and Lane, H.C. (2020). Remdesivir for the treatment of covid-19 - Final Report. *The New England Journal of Medicine*, 383(19), pp. 1813-1826. doi: 10.1056/NEJMoa2007764.

Belov, G. A., Nair, V., Hansen, B. T., Hoyt, F. H., Fischer, E. R. and Ehrenfeld, E. (2012) Complex dynamic development of poliovirus membranous replication complexes. *Journal of Virology*, 86(1), pp. 302-312. doi: 10.1128/jvi.05937-11.

Berg, K., Zhai, L., Chen, M., Kharazmi, A. and Owen, T.C. (1999). The use of a water soluble formazan complex to quantitate the cell number and mitochondrial function of Leishmania major promastigotes. *Parasitology Research*, 80, pp. 235-239. doi: 10.1007/BF00932680.

Beske, O. and Goldbard, S. (2002). High-throughput cell analysis using multiplexed array technologies. *Drug Discovery Today*, 7(18), pp. S131-S135. doi: 10.1016/s1359-6446(02)02388-7.

Bigouette, J. P., Wilkinson, A. L., Tallis, G., Burns, C. C., Wassilak, S. G. F. and Vertefeuille, J. F. (2021). Progress toward polio eradication — worldwide, January 2019–June 2021. *MMWR. Morbidity and Mortality Weekly Report*, 70(34), pp. 1129-1135. doi: 10.15585/mmwr.mm7034a1.

Biota. (2015). Biota doses first patient in Phase IIb trial of vapendavir to treat HRV. Available at: https://www.clinicaltrialsarena.com/news/newsbiota-doses-first-patient-in-phase-iib-trial-of-vapendavir-to-treat-hrv-4525170/ (Accessed: 4 January 2022).

Boivin, G., Abed, Y. and Boucher, F. (2005). Human parechovirus 3 and neonatal infections. *Emerging Infectious Diseases*, 11(1), pp. 103-107. doi: 10.3201/eid1101.040606.

Bolken, T.C., Laquerre, S., Zhang, Y., Bailey, T.R., Pevear, D.C., Kickner, S.S., Sperzel, L.E., Jones, K.F., Warren, T.K., Lund, S.A., Kirkwood-Watts, D.L., King, D.S., Shurtleff, A.C., Guttieri, M.C., Deng, Y., Bleam, M. and Hruby, D.E. (2006). Identification and characterization of potent small molecule inhibitor of hemorrhagic fever New World arenaviruses. *Antiviral Research*, 69(2), pp. 86-97. doi: 10.1016/j.antiviral.2005.10.008.

Cao, J., Isaacson, J., Patick, A. K., & Blair, W. S. (2005). High-throughput human immunodeficiency virus type 1 (HIV-1) full replication assay that includes HIV-1 VIF as an antiviral target. *Antimicrobial Agents and Chemotherapy*, 49(9), pp. 3833-3841. doi: 10.1128/aac.49.9.3833-3841.2005.

Carocci, M. and Bakkali-Kassimi, L. (2012). The encephalomyocarditis virus. *Virulence*, 3(4), pp. 351-367. doi: 10.4161/viru.20573.

Castro, C.M.O., Cruz, A.C.R., Da Silva, E.E. and Gomes, M.L.C. (2005). Molecular and seroepidemiologic studies of Enterovirus 71 infection in the State of Pará, Brazil. *Revista do Instituto de Medicina Tropical de São Paulo,* 47(2), pp. 65-71.

Cathcart, A., Baggs, E. and Semler, B. (2015) Picornaviruses: Pathogenesis and molecular biology. *Reference Module in Biomedical Sciences*. doi: 10.1016/b978-0-12-801238-3.00272-5.

Chai, S. C., Goktug, A. N. and Chen, T. (2015). Assay validation in high throughput screening – from concept to application. In, *Drug Discovery and Development - From Molecules to Medicine*, Vallisuta, O. and Olimat, S. (Eds.). Intech Open, Thailand.

Che, P., Wang, L. and Li, Q. (2009). The development, optimization and validation of an assay for high throughput antiviral drug screening against Dengue virus. *International Journal of Clinical and Experimental Medicine*, 2(4), pp. 363-373. doi: https://www.ncbi.nlm.nih.gov/pmc/articles.

Chen, Y., Zeng, S., Hsu, J. T., Horng, J., Yang, H., Shih, S., Chu, Y. and Wu, T. (2008) Amantadine as a regulator of internal ribosome entry site. *Acta Pharmacologica Sinica*, 29(11), pp. 1327-1333. doi: 10.1111/j.1745-7254.2008.00876.x.

Chera, A. and Tanca, A. (2022). Remdesivir: the first FDA-approved anti-COVID-19 treatment for young children. *Discoveries*, 10(2). doi: https://www.ncbi.nlm.nih.gov/pmc/articles/PMC9491826/.

Chidambaram, S., El-Sheikh, M., Alfarhan, A., Radhakrishnan, S. and Akbar, I. (2021). Synthesis of novel coumarin analogues: Investigation of molecular docking interaction of SARS-CoV-2 proteins with natural and synthetic coumarin analogues and their pharmacokinetics studies. *Saudi Journal Of Biological Sciences*, 28(1), pp. 1100-1108. doi: 10.1016/j.sjbs.2020.11.03.

Chu, J.J., Lee, R.C., Ang, M.J., Wang, W.L., Lim, H.A., Wee, J.L., Joy, J., Hill, J. and Brian Chia, C.S. (2015). Antiviral activities of 15 dengue NS2B-NS3 protease inhibitors using a human cell-based viral quantification assay. *Antiviral Research*, 118, pp. 68–74. doi: 10.1016/j.antiviral.2015.03.010.

Chuchaona, W., Khamrin, P., Yodmeeklin, A., Saikruang, W., Kongsricharoern, T., Ukarapol, N., Okitsu, S., Hayakawa, S., Ushijima, H. and Maneekarn, N. (2015). Detection and characterisation of a novel human parechovirus genotype in Thailand. *Infection, Genetics and Evolution*, 31, pp. 300-304. doi: 10.1016/j.meegid.2015.02.003.

Conti, C. and Desideri, N. (2009). Synthesis and antirhinovirus activity of new 3-benzyl chromene and chroman derivatives. *Bioorganic and Medicinal Chemistry*, 17(10), pp. 3720-3727. doi: 10.1016/j.bmc.2009.03.051.

Conti, C. and Desideri, N. (2010). New 4H-chromen-4-one and 2H-chromene derivatives as anti-picornavirus capsid-binders. *Bioorganic and Medicinal Chemistry*, 18(17), pp. 6480-6488. doi: 10.1016/j.bmc.2010.06.103.

Crotty, S., Cameron, C. and Andino, R. (2002). Ribavirin's antiviral mechanism of action: lethal mutagenesis? *Journal of Molecular Medicine*, 80(2), pp. 86-95. doi: 10.1007/s00109-001-0308-0.

Crotty, S., Maag, D., Arnold, J. J., Zhong, W., Lau, J. Y. N., Hong, Z., Andino, R. and Cameron, C. E. (2000). The broad-spectrum antiviral ribonucleoside ribavirin is an RNA virus mutagen. *Nature Medicine*, 6(12), pp. 1375-1379. doi: 10.1038/82191.

Cruz, D. J. M., Bonotto, R. M., Gomes, R. G. B., da Silva, C. T., Taniguchi, J. B., No, J. H., Lombardot, B., Schwartz, O., Hansen, M. A. E. and Freitas-Junior, L. H. (2013). Identification of novel compounds inhibiting chikungunya virus-induced cell death by high throughput screening of a kinase inhibitor library. *Public Library of Science: Neglected Tropical Diseases*, 7(10). doi: 10.1371/journal.pntd.0002471.

Cui, F., Liang, X., Wang, F., Zheng, H., Hutin, Y. J. and Yang, W. (2014). Development, production, and postmarketing surveillance of hepatitis A vaccines in China. *Journal of Epidemiology*, 24(3), pp. 169-177. doi: 10.2188/jea.je20130022.

Da Costa, E.C., Amorim, R., da Silva, F.C., Rocha, D.R., Papa, M.P., de Arruda, L.B., Mohana-Borges, R., Ferreira, V.F., Tanuri, A., da Costa, L.J. and Ferreira, S.B. (2013). Synthetic 1,4-pyran naphthoquinones are potent inhibitors of dengue virus replication. *Public Library of Science: ONE*, 8(12), e82504. doi: 10.1371/journal.pone.0082504.

Dai, W., Bi, J., Li, F., Wang, S., Huang, X., Meng, X., Sun, B., Wang, D., Kong, W., Jiang, C. and Su, W. (2019). Antiviral efficacy of flavonoids against enterovirus 71 infection in vitro and in newborn mice. *Viruses*, 11(7), pp. 625. doi: 10.3390/v11070625.

de Jesus, N. (2007). Epidemics to eradication: the modern history of poliomyelitis. *Virology Journal*, 4(1), pp. 70. doi: 10.1186/1743-422x-4-70.

de Wit, E., Feldmann, F., Cronin, J., Jordan, R., Okumura, A., Thomas, T., Scott, D., Cihlar, T, and Feldmann, H. (2020). Prophylactic and therapeutic remdesivir (GS-5734) treatment in the rhesus macaque model of MERS-CoV infection. *Proceedings of the National Academy of Sciences of the United States of America*, 117(12), pp. 6771-6776. doi: 10.1073/pnas.1922083117.

Debing, Y., Kaplan, G., Neyts, J. and Jochmans, D. (2013). Rapid and convenient assays to assess potential inhibitory activity on in vitro hepatitis A replication. *Antiviral Research*, 98(2), pp. 325-331. doi: 10.1016/j.antiviral.2013.03.016.

Delang, L., Abdelnabi, R. and Neyts, J. (2018). Favipiravir as a potential countermeasure against neglected and emerging RNA viruses. *Antiviral Research*, 153, pp. 85–94. doi: 10.1016/j.antiviral.2018.03.003.

Delhaye, S., Van Pesch, V. and Michiels, T. (2004). The leader Protein of Theiler's Virus Interferes with Nucleocytoplasmic Trafficking of Cellular Proteins. *Journal of Virology*, 78(8), pp. 4357-4362. doi: https://journals.asm.org/doi/full/10.1128/JVI.78.8.4357-4362.

Domingo, E., Baranowski, E., Escarmís, C., Sobrino, F. and Holland, J. J. (2014). Error frequencies of picornavirus rna polymerases: evolutionary implications for virus populations. *Molecular Biology of Picornavirus*, pp. 285-298. doi: 10.1128/9781555817916.ch23.

Dorobantu, C. M., Albulescu, L., Harak, C., Feng, Q., van Kampen, M., Strating, J. R. P. M., Gorbalenya, A. E., Lohmann, V., van der Schaar, H. M. and van Kuppeveld, F. J. M. (2015). Modulation of the host lipid landscape to promote RNA virus replication: The picornavirus encephalomyocarditis virus converges on the pathway used by Hepatitis C Virus. *Public Library of Science: Pathogens*, 11(9), e1005185. doi: 10.1371/journal.ppat.1005185.

Dragovich, P.S., Prins, T.J., Zhou, R., Johnson, T.O., Hua, Y., Luu, H.T., Sakata, S.K., Brown, E.L., Maldonado, F.C., Tuntland, T., Lee, C.A., Fuhrman, S.A., Zalman, L.S., Patick, A.K., Matthews, D.A., Wu, E.Y., Guo, M., Borer, B.C., Nayyar, N.K., Moran, T., Chen, L., Guzman, M.C., Dovalsantos, E.Z., Lee, S., McGee, K., Mohajeri, M., Liese, A., Tao, J., Kosa, M.B., Liu, B., Batugo, M.R., Gleeson, J.R., Wu, Z.P., Liu, J., Meador, J.W. and Ferre, R.A. (2003). Structure-based design, synthesis, and biological evaluation of irreversible human rhinovirus 3C protease inhibitors. 8. Pharmacological optimisation of orally bioavailable 2-pyridone-containing peptidomimetics. *Journal of Medicinal Chemistry*, 46(21), pp. 4572–4585. doi: https://doi.org/10.1021/jm030166l.

Duellman, S.J., Zhou, W., Meisenheimer, P., Vidugiris, G., Cali, J.J., Gautam, P., Wennerberg, K. and Vidugiriene, J. (2015). Bioluminescent, nonlytic, real-time cell viability assay and use in inhibitor screening. *Assay and Drug Development Technologies*, 13(8), pp. 456-465. doi: 10.1089/adt.2015.669.

Edwards, M. R., Bartlett, N. W., Hussell, T., Openshaw, P. and Johnston, S. L. (2012). The microbiology of asthma. *Nature Reviews Microbiology*, 10(7), pp. 459-471. doi: 10.1038/nrmicro2801.

Egorova, A., Kazakova, E., Jahn, B., Ekins, S., Makarov, V. and Schmidtke, M. (2020). Novel pleconaril derivatives: Influence of substituents in the isoxazole and phenyl rings on the antiviral activity against enteroviruses. *European Journal of Medicinal Chemistry*, 188, pp. 112007. doi: 10.1016/j.ejmech.2019.112007.

Emerson, S. U., Nguyen, H., Graff, J., Stephany, D. A., Brockington, A. and Purcell, R. H. (2004). In vitro replication of hepatitis E virus (HEV) genomes and of an HEV replicon expressing green fluorescent protein. *Journal of Virology,* 78(9), pp. 4838-4846. doi: 10.1128/jvi.78.9.4838-4846.2004.

Erb, R. and Ehlers, M. (1950). Resazurin reducing time as an indicator of bovine semen fertilizing capacity. *Journal of Dairy Science*, 33(12), pp. 853-864. doi: 10.3168/jds.s0022-0302(50)91981-3.

Erdem, R., De Coster, I., Withanage, K., Mercer, L. D., Marchant, A., Taton, M., Cools, N., Lion, E., Cassels, F., Higgins, D., Ivinson, K., Locke, E., Mahmood, K., Wright, P. F., Gast, C., White, J. A., Ackerman, M. E., Konopka-Anstadt, J. L., Mainou, B. A. and Van Damme, P. (2023). Safety, tolerability, and immunogenicity of inactivated poliovirus vaccine with or without E.coli double mutant heat-labile toxin (dmLT) adjuvant in healthy adults; a phase 1 randomized study. *Vaccine*. doi: 10.1016/j.vaccine.2023.01.048.

Faridi, M.M., Shah, N., Ghosh, T.K., Sankaranarayanan, V.S., Arankalle, V., Aggarwal, A., Sathiyasekaran, M., Bhattacharya, N., Vasanthi, T., Chatterjee, S., Choudhury, J. and Mitra, M. (2009). Immunogenicity and safety of live attenuated hepatitis A vaccine: a multicentric study. *Indian Pediatrics*., 46(1), pp. 29-34. PMID: 19179715.

Fata-Hartley, C.L. and Palmenberg, A.C. (2005). Dipyridamole reversibly inhibits mengovirus RNA replication. *Journal of Virology*, 79(17), pp. 11062-11070. doi: 10.1128/JVI.79.17.11062-11070.2005.

Foglia, E. A., Pezzoni, G., Bonilauri, P., Torri, D., Grazioli, S. and Brocchi, E. (2023). A recent view about encephalomyocarditis virus circulating in compartmentalised animal population in Northern Italy. *Scientific Reports*, 13(1). doi: 10.1038/s41598-023-27828-5.

Francisco-Velilla, R., Embarc-Buh, A., Abellan, S. and Martinez-Salas, E. (2022). Picornavirus translation strategies. *FEBS Open Bio*, 12: pp. 1125-1141. doi: https://doi.org/10.1002/2211-5463.13400.

Freundt, E., Drappier, M. and Michiels, T. (2018). Innate immune detection of cardioviruses and viral disruption of interferon signaling, *Frontiers in Microbiology*. doi: 10.3389/fmicb.2018.02448.

Furuse, Y., Chaimongkol, N., Okamoto, M., Imamura, T., Saito, M., Tamaki, R., and Saito, M. (2015). Molecular epidemiology of enterovirus D68 from 2013 to 2014 in Philippines. *Journal of Clinical Microbiology*, 53(3), pp. 1015-1018. doi: doi/full/10.1128/JCM.03362-14.

Furuta, Y., Takahashi, K., Fukuda, Y., Kuno, M., Kamiyama, T., Kozaki, K., Nomura, N., Egawa, H., Minami, S., Watanabe, Y., Narita, H. and Shiraki, K. (2002). In vitro and in vivo activities of anti-influenza virus compound T-705. *Antimicrobial Agents and Chemotherapy*, 46(4), pp. 977-981. doi: 10.1128/AAC.46.4.977-981.2002.

Gao, Q., Yuan, S., Zhang, C., Wang, Y., Wang, Y., He, G., Zhang, S., Altmeyer, R. and Zou, G. (2015). Discovery of itraconazole with broad-spectrum *in vitro* anti enterovirus activity that targets nonstructural protein 3A. *Antimicrobial Agents and Chemotherapy*, 59(5), pp. 2654–2665. doi: https://doi.org/10.1128/aac.05108-14.

Gazina, E.V., Smidansky, E.D., Holien, J.K., Harrison, D.N., Cromer, B.A., Arnold, J.J., Parker, M.W., Cameron, C.E. and Petrou, S. (2011). Amiloride is a competitive inhibitor of coxsackievirus b3 rna polymerase. *Journal of Virology*, 85(19), pp. 10364-10374. doi: https://journals.asm.org/doi/full/10.1128/JVI.05022-11.

Geller, R., Vignuzzi, M., Andino, R. and Frydman, J. (2007). Evolutionary constraints on chaperone-mediated folding provide an antiviral approach refractory to development of drug resistance. *Genes & Development*, 21(2), pp. 195-205. doi: 10.1101/gad.1505307.

Geraghty, R., Aliota, M. and Bonnac, L. (2021). Broad-spectrum antiviral strategies and nucleoside analogues. *Viruses*, 13(4), pp. 667. doi: 10.3390/v13040667.

Gerhauser, I., Hansmann, F., Ciurkiewicz, M., Löscher, W. and Beineke, A. (2019). Facets of theiler's murine encephalomyelitis virus-induced diseases: an update. *International Journal of Molecular Sciences*, 20(2), pp. 448. doi: 10.3390/ijms20020448.

Gibbs, C.R. and Lip, G.Y. (1998). Do we still need dipyridamole? *British Journal of Clinical Pharmacology*, 45(4), pp. 323-328. doi: 10.1046/j.1365-2125.1998.t01-1-00677.x.

Glanville, N. and Johnston, S. (2015). Challenges in developing a cross-serotype rhinovirus vaccine. *Current Opinion in Virology*, 11, pp. 83-88. doi: 10.1016/j.coviro.2015.03.004.

Goegan, P., Johnson, G. and Vincent, R. (1995). Effects of serum protein and colloid on the alamarBlue assay in cell cultures. *Toxicology in Vitro*, 9(3), pp. 257-266. doi: 10.1016/0887-2333(95)00004-r.

Graci, J.D. and Cameron, C.E. (2006). Mechanisms of action of ribavirin against distinct viruses. *Reviews in Medical Virology*, 16, pp. 37–48. doi: 10.1002/rmv.483.

Grant, R.A., Filman, D.J., Fujinami, R.S., Icenogle, J.P. and Hogle, J.M. (1992). Three-dimensional structure of Theiler virus. *Proceedings of the National Academy of Sciences*, 89, pp. 2061–2065. doi: 10.1073/pnas.89.6.2061.

Green, N., D Ott, R., J Isaacs, R. and Fang, H. (2008). Cell-based assays to identify inhibitors of viral disease. *Expert Opinion on Drug Discovery,* 3(6), pp. 671-676. doi: 10.1517/17460441.3.6.671.

Grein, J., Ohmagari, N., Shin, D., Diaz, G., Asperges, E., Castagna, A., Feldt, T., Green, G., Green, M. L., Lescure, F., Nicastri, E., Oda, R., Yo, K., Quiros-Roldan, E., Studemeister, A., Redinski, J., Ahmed, S., Bernett, J., Chelliah, D., Chen, D., Chihara, S., Cohen, S. H., Cunningham, J., D'Arminio Monforte, A., Ismail, S., Kato, H., Lapadula, G., L'Her, E., Maeno, T., Majumder, S., Massari, M., Mora-Rillo, M., Mutoh, Y., Nguyen, D., Verweij, E., Zoufaly, A., Osinusi, A. O., DeZure, A., Zhao, Y., Zhong, L., Chokkalingam, A., Elboudwarej, E., Telep, L., Timbs, L., Henne, I., Sellers, S., Cao, H., Tan, S. K., Winterbourne, L., Desai, P., Mera, R., Gaggar, A., Myers, R. P., Brainard, D. M., Childs, R. and Flanigan, T. (2020). Compassionate use of remdesivir for patients with severe covid-19. *New England Journal of Medicine*, 382(24), pp. 2327-2336. doi: 10.1056/nejmoa2007016.

Gu, L., Schneller, S. and Li, Q. (2013). Assays for the identification of novel antivirals against bluetongue virus. *Journal of Visualized Experiments*, (80). doi: 10.3791/50820.

Hampton, L. M., Farrell, M., Ramirez-Gonzalez, A., Menning, L., Shendale, S., Lewis, I., Rubin, J., Garon, J., Harris, J., Hyde, T., Wassilak, S., Patel, M., Nandy, R., Chang-Blanc, D., and Immunization systems

management group of the Global Polio Eradication Initiative. (2016). Cessation of trivalent oral poliovirus vaccine and introduction of inactivated poliovirus vaccine — worldwide. *Morbidity and Mortality Weekly Report*, 65(35), pp. 934–938. doi: https://www.jstor.org/stable/24858956.

Han, Y., Mesplède, T., Xu, H., Quan, Y. and Wainberg, M.A. (2018). The antimalarial drug amodiaquine possesses anti-ZIKA virus activities. *Journal of Medical Virology*, 90, pp. 796– 802. doi:https://doi.org/10.1002/jmv.25031.

Hannemann, H. (2020). Viral replicons as valuable tools for drug discovery. *Drug Discovery Today*, 25(6), pp. 1026-1033. doi: 10.1016/j.drudis.2020.03.010.

Hao, T., Li, Y., Fan, S., Li, W., Wang, S., Li, S., Cao, R. and Zhong, W. (2019). Design, synthesis and pharmacological evaluation of a novel mtor-targeted anti-ev71 agent. *European Journal of Medicinal Chemistry*, 175, pp. 172–186. doi: https://doi.org/10.1016/j.ejmech.2019.04.048.

Hardham, J. M., Krug, P., Pacheco, J. M., Thompson, J., Dominowski, P., Moulin, V., Gay, C. G., Rodriguez, L. L. and Rieder, E. (2020). Novel foot-and-mouth disease vaccine platform: Formulations for safe and DIVA-compatible FMD vaccines with improved potency. *Frontiers in Veterinary Science*, 7. doi: 10.3389/fvets.2020.554305.

Harvala, H. and Simmonds, P. (2009). Human parechoviruses: Biology, epidemiology and clinical significance. *Journal of Clinical Virology*, 45(1), pp. 1-9. doi: 10.1016/j.jcv.2009.03.009.

Hayden, F. G., Herrington, D. T., Coats, T. L., Kim, K., Cooper, E. C., Villano, S. A., Liu, S., Hudson, S., Pevear, D. C., Collett, M. and McKinlay, M. (2003). Efficacy and safety of oral pleconaril for treatment of colds due to picornaviruses in adults: Results of 2 double-blind, randomized, placebo-controlled trials. *Clinical Infectious Diseases*, 36(12), pp. 1523-1532. doi: 10.1086/375069.

Hayden, F.G., Coats, T., Kim, K., Hassman, H.A., Blatter, M.M., Zhang, B. and Liu, S. (2002). Oral pleconaril treatment of picornavirus-associated viral respiratory illness in adults: efficacy and tolerability in phase II clinical trials. *Antiviral therapy*, 7(1), pp.53-65. doi: https://doi.org/10.1177/135965350200700107.

Heikkinen, T. and Järvinen, A. (2003). The common cold. *The Lancet*, 361(9351), pp. 51-59. doi: 10.1016/s0140-6736(03)12162-9.

Hossain, M., Mori, I., Dong, L., Liu, B. and Kimura, Y. (2007). Fetal calf serum inhibits virus genome expression in Madin-Darby canine kidney cells persistently infected with influenza A virus. *Medical Microbiology And Immunology*, 197(1), pp. 21-27. doi: 10.1007/s00430-007-0054-1.

Hossan, M.S., Fatima, A., Rahmatullah, M., Khoo, T.J., Nissapatorn, V., Galochkina, A.V., Slita, V., Shtro, A.A., Nikolaeva, V.V., Zarubaev, V.V. and Wiart, C. (2018). Antiviral activity of Embelia ribes Burm. f. against influenza virus in vitro. *Archives of Virology*, 163(8), pp. 2121–2131. doi: 10.1007/s00705-018-3842-6.

Hsu, N.Y., Ilnytska, O., Belov, G., Santiana, M., Chen, Y. H., Takvorian, P. M., Pau, C., van der Schaar, H., Kaushik-Basu, N., Balla, T., Cameron, C.E., Ehrenfeld, E., van Kuppeveld, F.J.M. and Altan-Bonnet, N. (2010). Viral reorganisation of the secretory pathway generates distinct organelles for RNA replication. *Cell,* 141(5), pp. 799–811. doi: 10.1016/j.cell.2010.03.050.

Hu, Y., Ma, C. and Wang, J. (2022). Cytopathic effect assay and plaque assay to evaluate *in vitro* activity of antiviral compounds against human coronaviruses 229e, oc43, and nl63. *Bio-Protocol*, 12(3), e4314. doi: 10.21769/BioProtoc.4314.

Hu, Y., Zeng, G., Chu, K., Zhang, J., Han, W., Zhang, Y., Li, J. and Zhu, F. (2018). Five-year immunity persistence following immunization with inactivated enterovirus 71 type (EV71) vaccine in healthy children: A further observation. *Human Vaccines & Immunotherapeutics*, 14(6), pp. 1517-1523. doi: 10.1080/21645515.2018.1442997.

Hughes, J., Rees, S., Kalindjian, S. and Philpott, K. (2011). Principles of early drug discovery. *British Journal of Pharmacology*, 162(6), pp. 1239-1249. doi: 10.1111/j.1476-5381.2010.01127.x.

Ianevski, A., Zusinaite, E., Tenson, T., Oksenych, V., Wang, W., Afset, J. E., Bjørås, M. and Kainov, D. E. (2022). Novel synergistic anti-enteroviral drug combinations. *Viruses*, 14(9), pp. 1866. doi: 10.3390/v14091866.

ICTV. (2022). Available at: https://talk.ictvonline.org/ (Accessed: 3 February 2022).

Iki, S., Yokota, S., Okabayashi, T., Yokosawa, N., Nagata, K. and Fujii, N. (2005). Serum-dependent expression of promyelocytic leukemia protein suppresses propagation of influenza virus. *Virology*, 343(1), pp. 106-115. doi: 10.1016/j.virol.2005.08.010.

Irvine, J. D., Takahashi, L., Lockhart, K., Cheong, J., Tolan, J. W., Selick, H. and Grove, J. (1999). MDCK (Madin-Darby Canine Kidney) Cells: A tool for membrane permeability screening. *Journal Of Pharmaceutical Sciences*, 88(1), pp. 28-33. doi: 10.1021/js9803205.

Jackson, T. and Belsham, G. (2021). Picornaviruses: A view from 3A. *Viruses*, 13(3), pp. 456. doi: 10.3390/v13030456.

Jackson, T., Sheppard, D., Denyer, M., Blakemore, W. and King, A.M. (2000). The epithelial integrin αvβ6 is a receptor for foot-and-mouth disease virus. *Journal of virology*, 74(11), pp. 4949-4956. doi: https://journals.asm.org/doi/full/10.1128/JVI.74.11.4949-4956.2000.

Jauka, T., Mutsvunguma, L., Boshoff, A., Edkins, A.l. and Knox, C. (2010). Localisation of Theiler's murine encephalomyelitis virus protein 2C to the Golgi apparatus using antibodies generated against a peptide region. *Journal of Virological Methods,* 168(1-2), pp. 162-169. doi: 10.1016/j.jviromet.2010.05.009.

Jeon, S., Ko, M., Lee, J., Choi, I., Byun, S. Y., Park, S., Shum, D. and Kim, S. (2020). Identification of antiviral drug candidates against SARS-COV-2 from FDA-approved drugs. *Antimicrobial Agents and Chemotherapy*, 64(7). doi: https://doi.org/10.1128/aac.00819-20.

Jiang, P., Liu, Y., Ma, H., Paul, A. V. and Wimmer, E. (2014). Picornavirus Morphogenesis. *Microbiology and Molecular Biology Reviews*, 78(3), pp. 418-437. doi: 10.1128/mmbr.00012-14.

Jiang, W.P., Wang, Y.L., Chen, W.Y., Xu, W.G., Chen, J.T., Wang, X., Liu, Y. and Yin, W.D. (2008). Immunogenicity and safety of three consecutive lots on an inactivated hepatitis A vaccine: a double-blind, immunogenicity and safety of three consecutive lots on a inactivated hepatitis A vaccine:a double-blind, randomized and controlled trial in children. *Zhonghua Liu Xing Bing Xue Za Zhi*, 29(6), pp. 556-9. PMID: 19040036.

Johannessen, I. and Burns, S.M. (2012). Picornaviruses: meningitis; paralysis; rashes; intercostal myositis; myocarditis; infectious hepatitis; common cold. *Medical microbiology,* pp. 483-496.

John, C.K. (1939). Place of the methylene blue and resazurin reduction tests in a milk control program. *American Journal of Public Health and the Nation's Health*, 29(3), pp. 239–247. doi: 10.2105/ajph.29.3.239.

Johns, H.L., Berryman, S., Monaghan, P., Belsham, G.J. and Jackson, T. (2009). A dominant negative mutant of rab5 inhibits infection of cells by foot-and-mouth disease virus; implications for virus entry. *Journal of Virology,* 83(12), pp. 6247–6256. doi: https://journals.asm.org/doi/epub/10.1128/JVI.02460-08.

Johnston, G. (2010). Automated handled instrument improves counting precision across multiple cell lines. *BioTechniques*, 48, pp. 325-327.

Jones, M.S., Lukashov, V.V., Ganac, R.D. and Schnurr, D.P. (2007). Discovery of a novel human picornavirus in a stool sample from a pediatric patient presenting with fever of unknown origin, *Journal of Clinical Microbiology*, 45(7), pp. 2144-2150. doi: doi/full/10.1128/JCM.00174-07.

Jung, E., Lee, J., Kim, H. J., Ryu, C., Lee, K., Kim, M., Lee, C. and Go, Y. Y. (2018). Identification of quinone analogues as potential inhibitors of picornavirus 3C protease in vitro. *Bioorganic & Medicinal Chemistry Letters*, 28(14), pp. 2533-2538. doi: 10.1016/j.bmcl.2018.05.046.

Kalinski, J. J., Krause, R. W. M., Parker-Nance, S., Waterworth, S. C. and Dorrington, R. A. (2021). Unlocking the diversity of pyrroloiminoquinones produced by latrunculid sponge species. *Marine Drugs*, 19(2), pp. 68. doi: 10.3390/md19020068.

Kang, H., Kim, C., Kim, D., Song, J., Choi, M., Choi, K., Kang, M., Lee, K., Kim, H. S., Shin, J. S., Kim, J., Han, S., Lee, M., Lee, S. U., Lee, C., Kim, M., Ko, H., van Kuppeveld, F. J. and Cho, S. (2015). Synergistic antiviral activity of gemcitabine and ribavirin against enteroviruses. *Antiviral Research*, 124, pp. 1-10. doi: 10.1016/j.antiviral.2015.10.011.

Kankam, M.K., Burns, J.M., Collett, M.S., Corrado, M.L. and Hincks, J.R. (2021). A Phase 1 study of the safety, tolerability, and pharmacokinetics of single and multiple oral doses of V-7404 in healthy adult

volunteers. *Antimicrobial. Agents and Chemotherapy*, 65(10), e0102921. doi: https://doi.org/10.1128/AAC.01029-21.

Kassem, A. F., Batran, R. Z., Abbas, E. M., Elseginy, S. A., Shaheen, M. N. and Elmahdy, E. M. (2019). New 4-Phenylcoumarin derivatives as potent 3C protease inhibitors: Design, synthesis, anti-HAV effect and molecular modeling. *European Journal Of Medicinal Chemistry*, 168, pp. 447-460. doi: 10.1016/j.ejmech.

Khatami, A., McMullan, B. J., Webber, M., Stewart, P., Francis, S., Timmers, K. J., Rodas, E., Druce, J., Mehta, B., Sloggett, N. A., Cumming, G., Papadakis, G. and Kesson, A. M. (2014). Sepsis-like disease in infants due to human parechovirus Type 3 during an outbreak in Australia. *Clinical Infectious Diseases*, 60(2), pp. 228-236. doi: 10.1093/cid/ciu784.

Khetsuriani, N., LaMonte, A., Oberste, M. S. and Pallansch, M. (2006). Neonatal enterovirus infections reported to the national enterovirus surveillance system in the United States, 1983-2003. *The Pediatric Infectious Disease Journal*, 25(10), pp. 889-893. doi: 10.1097/01.inf.0000237798.07462.32.

Kim, H.H. and Liao, J.K. (2008). Translational therapeutics of dipyridamole. *Arteriosclerosis, Thrombosis, and Vascular Biology*, 28(3), pp. 39-42. doi: 10.1161/ATVBAHA.107.160226.

Kim, J., Tang, J. Y., Gong, R., Kim, J., Lee, J. J., Clemons, K. V., Chong, C. R., Chang, K. S., Fereshteh, M., Gardner, D., Reya, T., Liu, J. O., Epstein, E. H., Stevens, D. A. and Beachy, P. A. (2010). Itraconazole, a commonly used antifungal that inhibits hedgehog pathway activity and cancer growth. *Cancer Cell*, 17(4), pp. 388–399. doi: https://doi.org/10.1016/j.ccr.2010.02.027.

Kinobe, R., Wiyatno, A., Artika, I.M. and Safari, D. (2022). Insight into the enterovirus A71: A review. *Reviews in Medical Virology*, 32(6), e2361. doi: https://doi.org/10.1002/rmv.2361.

Kuhn, J. H., Sibley, S. D., Chapman, C. A., Knowles, N. J., Lauck, M., Johnson, J. C., Lawson, C. C., Lackemeyer, M. G., Valenta, K., Omeja, P., Jahrling, P. B., O'Connor, D. H. and Goldberg, T. L. (2020). Discovery of lanama virus, a distinct member of species kunsagivirus c (Picornavirales: Picornaviridae), in wild vervet monkeys (Chlorocebus pygerythrus). *Viruses*, 12(12), pp. 1436. doi: 10.3390/v12121436.

Kwong, A. D., Kauffman, R. S., Hurter, P. and Mueller, P. (2011). Discovery and development of telaprevir: an NS3-4A protease inhibitor for treating genotype 1 chronic hepatitis C virus. *Nature Biotechnology*, 29(11), pp. 993-1003. doi: 10.1038/nbt.2020.

Lage, O., Ramos, M., Calisto, R., Almeida, E., Vasconcelos, V. and Vicente, F. (2018). Current screening methodologies in drug discovery for selected human diseases. *Marine Drugs*, 16(8), pp. 279. doi: 10.3390/md16080279.

Lamarche, M. J., Borawski, J., Bose, A., Capacci-Daniel, C., Colvin, R., Dennehy, M., Ding, J., Dobler, M., Drumm, J., Gaither, L.A. and Gao, J. (2012). Anti-hepatitis C virus activity and toxicity of type III phosphatidylinositol-4-kinase beta inhibitors. *Antimicrobial. Agents and Chemotherapy.* 56(10), pp. 5149–5156. doi: 10.1128/aac.00946-12.

Lani, R., Hassandarvish, P., Shu, M., Phoon, W. H., Chu, J. J. H., Higgs, S., Vanlandingham, D., Abu Bakar, S. and Zandi, K. (2016). Antiviral activity of selected flavonoids against Chikungunya virus. *Antiviral Research*, 133, pp. 50-61. doi: 10.1016/j.antiviral.2016.07.009.

Lanke, K., Krenn, B., Melchers, W., Seipelt, J. and van Kuppeveld, F. (2007). PDTC inhibits picornavirus polyprotein processing and RNA replication by transporting zinc ions into cells. *Journal Of General Virology*, 88(4), pp. 1206-1217. doi: 10.1099/vir.0.82634-0.

Lanko, K., Ma, Y., Delang, L., Mirabelli, C. and Neyts, J. (2019). Antiviral effects of selected nucleoside analogues against human parechoviruses A1 and A3. *Antiviral Research*, 162, pp. 51-53. doi: 10.1016/j.antiviral.2018.12.009.

Lee, J.S., Choi, H.J., Song, J.H., Ko, H.J., Yoon, K. and Seong, J.M. (2017). Antiviral activity of itraconazole against echovirus 30 infection *in vitro*. *Osong Public Health and Research Perspectives*, 8(5), pp. 318–324. doi: https://doi.org/10.24171/j.phrp.2017.8.5.05.

Lehrich, J., Arnason, B. and Hochberg, F. (1976). Demyelinating myelopathy in mice induced by the DA virus. *Journal of neurological science,* 29, pp. 149-160. doi: https://doi.org/10.1016/0022-510x(76)90167-2.

Lei, D., Griffiths, E. and Martin, J. (2020). WHO working group meeting to develop WHO Recommendations to assure the quality, safety and efficacy of enterovirus 71 vaccines. *Vaccine*, 38(32), pp. 4917-4923. doi: 10.1016/j.vaccine.2020.05.001.

Lemon, S. (2022). Hepatitis A: Current view of an ancient disease. *Journal of Hepatology*, 77(1), pp. 243-244. doi: 10.1016/j.jhep.2021.09.028.

Lestner, J. and Hope, W.W. (2013). Itraconazole: an update on pharmacology and clinical use for treatment of invasive and allergic fungal infections. *Expert Opinion On Drug Metabolism and Toxicology*, 9, pp. 911-926. doi: https://www.tandfonline.com/doi/full/10.1.

Levy, H.C., Bostina, M., Filman, D.J., Hogle, J.M. (2010). Catching a virus in the act of RNA release: a novel poliovirus uncoating intermediate characterised by cryo-electron microscopy. *Journal of Virology,* 84(9), pp. 4426-4441. doi: https://journals.asm.org/doi/epub/10.1128/JVI.02393-09.

Li, J.Q., Deng, C.L., Gu, D., Li, X., Shi, L., He, J., Zhang, Q.Y., Zhang, B. and Ye, H.Q. (2018). Development of a replicon cell line-based high throughput antiviral assay for screening inhibitors of Zika virus. *Antiviral Research*, 150, pp. 148-154. doi: 10.1016/j.antiviral.2017.12.017.

Li, M.L., Shih, S.R., Tolbert, B.S. and Brewer, G. (2021). Enterovirus A71 vaccines. *Vaccines*, 9, pp. 1-10. doi: https://doi.org/10.3390/vaccines9030199.

Li, Q., Maddox, C., Rasmussen, L., Hobrath, J.V. and White, L.E. (2009). Assay development and high-throughput antiviral drug screening against Bluetongue virus. *Antiviral Research*, 83(3), pp. 267-73. doi: 10.1016/j.antiviral.2009.06.004.

Li, S., Chen, C., Zhang, H., Guo, H., Wang, H., Wang, L., Zhang, X., Hua, S., Yu, J. and Xiao, P. (2005). Identification of natural compounds with antiviral activities against SARS-associated coronavirus. *Antiviral Research*, 67(1), pp. 18-23. doi: 10.1016/j.antiviral.2005.02.007.

Li, X., Li, Y., Fan, S., Cao, R., Li, X., He, X., Li, W., Xu, L., Cheng, T., Li, H. and Zhong, W. (2022). Discovery and optimization of quinoline analogues as novel potent antivirals against enterovirus D68. *Journal of Medicinal Chemistry*, 65(21), pp. 14792–14808. doi: https://doi.org/10.1021/acs.jmedchem.2c01311.

Lim, H.X. and Poh, C.L. (2019). Insights into innate and adaptive immune responses in vaccine development against EV-A71. *Therapeutic Advances in Vaccines and Immunotherapy*, 7. doi: 10.1177/2515135519888998.

Lin, J.Y., Kung, Y.A. and Shih, S.R. (2019). Antivirals and vaccines for Enterovirus A71. *Journal of Biomedical Science*, 26, pp. 1-10. doi: https://doi.org/10.1186/s12929-019-0560-7.

Lin, Y., Chang, Y., Hsiao, N., Hsieh, J., Wang, C., Kung, S., Tsai, F., Lan, Y. and Lin, C. (2012). Fisetin and rutin as 3C protease inhibitors of enterovirus A71. *Journal of Virological Methods*, 182(1-2), pp. 93-98. doi: 10.1016/j.jviromet.2012.03.020.

Lipton, H.L. (1980). Persistent Theiler's murine encephalomyelitis virus infection in mice depends on plaque size. *Journal of general virology,* 46, pp. 169-177. doi: https://doi.org/10.1099/0022-1317-46-1-169.

Liu, N. and Xu, X. (2006). β-tubulin is a more suitable internal control than β-actin in western blot analysis of spinal cord tissues after traumatic injury. *Journal of Neurotrauma*, 23(12), pp. 1794-1801. doi: 10.1089/neu.2006.23.1794.

Liu, X., Li, Z., Liu, S., Sun, J., Chen, Z., Jiang, M., Zhang, Q., Wei, Y., Wang, X., Huang, Y., Shi, Y., Xu, Y., Xian, H., Bai, F., Ou, C., Xiong, B., Lew, A. M., Cui, J., Fang, R., Huang, H., Zhao, J., Hong, X., Zhang, Y., Zhou, F. and Luo, H. (2020). Potential therapeutic effects of dipyridamole in the severely ill patients with COVID-19. *Acta Pharmaceutica Sinica B*, 10(7), pp. 1205-1215. doi: 10.1016/j.apsb.2020.04.008.

Liu, Z., Wei, F., Chen, L.J., Xiong, H.R., Liu, Y.Y., Luo, F., Hou, W., Xiao, H. and Yang, Z.Q. (2013). In vitro and in vivo studies of the inhibitory effects of emodin isolated from Polygonum cuspidatum on Coxsakievirus B(4). *Molecules*, 18(10), pp. 11842–11858. doi: 10.3390/molecules181011842.

Lohmann, V., Körner, F., Koch, J., Herian, U., Theilmann, L. and Bartenschlager, R. (1999). Replication of subgenomic hepatitis C virus RNAS in a hepatoma cell line. *Science,* 285(5424), 110-113. doi: 10.1126/science.285.5424.110.

Louten, J. (2016). Virus structure and classification. *Essential Human Virology*, pp. 19-29. doi: 10.1016/b978-0-12-800947-5.00002-8.

Lugo, D. and Krogstad, P. (2016). Enteroviruses in the early 21st century. *Current Opinion in Pediatrics*, 28(1), pp. 107-113. doi: 10.1097/mop.0000000000000303.

Lundholt, B.K., Scudder, K.M. and Pagliaro, L. (2003). A simple technique for reducing edge effect in cell-based assays. *Journal of Biomolecular Screening*, 8(5), pp. 566-570. doi: 10.1177/1087057103256465.

Luo, M., He, C., Toth, K.S., Zhang, C.X. and Lipton, H.L. (1992). Three-dimensional structure of Theiler murine encephalomyelitis virus (BeAn strain). *Proceedings of the National Academy of Sciences*, 89, pp. 2409–2413. doi: 10.1073/pnas.89.6.2409.

Maddox, C.B., Rasmussen, L. and White, E.L. (2008). Adapting cell-based assays to the high-throughput screening platform: problems encountered and lessons learned. *JALA: Journal of the Association for Laboratory Automation*, 13(3), pp. 168–173. doi: https://doi.org/10.1016/j.jala.2008.02.002.

Mahajan, S., Sharma, G. K., Bora, K. and Pattnaik, B. (2021). Identification of novel interactions between host and non-structural protein 2C of foot-and-mouth disease virus. *Journal of General Virology*, 102(3). doi: 10.1099/jgv.0.001577.

Maehara, Y., Anai, H., Tamada, R. and Sugimachi, K. (1987). The ATP assay is more sensitive than the succinate-dehydrogenase inhibition test for predicting cell viability. *European Journal of Cancer & Clinical Oncology*, 23, pp. 273-276.

Matrosovich, M., Matrosovich, T., Garten, W. and Klenk, H.D. (2006). New low-viscosity overlay medium for viral plaque assays. *Virology Journal*, 3(1), pp. 63. doi: https://doi.org/10.1186/1743-422x-3-63.

McIntyre, C., Knowles, N. and Simmonds, P. (2013). Proposals for the classification of human rhinovirus species A, B and C into genotypically assigned types. *Journal of General Virology*, 94(8), pp. 1791-1806. doi: 10.1099/vir.0.053686-0.

Mendoza, E.J., Manguiat, K., Wood, H., and Drebot, M. (2020). Two detailed plaque assay protocols for the quantification of infectious SARS-CoV-2. *Current Protocols in Microbiology*, 57, e105. doi: 10.1002/cpmc.105.

Mesmin, B., Bigay, J., Moser von Filseck, J., Lacas-Gervais, S., Drin, G. and Antonny, B. (2013). A four-step cycle driven by PI(4)P hydrolysis directs sterol/PI(4)P exchange by the ER-Golgi tether OSBP. *Cell*, 155(4), pp. 830-843. doi: 10.1016/j.cell.2013.09.056.

Messacar, K., Abzug, M. and Dominguez, S. (2015). 2014 outbreak of enterovirus D68 in North America. *Journal of Medical Virology*, 88(5), pp. 739-745. doi: 10.1002/jmv.24410.

Migueres, M., Lhomme, S. and Izopet, J. (2021). Hepatitis A: Epidemiology, high-risk groups, prevention and research on antiviral treatment. *Viruses*, 13(10), pp. 1900. doi: 10.3390/v13101900.

Mirabelli, C., Scheers, E. and Neyts, J. (2017). Novel therapeutic approaches to simultaneously target rhinovirus infection and asthma/COPD pathogenesis. *F1000Research*, 6, pp. 1860. doi: 10.12688/f1000research.11978.1.

Mishra, S., Pandey, A. and Manvati, S. (2020). Coumarin: An emerging antiviral agent. *Heliyon*, 6(1). doi: https://doi.org/10.1016/j.heliyon.2020.e03217.

Mokrejš, M., Mašek, T., Vopálenský, V., Hlubuček, P., Delbos, P. and Pospíšek, M. (2010). IRESite—a tool for the examination of viral and cellular internal ribosome entry sites. *Nucleic Acids Research*, 38(1), pp. 131-136. doi: 10.1093/nar/gkp981.

Monteiro, M.C., de la Cruz, M., Cantizani, J., Moreno, C., Tormo, J.R., Mellado, E., de Lucas, J.R., Asensio, F., Valiante, V., Brakhage, A.A., Latge, J., Genilloud, O. and Vicente, F. (2012). A new approach to drug discovery: high-throughput screening of microbial natural extracts against Aspergillus fumigatus using resazurin. *Journal of Biomolecular Screening*, 17(4), pp. 542-549. doi: 10.1177/1087057111433459.

Muckelbauer, J. K., Kremer, M., Minor, I., Diana, G., Dutko, F. J., Groarke, J., Pevear, D. C. and Rossmann, M. G. (1995). The structure of coxsackievirus B3 at 3.5 å resolution. *Structure*, 3(7), pp. 653-667. doi: 10.1016/s0969-2126(01)00201-5.

Musarra-Pizzo, M., Pennisi, R., Ben-Amor, I., Mandalari, G. and Sciortino, M. T. (2021). Antiviral activity exerted by natural products against human viruses. *Viruses*, 13(5), pp. 828. doi: 10.3390/v13050828.

Mutsvunguma, L. Z., Moetlhoa, B., Edkins, A. L., Luke, G. A., Blatch, G. L. and Knox, C. (2011). Theiler's murine encephalomyelitis virus infection induces a redistribution of heat shock proteins 70 and 90 in BHK-21 cells, and is inhibited by novobiocin and geldanamycin. *Cell Stress and Chaperones*, 16(5), pp. 505-515. doi: 10.1007/s12192-011-0262-x.

Nacev, B. A., Grassi, P., Dell, A., Haslam, S. M. and Liu, J. O. (2011). The antifungal drug itraconazole inhibits vascular endothelial growth factor receptor 2 (VEGFR2) glycosylation, trafficking, and signaling in endothelial cells. *Journal of Biological Chemistry*, 286(51), pp. 44045–44056. doi: https://doi.org/10.1074/jbc.m111.278754.

Neubauer, D., Steinberger, J. and Skern, T. (2009). Picornaviruses. *Viral Proteases and Antiviral Protease Inhibitor Therapy*, pp. 101-130. doi: 10.1007/978-90-481-2348-3_6.

Neyts, J., De Clercq, E., Singha, R., Chang, Y.H., Das, A.R., Chakraborty, S.K., Hong, S.C., Tsay, S.C., Hsu, M.H. and Hwu, J.R. (2009). Structure-activity relationship of new anti-hepatitis C virus agents: heterobicycle-coumarin conjugates. *Journal of Medicinal Chemistry*, 52(5), pp. 1486-90. doi: 10.1021/jm801240d.

Nie, X., Li, C., Hu, S., Xue, F., Kang, Y. and Zhang, W. (2017). An appropriate loading control for western blot analysis in animal models of myocardial ischemic infarction. *Biochemistry And Biophysics Reports*, 12, pp. 108-113. doi: 10.1016/j.bbrep.2017.09.00.

Noah, J. W., Severson, W., Noah, D. L., Rasmussen, L., White, E. L. and Jonsson, C. B. (2007). A cell-based luminescence assay is effective for high-throughput screening of potential influenza antivirals. *Antiviral Research*, 73(1), pp. 50-59. doi: 10.1016/j.antiviral.2006.07.006.

Nobori, H., Toba, S., Yoshida, R., Hall, W., Orba, Y., Sawa, H. and Sato, A. (2018). Identification of Compound-B, a novel anti-dengue virus agent targeting the non-structural protein 4A. *Antiviral Research*, 155, pp. 60-66. doi: 10.1016/j.antiviral.2018.05.003.

Novikov, D. and Melentev, D. (2022). Enteroviral (Picornaviridae: Enterovirus) (nonpolio) vaccines. *Problems of Virology*, 67(3), pp. 185-192. doi: 10.36233/0507-4088-111.

O'brien, J., Wilson, I., Orton, T. and Pognan, F. (2003). Investigation of the alamarBlue (resazurin) fluorescent dye for the assessment of mammalian cell cytotoxicity. *European Journal of Biochemistry*, 267, pp. 5421-5426. doi: 10.1046/j.1432-1327.2000.01606.x.

O'Brien, P.J. (1991). Molecular mechanisms of quinone cytotoxicity. *Chemico-Biological Interactions*, 80 (1), pp. 1–41. doi: 10.1016/0009-2797(91)90029-7.

Oberste, M. S., Maher, K., Kilpatrick, D. R., Flemister, M. R., Brown, B. A. and Pallansch, M. A. (1999). Typing of human enteroviruses by partial sequencing of VP1. *Journal of Clinical Microbiology*, 37(5), pp. 1288-1293. doi: 10.1128/jcm.37.5.1288-1293.1999.

Oberste, M. S., Moore, D., Anderson, B., Pallansch, M. A., Pevear, D. C. and Collett, M. S. (2009). In vitro antiviral activity of V-073 against polioviruses. *Antimicrobial Agents and Chemotherapy*, *53*(10), pp. 4501–4503. doi: https://doi.org/10.1128/aac.00671-09.

Oehring, H. and Schmidt, J. (1978). The antiviral action of dipyridamole on rhinoviruses. *Zeitschrift fur Attgemeine Mikrobiologie, Morphologic, Physiologic, Genetik und Okologie der Microorganismen*, 24(6), pp. 447-449. doi: https://www.cabdirect.org/cabdirect/abstract/19802700534.

Oleszak, E.L., Chang, J.R., Friedman, H., Katsetos, C.D. and Platsoucas, C.D. (2004). Theiler's virus infection: a model for multiple sclerosis. *Clinical Microbiology Reviews*, 17(1), pp. 174-207. doi: https://journals.asm.org/doi/full/10.1128/CMR.17.1.174-207.

Omura, S., Kawai, E., Sato, F., Martinez, N. E., Minagar, A., Al-Kofahi, M., Yun, J. W., Cvek, U., Trutschl, M., Alexander, J. S., and Tsunoda, I. (2018). Theiler's virus-mediated immunopathology in the CNS and heart: roles of organ-specific cytokine and lymphatic responses. *Frontiers in Immunology*, 9. doi: https://doi.org/10.3389/fimmu.2018.02870.

Orabi, R.M, Reference Laboratory for Foot-and-Mouth Disease. (2022). South Africa (08): cattle, spread, control strategy | Reference Laboratory for Foot-and-Mouth Disease**.** Available at: https://www.foot-and-mouth.org/news/2022/08/south-africa-08-cattle-spread-control-strategy (Accessed: 21 January 2023).

Page, B., Page, M. and Noel, C. (1993). A new fluorometric assay for cytotoxicity measurements in vitro. *International Journal of Oncology*, 3, pp. 473-476. doi: 10.3892/ijo.3.3.473.

Palma, A. M. D., Heggermont, W., Leyssen, P., Pürstinger, G., Wimmer, E., Clercq, E. D., Rao, A., Monforte, A., Chimirri, A. and Neyts, J. (2007). Anti-enterovirus activity and structure–activity relationship of a series of 2,6-dihalophenyl-substituted 1H,3H-thiazolo[3,4-a]benzimidazoles. *Biochemical And Biophysical Research Communications*, 353(3), pp. 628-632. doi: 10.1016/j.bbrc.2006.12.063.

Palmenberg, A. C. (1990). Proteolytic processing of picornaviral polyprotein. *Annual Review of Microbiology,* 44, pp. 603-623. doi: doi/abs/10.1146/annurev.mi.44.100190.003131?journalCode=micro.

Palmenberg, A. C., Spiro, D., Kuzmickas, R., Wang, S., Djikeng, A., Rathe, J. A., Fraser-Liggett, C. M. and Liggett, S. B. (2009). Sequencing and analyses of all known human rhinovirus genomes reveal structure and evolution. *Science*, 324(5923), pp. 55-59. doi: 10.1126/science.1165557.

Panjwani, A., Strauss, M., Gold, S., Wenham, H., Jackson, T., Chou, J. J., Rowlands, D. J., Stonehouse, N. J., Hogle, J. M. and Tuthill, T. J. (2014). Capsid protein vp4 of human rhinovirus induces membrane permeability by the formation of a size-selective multimeric pore. *Public Library of Science: Pathogens*, 10(8), e1004294. doi: 10.1371/journal.ppat.1004294.

Papadopoulos, N.G., Moustaki , M., Tsolia , M., Bossios , A., Astra , E., Prezerakou , A., Gourgiotis , D., and Kafetzis D. (2022). Association of rhinovirus infection with increased disease severity in acute bronchiolitis. *American Journal of Respiratory and Critical Care Medicine,*165(9), pp. 1285-1289. doi: doi/full/10.1164/rccm.200112-118BC.

Papi, A. and Contoli, M. (2010). Rhinovirus vaccination: the case against. *European Respiratory Journal*, 37(1), pp. 5-7. doi: 10.1183/09031936.00145710.

Parvez, M.K., Rehman, T., Alam, P., Al-Dosari, M.S., Alqasoumi, S.I., Mohammed, F. and Alajmi, M.F. (2019). Plant-derived antiviral drugs as novel hepatitis B virus inhibitors: Cell culture and molecular docking study. *Saudi Pharmaceutical Journal*, 27(3), pp. 389–400. doi: 10.1016/j.jsps.2018.12.008.

Patick, A.K., Brothers, M.A., Maldonado, F., Binford, S., Maldonado, O., Fuhrman, S., Petersen, A., Smith III, G.J., Zalman, L.S., Burns-Naas, L.A. and Tran, J.Q. (2005). In vitro antiviral activity and single-dose pharmacokinetics in humans of a novel, orally bioavailable inhibitor of human rhinovirus 3C protease. *Antimicrobial Agents and Chemotherapy*, 49(6), pp. 2267-2275. doi: https://journals.asm.org/doi/full/10.1128/AAC.49.6.2267-2275.2005.

Paton, D. J., Di Nardo, A., Knowles, N. J., Wadsworth, J., Pituco, E. M., Cosivi, O., Rivera, A. M., Kassimi, L. B., Brocchi, E., de Clercq, K., Carrillo, C., Maree, F. F., Singh, R. K., Vosloo, W., Park, M., Sumption, K. J., Ludi, A. B. and King, D. P. (2021). The history of foot-and-mouth disease virus serotype C: the first known extinct serotype. *Virus Evolution*, 7(1). doi: 10.1093/ve/veab009.

Pauwels, R., Balzarini, J., Baba, M., Snoeck, R., Schols, D., Herdewijn, P., Desmyter, J. and De Clercq, E. (1988). Rapid and automated tetrazolium-based colorimetric assay for the detection of anti-HIV compounds. *Journal of virological methods*, 20(4), pp.309-321. doi: 10.1016/0166-0934(88)90134-6.

Payne, S. (2017). Methods to study viruses. *Viruses*, pp. 37-52. doi: 10.1016/b978-0-12-803109-4.00004-0.

Pelkmans, L., Puntener, D., and Helenius, A. (2002). Local actin polymerisation and dynamin recruitment in SV40-induced internalisation of caveolae. *Science,* 296, pp. 535-539. doi: https://www.science.org/doi/pdf/10.1126/science.1069784?casa_token=h9dDYnVlJY8AAAAA:VzbmhKF56WQJ-OJXzbz7Y4BFqftnaMkgVKOZ.

Pettke, A., Tampere, M., Pronk, R., Wallner, O., Falk, A., Warpman, B.U., Helleday, T., Mirazimi, A. and Puumalainen, M.R. (2020). Broadly active antiviral compounds disturb Zika virus progeny release rescuing virus-induced toxicity in brain organoids. *Viruses*, 13(1). doi: 10.3390/v13010037.

Pinto, A.M., Leite, J.P., Neves, A.P., da Silva, G.B., Vargas, M.D. and Paixao, I.C. (2014). Synthetic aminomethylnaphthoquinones inhibit the in vitro replication of bovine herpesvirus 5. *Archives of Virology*, 159(7), pp. 1827–1833. doi: 10.1007/s00705-014-1989-3.

Pons-Salort, M., Parker, E.P. and Grassly, N.C. (2015). The epidemiology of non-polio enteroviruses: recent advances and outstanding questions. *Current Opinion in Infectious Diseases*, 28(5), pp. 479-87. doi: 10.1097/QCO.0000000000000187.

Präbst, K., Engelhardt, H., Ringgeler, S. and Hübner, H. (2017). Basic colorimetric proliferation assay: MTT, WST and Resazurin. *Cell Viability Assays, Methods and Protocols*, 1601, pp.1-17. doi: https://doi.org/10.1007/978-1-4939-6960-9_1.

Qin, Z., Ju, H., Liu, Y., Gao, T., Wang, W., Aurelian, L. Zhao, P. and Qi, Z. (2013). Fetal bovine serum inhibits hepatitis C virus attachment to host cells. *Journal Of Virological Methods*, 193(2), pp. 261-269. doi: 10.1016/j.jviromet.2013.06.024.

Qing, M., Liu, W., Yuan, Z., Gu, F. and Shi, P. Y. (2010). A high-throughput assay using dengue-1 virus-like particles for drug discovery. *Antiviral Research*, 86(2), pp. 163-171. doi: 10.1016/j.antiviral.2010.02.313.

Rampersad, S.N. (2012). Multiple applications of alamar blue as an indicator of metabolic function and cellular health in cell viability bioassays. *Sensors*, 12(9), pp. 12347-12360. doi: 10.3390/s120912347.

Rausch, K., Hackett, B.A., Weinbren, N.L., Reeder, S.M., Sadovsky, Y., Hunter, C.A., Schultz, D.C., Coyne, C.B. and Cherry, S. (2017). Screening bioactives reveals Nanchangmycin as a broad spectrum antiviral active against Zika Virus. *Cell Reports*, 18(3), pp. 804-815. doi: 10.1016/j.celrep.2016.12.068.

Renwick, N., Schweiger, B., Kapoor, V., Liu, Z., Villari, J., Bullmann, R., Miething, R., Briese, T. and Lipkin, W. (2007). A recently identified rhinovirus genotype is associated with severe respiratory-tract infection in children in Germany. *The Journal of Infectious Diseases*, 196(12), pp. 1754-1760. doi: 10.1086/524312.

Rhoden, E., Liu, H., Wang-Chern, S. and Oberste, M. (2013). Anti-poliovirus activity of protease inhibitor AG-7404, and assessment of in vitro activity in combination with antiviral capsid inhibitor compounds. *Antiviral Research*, 98(2), pp. 186-191. doi: 10.1016/j.antiviral.2013.03.003.

Rhoden, E., Nix, W., Weldon, W. and Selvarangan, R. (2018). Antifungal azoles itraconazole and posaconazole exhibit potent in vitro antiviral activity against clinical isolates of parechovirus A3 (Picornaviridae). *Antiviral Research*, 149, pp. 75-77. doi: 10.1016/j.antiviral.2017.11.011.

Rhoden, E., Zhang, M., Nix, W.A. and Oberste, M.S. (2015). In vitro efficacy of antiviral compounds against Enterovirus D68. *Antimicrobial Agents and Chemotherapy*, 59(12), pp. 7779-7781. doi: 10.1128/AAC.00766-15.

Riss, T.L. and Moravec, R.A. (1992). Comparison of MTT, XTT and a novel tetrazolium compound MTS for in vitro proliferation and chemosensitivity assays. *Molecular Biology of the Cell*, 184a (3).

Ross, C., Upfold, N., Luke, G. A., Bishop, Ö. T. and Knox, C. (2016). Subcellular localisation of Theiler's murine encephalomyelitis virus (TMEV) capsid subunit VP1 vis-á-vis host protein Hsp90. *Virus Research*, 222, pp. 53-63. doi: 10.1016/j.virusres.2016.06.003.

Rossmann, M. (2014). Picornavirus structure overview. *Molecular Biology of Picornavirus*, pp. 25-38. doi: 10.1128/9781555817916.ch3.

Rotter, B.A., Thompson, B.K., Clarkin, S. and Owen, T.C. (1993). Rapid colorimetric bioassay for screening of Fusarium mycotoxins. *Natural Toxins*, 1, pp. 303-307. doi: 10.1002/nt.2620010509/full.

Rübsamen-Schaeff, H. and Buschmann, H. (2021). New drug development for known and emerging viruses. *Methods and Principles in Medicinal Chemistry*. doi: 10.1002/9783527810697.

Ruiz, A. and Russell, S. (2012). A new paradigm in viral resistance. *Cell Research*, 22(11), pp. 1515-1517. doi: 10.1038/cr.2012.139.

Runfeng, L., Yunlong, H., Jicheng, H., Weiqi, P., Qinhai, M., Yongxia, S., Chufang, L., Jin, Z., Zhenhua, J., Haiming, J., Kui, Z., Shuxiang, H., Jun, D., Xiaobo, L., Xiaotao, H., Lin, W., Nanshan, Z. and Zifeng, Y. (2020). Lianhuaqingwen exerts antiviral and anti-inflammatory activity against novel coronavirus (SARS-CoV-2). *Pharmacological Research,* 156, pp. 104761. doi: 10.1016/j.phrs.2020.104761.

Sanaki, T., Wakabayashi, M., Yoshioka, T., Yoshida, R., Shishido, T., Hall, W.W., Sawa, H. and Sato, A. (2019). Inhibition of dengue virus infection by 1-stearoyl-2-arachidonoyl-phosphatidylinositol in vitro. *The FASEB Journal*, 33: pp. 13866-13881. doi: https://doi.org/10.1096/fj.201901095RR.

Sarry, M., Romey, A., Lefebvre, D., Benfrid, S., Dufour, B., Durand, B., Zanella, G., De Regge, N., Zientara, S., Bakkali Kassimi, L. and Blaise-Boisseau, S. (2022). Foot and mouth disease virus: transmission, pathogenesis, diagnosis and surveillance. Virologie, 26(5), pp. 355-373. doi: 10.1684/vir.2022.0972.

Schuffenecker, I., Javouhey, E., Gillet, Y., Kugener, B., Billaud, G., Floret, D., Lina, B. and Morfin, F. (2012). Human parechovirus infections, Lyon, France, 2008–10: Evidence for severe cases. *Journal of Clinical Virology*, 54(4), pp. 337-341. doi: 10.1016/j.jcv.2012.04.016.

Senior, K. (2002). FDA panel rejects common cold treatment. *The Lancet Infectious Diseases*, 2(5), pp. 264. doi: 10.1016/s1473-3099(02)00277-3.

Sethi, Y., Kaka, N., Chopra, H., Aggarwal, N., Arora, S. and Emran, T. B. (2022). Recent poliovirus outbreaks and vaccination: A perspective. *Annals of Medicine and Surgery*, 84, pp. 104970. doi: 10.1016/j.amsu.2022.104970.

Severson, W. E., McDowell, M., Ananthan, S., Chung, D., Rasmussen, L., Sosa, M. I., White, E. L., Noah, J. and Jonsson, C. B. (2008). High-Throughput screening of a 100,000-compound library for inhibitors of Influenza A Virus (H3N2). *SLAS Discovery*, 13(9), pp. 879-887. doi: 10.1177/1087057108323123.

Severson, W.E., Shindo, N., Sosa, M., Fletcher, T. 3rd, White, E.L., Ananthan, S. and Jonsson, C.B. (2007). Development and validation of a high-throughput screen for inhibitors of SARS CoV and its application in screening of a 100,000-compound library. *Journal of Biomolecular Screening*, 12(1), pp. 33-40. doi: 10.1177/1087057106296688.

Shen, L., Yang, Y., Ye. F., Liu, G., Desforges, M., Talbot, P.J, and Tan, W. (2016). Safe and sensitive antiviral screening platform based on recombinant human Coronavirus OC43 expressing the luciferase reporter gene. *Antimicrobial Agents and Chemotherapy*, 60(9), pp. 5492-5503. doi: 10.1128/AAC.00814-16.

Shen, Y., Gu, X. and Zhou, J. (2008). Protective effect of inactivated hepatitis A vaccine against the outbreak of hepatitis A in an open rural community. *World Journal of Gastroenterology*, 14(17), 14(17), pp. 2771-2775. doi: 10.3748/wjg.14.2771.

Sherry, L., Grehan, K., Snowden, J.S., Knight, M.L., Adeyemi, O.O., Rowlands, D.J. and Stonehouse, N.J. (2020). Comparative molecular biology approaches for the production of poliovirus virus-like particles using pichia pastoris. *mSphere,* 5(2), e00838-19. doi: doi/full/10.1128/mSphere.00838-19.

Shim, A., Song, J., Kwon, B., Lee, J., Ahn, J., Kim, Y., Rhee, K., Chang, S., Cha, Y., Lee, Y., Kweon, M., Park, K. S., Kim, D., Cho, S., Cho, H. and Ko, H. (2016). Therapeutic and prophylactic activity of itraconazole against human rhinovirus infection in a murine model. *Scientific Reports*, 6(1). doi: 10.1038/srep23110.

Simmonds, P., McIntyre, C., Savolainen-Kopra, C., Tapparel, C., Mackay, I. M. and Hovi, T. (2010). Proposals for the classification of human rhinovirus species C into genotypically assigned types. *Journal of General Virology*, 91(10), pp. 2409-2419. doi: 10.1099/vir.0.023994-0.

Sinclair, W. and Omar, M. (2021). Enterovirus. *Statpearls Publishing*. https://www.ncbi.nlm.nih.gov/books/NBK562330/.

Skancke, A. and Skancke, P.N. (1988). General and theoretical aspects of quinones. In, *The quinonoid compounds*, Patai, S. and Rappoport, Z (Eds.). 2nd vol., John Wiley and Sons Ltd, Jerusalem, pp. 1-5.

Smee, D. F., Evans, W. J., Nicolaou, K. C., Tarbet, E. B. and Day, C. W. (2016). Susceptibilities of enterovirus D68, enterovirus 71, and rhinovirus 87 strains to various antiviral compounds. *Antiviral Research*, 131, pp. 61–65. doi: https://doi.org/10.1016/j.antiviral.2016.04.003.

Smee, D. F., Hurst, B. L., Evans, W. J., Clyde, N., Wright, S., Peterson, C., Jung, K. and Day, C. W. (2017). Evaluation of cell viability dyes in antiviral assays with RNA viruses that exhibit different cytopathogenic properties. *Journal Of Virological Methods*, 246, pp. 51-57. doi: 10.1016/j.jviromet.2017.03.012.

Smith, D. and Simmonds, P. (2018). Classification and genomic diversity of enterically transmitted hepatitis viruses. *Cold Spring Harbor Perspectives in Medicine*, 8(9), a031880. doi: 10.1101/cshperspect.a031880.

Solomon, T., Lewthwaite, P., Perera, D., Cardosa, M.J., McMinn, P. and Ooi, M.H. (2010). Virology, epidemiology, pathogenesis, and control of enterovirus 71. *The Lancet Infectious Diseases*, 10 (11), pp. 778-790. doi: 10.1016/s1473-3099(10)70194-8.

Steil, B. and Barton, D. (2009). Cis-active RNA elements (CREs) and picornavirus RNA replication. *Virus Research*, 139(2), pp. 240-252. doi: 10.1016/j.virusres.2008.07.027.

Stone, J.K., Rijnbrand, R., Stein, D.A., Ma, Y., Yang, Y., Iversen, P.L. and Andino, R. (2008). A morpholino oligomer targeting highly conserved internal ribosome entry site sequence is able to inhibit multiple species of picornavirus. *Antimicrobial Agents and Chemotherapy*, 52(6), pp. 1970-1981. doi: https://journals.asm.org/doi/full/10.1128/AAC.00011-08.

Stone, V., Johnston, H. and Schins, RPF. (2009). Development of in vitro systems for nanotoxicology: Methodological considerations. *Critical Reviews in Toxicology*, 39(7), pp. 613-626. doi: 10.1080/10408440903120975.

Strating, J., van der Linden, L., Albulescu, L., Bigay, J., Arita, M., Delang, L., Leyssen, P., van der Schaar, H., Lanke, K., Thibaut, H., Ulferts, R., Drin, G., Schlinck, N., Wubbolts, R., Sever, N., Head, S., Liu, J., Beachy, P., De Matteis, M., Shair, M., Olkkonen, V., Neyts, J. and van Kuppeveld, F. (2015). Itraconazole inhibits enterovirus replication by targeting the oxysterol-binding protein. *Cell Reports*, 10(4), pp. 600-615. doi: 10.1016/j.celrep.2014.12.054.

Strober, W. (2001). Trypan blue exclusion test of cell viability. *Current Protocols in Immunology*, 21(3B). doi: 10.1002/0471142735.ima03bs21.

Sui, Y. and Wu, Z. (2007). Alternative statistical parameter for high-throughput screening assay quality assessment. *Journal of Biomolecular Screening*, 12(2). doi: 10.1177/1087057106296498.

Świerczyńska, M., Mirowska-Guzel, D. and Pindelska, E. (2022). Antiviral drugs in influenza. *International Journal of Environmental Research and Public Health*, 19(5), pp. 3018. doi: 10.3390/ijerph19053018.

Sykes, M.L. and Avery, V.M. (2009). Development of an Alamar Blue viability assay in 384-well format for high throughput whole cell screening of Trypanosoma brucei brucei bloodstream form strain 427. *The American Journal of Tropical Medicine and Hygiene*, 81(4), pp. 665–674. doi: 10.4269/ajtmh.2009.09-0015.

Szebeni, J., Wahl, S.M., Popovic, M., Wahl, L.M., Gartner, S., Fine, R.L., Skaleric, U., Friedmann, R.M. and Weinstein, J.N. (1989). Dipyridamole potentiates the inhibition by 3'-azido-3'-deoxythymidine and other dideoxynucleosides of human immunodeficiency virus replication in monocyte-macrophages. *Proceedings of the National Academy of Sciences of the United States of America*, 86(10), pp. 3842-3846. doi: 10.1073/pnas.86.10.3842.

Tammaro, C., Guida, M., Appetecchia, F., Biava, M., Consalvi, S. and Poce, G. (2023). Direct-acting antivirals and host-targeting approaches against enterovirus B infections: Recent advances. *Pharmaceuticals*, 16(2), pp. 203. doi: 10.3390/ph16020203.

Taneja, N.K. and Tyagi, J.S. (2007). Resazurin reduction assays for screening of antitubercular compounds against dormant and actively growing Mycobacterium tuberculosis, Mycobacterium bovis BCG and Mycobacterium smegmatis. *The Journal of Antimicrobial Chemotherapy*, 60(2), pp. 288–293. doi: 10.1093/jac/dkm207.

Tapparel, C., Siegrist, F., Petty, T. J. and Kaiser, L. (2013). Picornavirus and enterovirus diversity with associated human diseases. *Infection, Genetics and Evolution*, 14, pp. 282-293. doi: 10.1016/j.meegid.2012.10.016.

Tchesnokov, E.P., Feng, J.Y., Porter, D.P., Götte, M., Tchesnokov, E., Feng, J. and Porter, D. (2019). Mechanism of inhibition of Ebola virus RNA-dependent RNA polymerase by remdesivir. *Viruses*, 11, pp. 326. doi: 10.3390/v11040326.

Tenser, R.B., Gaydos, A. and Hay, K.A. (2001). Inhibition of herpes simplex virus reactivation by dipyridamole. *Antimicrobial Agents and Chemotherapy*, 45, pp. 3657-3659. doi: https://doi.org/10.1128/AAC.45.12.3657-3659.2001.

Theiler, M. and Gard S (1940) Encephalomyelitis of mice. 1. Characteristics and pathogenesis of the virus. *Journal of experimental medicine,* 72, pp. 49-67. doi: https://doi.org/10.1084/jem.72.1.49.

Tietjen, I., Cassel, J., Register, E. T., Zhou, X. Y., Messick, T. E., Keeney, F., Lu, L. D., Beattie, K. D., Rali, T., Tebas, P., Ertl, H. C., Salvino, J. M., Davis, R. A. and Montaner, L. J. (2021). The natural stilbenoid (–)-hopeaphenol inhibits cellular entry of SARS-COV-2 USA-WA1/2020, B.1.1.7, and B.1.351 variants. *Antimicrobial Agents and Chemotherapy*, 65(12). doi: https://doi.org/10.1128/aac.00772-21.

Tmizutani, E, Inagaki, H., Hayasaka, D., Kariwa, H. and Takashima, I. (1999). Enhancement of borna disease virus transcription in persistently infected cells by serum starvation. *Journal of Veterinary Medical Science*, 61(7), pp. 831–834. doi: https://doi.org/10.1292/jvms.61.831.

Tobita, K., Tanaka, T. and Hayase, Y. (1997). Spontaneous excretion of virus from MDCK cells persistently infected with influenza virus A/PR/8/34. *Journal Of General Virology*, 78(3), pp. 563-566. doi: 10.1099/0022-1317-78-3-563.

Tomeczkowski, J., Ludwig, A. and Kretzmer, G. (1993). Effect of cholesterol addition on growth kinetics and shear stress sensitivity of adherent mammalian cells. *Enzyme and Microbial Technology*, 15(10), pp. 849-853. doi: 10.1016/0141-0229(93)90096-k.

Tominaga, H., Ishiyama, M., Ohseto, F., Sasamoto, K., Hamamoto, T., Suzuki, K. and Watanabe, M. (1999). A water-soluble tetrazolium salt useful for colorimetric cell viability assay. *Analytical Communications*, 36, pp. 47-50. doi: 10.1039/A809656B.

Tonew, E., Indulen, M.K. and Dzeguze, D.R. (1982). Antiviral action of dipyridamole and its derivatives against influenza virus A. *Acta Virologica*, 26(3), pp. 125-129.

Tonew, M. and Dzeguze, D.R. (1977) Dipyridamole, an inhibitor of Mengovirus replication in FL and L Cells. *Chemotherapy*, 23(3), pp. 149-158. doi: 10.1159/000221983.

Tonew, M., Tonew, E. and Mentel, R. (1977). The antiviral activity of dipyridamole. *Acta Virologica.* 21(2), pp. 146-150.

Torres-Torres, S., Myers, A. L., Klatte, J. M., Rhoden, E. E., Oberste, M. S., Collett, M. S. and McCulloh, R. J. (2015). First Use of Investigational Antiviral Drug Pocapavir (V-073) for Treating Neonatal Enteroviral Sepsis. *Pediatric Infectious Disease Journal*, 34(1), pp. 52-54. doi: 10.1097/inf.0000000000000497.

Travnickova, E., Mikula, P., Oprsal, J., Bohacova, M., Kubac, L., Kimmer, D., Soukupova, J. and Bittner, M. (2019). Resazurin assay for assessment of antimicrobial properties of electrospun nanofiber filtration membranes. *Applied Microbiology and Biotechnology Express*, 9(1). doi: 10.1186/s13568-019-0909-z.

Tsai, F., Lin, C., Lai, C., Lan, Y., Lai, C., Hung, C., Hsueh, K., Lin, T., Chang, H. C., Wan, L., Sheu, J. J. and Lin, Y. (2011). Kaempferol inhibits enterovirus 71 replication and internal ribosome entry site (IRES) activity through FUBP and HNRP proteins. *Food Chemistry*, 128(2), pp. 312-322. doi: 10.1016/j.foodchem.2011.03.022.

Tsou, Y., Lin, Y., Chang, H., Lin, H., Shao, H., Yu, S., Liu, C., Chitra, E., Sia, C. and Chow, Y. (2013). Heat shock protein 90: role in enterovirus 71 entry and assembly and potential target for therapy. *Public Library of Science: ONE*, 8(10), e77133. doi: 10.1371/journal.pone.0077133.

Tulloch, F., Luke, G. and Ryan, M. (2018). Problems in FMD eradication: a way forward? *Journal of Veterinary Medicine and Research*. doi: https://research-repository.st-andrews.ac.uk/handle/10023/15532.

Tuthill, T. J., Groppelli, E., Hogle, J. M. and Rowlands, D. J. (2010). Picornaviruses. *Current Topics in Microbiology and Immunology*, pp. 43-89. doi: 10.1007/82_2010_37.

Uemura, K., Nobori, H., Sato, A., Sanaki, T., Toba, S., Sasaki, M., Murai, A., Saito-Tarashima, N., Minakawa, N., Orba, Y., Kariwa, H., Hall, W.W., Sawa, H., Matsuda, A. and Maenaka, K. (2021). 5-Hydroxymethyltubercidin exhibits potent antiviral activity against flaviviruses and coronaviruses, including SARS-CoV-2. *iScience*, 24(10). doi: 10.1016/j.isci.2021.103120.

Upfold, N. (2019). Exploring the structural integrity of the picornavirus capsid. PhD thesis, Rhodes University, Grahamstown.

Upfold, N., Ross, C., Bishop, Ö. T., Luke, G. A. and Knox, C. (2018). The generation and characterisation of neutralising antibodies against the Theiler's murine encephalomyelitis virus (TMEV) GDVII capsid reveals the potential binding site of the host cell co-receptor, heparan sulfate. *Virus Research*, 244, pp. 153-163. doi: 10.1016/j.virusres.2017.11.017.

Uzunoglu, S., Karaca, B., Atmaca. H., Kisim, A., Sezgin, C., Karabulut, B. and Uslu. R. (2010). Comparison of XTT and Alamar blue assays in the assessment of the viability of various human cancer cell lines by AT-101 (2/2 gossypol). *Toxicology Mechanisms and Methods*, 20(8), pp. 482–486. doi: 10.3109/15376516.2010.508080.

van Damme, E., De Meyer, S., Bojkova, D., Ciesek, S., Cinatl, J., De Jonghe, S., Jochmans, D., Leyssen, P., Buyck, C., Neyts, J. and Van Loock, M. (2021). In vitro activity of itraconazole against SARS-COV-2. *Journal of Medical Virology*, 93(7), pp. 4454–4460. doi: https://doi.org/10.1002/jmv.26917.

van der Grein, S. G., Defourny, K. A. Y., Rabouw, H. H., Galiveti, C. R., Langereis, M. A., Wauben, M. H. M., Arkesteijn, G. J. A., van Kuppeveld, F. J. M. and Nolte-'t Hoen, E. N. M. (2019). Picornavirus infection induces temporal release of multiple extracellular vesicle subsets that differ in molecular composition and infectious potential. *Public Library of Science: Pathogens*, 15(2). doi: 10.1371/journal.ppat.1007594.

van der Linden, L., Vives-Adrián, L., Selisko, B., Ferrer-Orta, C., Liu, X., Lanke, K., Ulferts, R., De Palma, A. M., Tanchis, F., Goris, N., Lefebvre, D., De Clercq, K., Leyssen, P., Lacroix, C., Pürstinger, G., Coutard, B., Canard, B., Boehr, D. D., Arnold, J. J., Cameron, C. E., Verdaguer, N., Neyts, J. and van Kuppeveld, F. J. M. (2015). The RNA template channel of the RNA-dependent RNA polymerase as a target for development of antiviral therapy of multiple genera within a virus family. *Public Library of Science: Pathogens*, 11(3). doi: 10.1371/journal.ppat.1004733.

van der Linden, L., Wolthers, K. and van Kuppeveld, F. (2015). Replication and inhibitors of enteroviruses and parechoviruses. *Viruses*, 7(8), pp. 4529-4562. doi: 10.3390/v7082832.

Venkatraman, S. (2012). Discovery of boceprevir, a direct-acting NS3/4A protease inhibitor for treatment of chronic hepatitis C infections. *Trends In Pharmacological Sciences*, 33(5), 289-294. doi: 10.1016/j.tips.2012.03.012.

Wang, G., Cao, R., Chen, R., Mo, L., Han, J., Wang, X., Xu, X., Jiang, T., Deng, Y., Lyu, K., Zhu, S., Qin, E., Tang, R. and Qin, C. (2013). Rational design of thermostable vaccines by engineered peptide-induced virus self-biomineralisation under physiological conditions. *Proceedings of the National Academy of Sciences*, 110(19), pp. 7619-7624. doi: 10.1073/pnas.1300233110.

Wang, H., Zhang, D., Ge, M., Li, Z., Jiang, J. and Li, Y. (2015). Formononetin inhibits enterovirus 71 replication by regulating COX- 2/PGE2 expression. *Virology Journal*, 12(1). doi: 10.1186/s12985-015-0264-x.

Wang, J., Du, J., Wu, Z. and Jin, Q. (2013). Quinacrine impairs enterovirus 71 rna replication by preventing binding of polypyrimidine-tract binding protein with internal ribosome entry sites. *Public Library of Science: ONE*, 8(1), e52954. doi: 10.1371/journal.pone.0052954.

Wang, J., Hu, Y. and Zheng, M. (2022). Enterovirus A71 antivirals: Past, present, and future. *Acta Pharmaceutica Sinica B*, 12(4), pp. 1542-1566. doi: 10.1016/j.apsb.2021.08.017.

Wang, M., Mou, C., Chen, M. and Chen, Z. (2021). Infectious recombinant Senecavirus A expressing novel reporter proteins. *Applied Microbiology and Biotechnology*, 105(6), pp. 2385-2397. doi: 10.1007/s00253-021-11181-6.

Wang, X.Y., Xu, Z.Y., Ma, J.C., von Seidlein, L., Zhang, Y., Hao, Z.Y., Han, O.P., Zhang, Y.L., Tian, M.Y., Ouyang, P.Y., Zhang, Z.Y., Han, C.Q., Xing, Z.C. and Chen, J.C. (2007). Long-term immunogenicity after single and booster dose of a live attenuated hepatitis A vaccine: results from 8-year follow-up. *Vaccine*, 25(3), pp. 446-9. doi: 10.1016/j.vaccine.2006.08.004.

Webster, D., Lee, T.D., Moore, J., Manning, T., Kunimoto, D., LeBlanc, D., Johnson, J.J. and Gray, C. (2010). Antimycobacterial screening of traditional medicinal plants using the microplate resazurin assay. *Canadian Journal of Microbiology*, 56(6), pp. 487–494. doi: 10.1139/w10-035.

Welinder, C. and Ekblad, L. (2011). Coomassie staining as loading control in western blot analysis. *Journal of Proteome Research*, 10 (3), pp. 1416-1419. doi: 10.1021/pr1011476.

Westby, M., Nakayama, G., Butler, S. and Blair, W. (2005). Cell-based and biochemical screening approaches for the discovery of novel HIV-1 inhibitors. *Antiviral Research*, 67(3), pp. 121-140. doi: 10.1016/j.antiviral.2005.06.006.

Whitton, J., Cornell, C. and Feuer, R. (2005). Host and virus determinants of picornavirus pathogenesis and tropism. *Nature Reviews Microbiology*, 3(10), pp. 765-776. doi: 10.1038/nrmicro1284.

Willems, T., Lefebvre, D., Neyts, J. and De Clercq, K. (2011). Diagnostic performance and application of two commercial cell viability assays in foot-and-mouth disease research. *Journal Of Virological Methods*, 173(1), pp. 108-114. doi: 10.1016/j.jviromet.2011.01.015.

World Health Organization. (2023). Poliomyelitis. Available at: https://www.who.int/teams/health-product-policy-and-standards/standards-and specifications/vaccines-quality/poliomyelitis. (Accessed: 7 February 2023).

World Health Organization. (2019). WHO immunological basis for immunization series: module 18: hepatitis A, update 2019. Available at: https://apps.who.int/iris/handle/10665/326501. (Accessed: 4 January 2022).

Wu, Y., Wu, M., He, G., Zhang, X., Li, W., Gao, Y., Li, Z., Wang, Z. and Zhang, C. (2012). Glyceraldehyde-3-phosphate dehydrogenase: A universal internal control for Western blots in prokaryotic and eukaryotic cells. *Analytical Biochemistry*, 423(1), pp. 15-22. doi: 10.1016/j.ab.2012.01.012.

Xiong, Q., Wang, Y., Xie, B., Pei, X. and Peng, Y. (2017). Single-step construction of a picornavirus replicon RNA with precise ends. *Journal of Virological Methods*, 248, pp. 87-91. doi: 10.1016/j.jviromet.2017.06.009.

Xu, J., Dang, Y., Ren, Y.R. and Liu, J.O. (2010). Cholesterol trafficking is required for mTOR activation in endothelial cells. *Proceedings of the national academy of sciences of the United States of America*, 107(10), pp. 4764‑4769. doi: https://doi.org/10.1073/pnas.0910872107.

Yang, H., Xie, Y. and Li, C. (2023). Understanding the mechanisms for COVID-19 vaccine's protection against infection and severe disease. *Expert Review of Vaccines*, doi: 10.1080/14760584.2023.2174529.

Yin, Y., Xu, Y., Ou, Z., Su, L. and Xia, H. (2015), A simple and highly repeatable viral plaque assay for enterovirus 71. *Journal of Basic Microbiology*, 55, pp. 538-541. doi: https://doi.org/10.1002/jobm.201400330.

Yip, D.K. and Auersperg, N. (1972). The dye-exclusion test for cell viability: Persistence of differential staining following fixation. *In Vitro*, 7(5), pp. 323-329.

Yiu, C.Y., Chen, S.Y., Yang, T.H., Chang, C.J., Yeh, D.B., Chen, Y.J. and Lin, T.P. (2014). Inhibition of Epstein-Barr virus lytic cycle by an ethyl acetate subfraction separated from Polygonum cuspidatum root and its major component, emodin. *Molecules*, 19(1), pp. 1258–1272. doi: 10.3390/molecules19011258.

Zell, R. (2017). Picornaviridae- the ever-growing virus family. *Archives of Virology*, 163(2), pp. 299-317. doi: 10.1007/s00705-017-3614-8.

Zell, R., Knowles, N.J. and Simmonds, P. (2021). A proposed division of the family *Picornaviridae* into subfamilies based on phylogenetic relationships and functional genomic organization. *Archives of Virology*, 166, pp. 2927–2935. doi: https://doi.org/10.1007/s00705-021-05178-9.

Zhang, J.H., Chung, T.D. and Oldenburg, K.R. (1999). A simple statistical parameter for use in evaluation and validation of high throughput screening assays. *Journal of Biomolecular Screening*, 4(2), pp. 67-73. doi: 10.1177/108705719900400206.

Zhang, M., Wu, F., Liang, M., Xian, J., Zheng, L., Li, Q. and Chen, Q. (2022). Parechovirus A infection and risk of gastroenteritis in children: A systematic review and meta-analysis. *Reviews in Medical Virology*, 32(6), e2380. doi: https://doi.org/10.1002/rmv.2380.

Zhao, X., Zhou, C., Zhang, X., Li, W., Wan, X., Wang, Y., Zeng, Y. and Zhang, W. (2017). The complete genome sequence of a human parechovirus from a child with diarrhea in china revealed intertypic recombination. *Genome Announcements*, 5(21), e00332-17. doi: doi/full/10.1128/genomeA.00332-17.

Zhao, Y. L., Meng, Z. D., Xu, Z. Y., Guo, J. J., Chai, S. A., Duo, C. G., Wang, X. Y., Yao, J. F., Liu, H. B., Qi, S. X. and Zhu, H. B. (2000). H2 strain attenuated live hepatitis A vaccines: Protective efficacy in a hepatitis A outbreak. *World Journal of Gastroenterology*, 6(6), pp. 829-832. https://doi.org/10.3748/wjg.v6.i6.829.

Zheng, W., Thorne, N. and McKew, J. (2013). Phenotypic screens as a renewed approach for drug discovery. *Drug Discovery Today*, 18(21-22), pp. 1067-1073. doi: 10.1016/j.drudis.2013.07.001.

Zhu, S., Zhang, C., Huang, L.S., Zhang, X.Q., Xu, Y., Fang, X., Zhou, J., Wu, M., Schooley, R.T., Huang, Z. and An, J. (2019). Discovery and computational analyses of novel small molecule Zika virus inhibitors. *Molecules*, 24(8). doi: https://doi.org/10.3390/molecules24081465.

Zoll, J., Erkens Hulshof, S., Lanke, K., Verduyn Lunel, F., Melchers, W. J. G., Schoondermark-van de Ven, E., Roivainen, M., Galama, J. M. D. and van Kuppeveld, F. J. M. (2009). Saffold virus, a human Theiler's-

like cardiovirus, is ubiquitous and causes infection early in life. *Public Library of Science: Pathogens*, 5(5), e1000416. doi: 10.1371/journal.ppat.1000416.

Zou, G., Xu, H. Y., Qing, M., Wang, Q. and Shi, P. (2011). Development and characterisation of a stable luciferase dengue virus for high-throughput screening. *Antiviral Research*, 91(1), pp. 11-19. doi: 10.1016/j.antiviral.2011.05.001.

Zuck, P., Murray, E. M., Stec, E., Grobler, J. A., Simon, A. J., Strulovici, B., Inglese, J., Flores, O. A. and Ferrer, M. (2004). A cell-based β-lactamase reporter gene assay for the identification of inhibitors of hepatitis C virus replication. *Analytical Biochemistry*, 334(2), pp. 344-355. doi: 10.1016/j.ab.2004.07.031.